



Calhoun: The NPS Institutional Archive DSpace Repository

Theses and Dissertations

1. Thesis and Dissertation Collection, all items

1992-03

Further studies in filmwise condensation of steam on horizontal finned tubes

Swensen, Keith Andrew

Monterey, California. Naval Postgraduate School

<http://hdl.handle.net/10945/23910>

This publication is a work of the U.S. Government as defined in Title 17, United States Code, Section 101. Copyright protection is not available for this work in the United States.

Downloaded from NPS Archive: Calhoun



<http://www.nps.edu/library>

Calhoun is the Naval Postgraduate School's public access digital repository for research materials and institutional publications created by the NPS community.

Calhoun is named for Professor of Mathematics Guy K. Calhoun, NPS's first appointed -- and published -- scholarly author.

Dudley Knox Library / Naval Postgraduate School
411 Dyer Road / 1 University Circle
Monterey, California USA 93943

DUDLEY KNOX LIBRARY
NAVAL POSTGRADUATE SCHOOL
MONTEREY CA 93943-5101

NAVAL POSTGRADUATE SCHOOL

Monterey , California



THEESIS

**FURTHER STUDIES IN FILMWISE
CONDENSATION OF STEAM ON
HORIZONTAL FINNED TUBES**

by

Keith Andrew Swensen

March, 1992

Thesis Co-Advisor
Thesis Co-Advisor

P.J. Marto
S.B. Memory

Approved for public release; distribution is unlimited.

T258717

Unclassified

CURITY CLASSIFICATION OF THIS PAGE

REPORT DOCUMENTATION PAGE

Form Approved
OMB No. 0704-0188

1. REPORT SECURITY CLASSIFICATION Unclassified			1b RESTRICTIVE MARKINGS		
2. SECURITY CLASSIFICATION AUTHORITY			3. DISTRIBUTION/AVAILABILITY OF REPORT Approved for public release; distribution is unlimited.		
4. DECLASSIFICATION/DOWNGRADING SCHEDULE					
PERFORMING ORGANIZATION REPORT NUMBER(S)			5. MONITORING ORGANIZATION REPORT NUMBER(S)		
6. NAME OF PERFORMING ORGANIZATION Naval Postgraduate School		6b OFFICE SYMBOL (If applicable) 34	7a. NAME OF MONITORING ORGANIZATION Naval Postgraduate School		
7. ADDRESS (City, State, and ZIP Code) Monterey, CA 93943-5000			7b. ADDRESS (City, State, and ZIP Code) Monterey, CA 93943-5000		
8. NAME OF FUNDING/SPONSORING ORGANIZATION		8b OFFICE SYMBOL (If applicable)	9. PROCUREMENT INSTRUMENT IDENTIFICATION NUMBER		
10. ADDRESS (City, State, and ZIP Code)			10. SOURCE OF FUNDING NUMBERS		
			PROGRAM ELEMENT NO	PROJECT NO	TASK NO
					WORK UNIT ACCESSION NO.
TITLE (Include Security Classification) FURTHER STUDIES IN FILMWISE CONDENSATION OF STEAM ON HORIZONTAL FINNED TUBES (Unclassified)					
PERSONAL AUTHOR(S) Keith Andrew Swensen					
a. TYPE OF REPORT Master's Thesis	13b TIME COVERED FROM _____ TO _____		14. DATE OF REPORT (Year, Month, Day) March 1992		15. PAGE COUNT 142
SUPPLEMENTARY NOTATION The views expressed in this thesis are those of the author and do not reflect the official policy or position of the Dept. of Defense or U.S. Government.					
COSATI CODES			18. SUBJECT TERMS (Continue on reverse if necessary and identify by block number) filmwise condensation, integral finned tubes, vapor velocity		
ABSTRACT (Continue on reverse if necessary and identify by block number) Over the years, there has been significant variation in the filmwise steam condensation data at NPS on horizontal low-integral finned tubes. With a view to increasing the accuracy of the data, inserts were used inside the tubes to reduce inside thermal resistance; however, significant discrepancies then occurred in the calculated outside heat-transfer coefficient when compared to data taken without an insert. These discrepancies arose due to the data reduction technique which assumes a known inside heat-transfer resistance and subtracts this from a measured overall resistance. If the assumed value on the inside is inaccurate, then the outside value is equally inaccurate. The present work uses an instrumented smooth tube to obtain accurate inside heat-transfer correlations both with and without inserts and uses these to obtain accurate outside coefficients for a family of uninstrumented finned tubes with a view to finding an optimum fin spacing for steam condensation.					
DISTRIBUTION/AVAILABILITY OF ABSTRACT <input checked="" type="checkbox"/> UNCLASSIFIED/UNLIMITED <input type="checkbox"/> SAME AS RPT <input type="checkbox"/> DTIC USERS			21. ABSTRACT SECURITY CLASSIFICATION Unclassified		
22a. NAME OF RESPONSIBLE INDIVIDUAL P.J. Marto			22b. TELEPHONE (Include Area Code) (408) 646-2989	22c. OFFICE SYMBOL 69Mx	

Approved for public release; distribution is unlimited.

Further Studies in Filmwise
Condensation of Steam on
Horizontal Finned Tubes

by

Keith Andrew Swensen
Lieutenant, United States Navy
B.S., Brigham Young University, 1985

Submitted in partial fulfillment
of the requirements for the degree of

MASTER OF SCIENCE IN MECHANICAL ENGINEERING

from the

ABSTRACT

Over the years, there has been significant variation in the filmwise steam condensation data at NPS on horizontal low-integral finned tubes. With a view to increasing the accuracy of the data, inserts were used inside the tubes to reduce inside thermal resistance; however, significant discrepancies then occurred in the calculated outside coefficient when compared to data taken without an insert. These discrepancies arose due to the data reduction technique which assumes a known inside heat-transfer resistance and subtracts this from a measured overall resistance. If the assumed value on the inside is inaccurate, then the outside value is equally inaccurate.

The present work uses an instrumented smooth tube to obtain accurate inside heat-transfer correlations both with and without inserts and uses these to obtain accurate outside coefficients for a family of uninstrumented finned tubes with a view to finding an optimum fin spacing for steam condensation.

TABLE OF CONTENTS

I. INTRODUCTION	1
A. BACKGROUND	1
B. CONDENSATION	2
C. CONDENSATION RESEARCH AT NAVAL POSTGRADUATE SCHOOL	4
D. OBJECTIVES	5
II. LITERATURE SURVEY	7
A. INTRODUCTION	7
B. VAPOR SIDE CONSIDERATIONS	8
C. COOLANT SIDE CONSIDERATIONS	11
III. APPARATUS AND SYSTEM INSTRUMENTATION	14
A. SYSTEM OVERVIEW	14
B. SYSTEM INSTRUMENTATION	17
C. SYSTEM MODIFICATIONS	20
IV EQUIPMENT OPERATION AND EXPERIMENTAL PROCEDURE .	23

A. SYSTEM STARTUP AND SHUTDOWN PROCEDURES	23
B. EXPERIMENTAL PROCEDURES AND OBSERVATIONS	29
C. TUBES TESTED	32
V. THEORETICAL BACKGROUND AND DATA REDUCTION	
PROCEDURES	36
A. THEORETICAL BACKGROUND	36
B. MODIFIED WILSON PLOT TECHNIQUE	40
C. INSTRUMENTED TUBE IMPROVEMENTS FOR DATA	
REDUCTION	43
D. ENHANCEMENT RATIO	44
VI. RESULTS AND DISCUSSION	47
A. DROPOWISE CONDENSATION	47
B. INSTRUMENTED TUBE RESULTS	49
C. INSIDE HEAT-TRANSFER CORRELATIONS FROM	
INSTRUMENTED TUBE RESULTS	57
D. ANALYSIS OF SMOOTH TUBE RESULTS	65
E. ANALYSIS OF FINNED TUBE RESULTS	69
VII. CONCLUSIONS AND RECOMMENDATIONS	74
A. CONCLUSIONS	74

B. RECOMMENDATIONS	74
APPENDIX A. PHYSICAL AND THERMODYNAMIC PROPERTIES OF WATER	75
APPENDIX B. SYSTEM CALIBRATIONS AND CORRECTIONS	77
APPENDIX C. SYSTEM INTEGRITY / LEAK TESTING	86
APPENDIX D. COMPARISON OF FIXED C_i vs FLOATING C_i SOLUTION METHODS FOR MODIFIED WILSON PLOT DATA REPROCESSING	89
APPENDIX E. UNCERTAINTY ANALYSIS	93
APPENDIX F. INSTRUMENTED TUBE CONSTRUCTION	104
APPENDIX G. DRPINST PROGRAM LISTING	107
LIST OF REFERENCES	125
INITIAL DISTRIBUTION LIST	127

LIST OF TABLES

Table 1. DATA ACQUISITION SYSTEM CHANNEL ASSIGNMENT	21
Table 2. DATA RUN SUMMARY	33
Table 3. PERFORMANCE COMPARISON OF TUBE INSERTS AT ATMOSPHERIC CONDITIONS	54
Table 4. COMPARISON OF EQUATIONS (6.1) AND (6.3) FOR $Pr^{1/3}(\mu_o/\mu_w)^{0.14} = 1.4$ (held constant for comparison)	63
Table 5. COMPARISON OF REYNOLDS NUMBER EXPONENTS FOR SIEDER-TATE-TYPE CORRELATIONS	65
Table 6. SMOOTH TUBE α SUMMARY; EFFECT OF PRESSURE AND VAPOR VELOCITY	69
Table B.1 QUARTZ THERMOMETER CALIBRATION DATA.	79
Table B.2 FRICTION TEMPERATURE RISE POLYNOMIALS.	84
Table D. COMPARISON OF FIXED C_i vs FLOATING C_i REPROCESSING METHODS	90

LIST OF FIGURES

Figure 1. Schematic of Single Tube Test Apparatus	15
Figure 2. Schematic of Test Section Insert	16
Figure 3. Schematic of Purging System and Cooling Water Sump	18
Figure 4. Comparison of Dropwise and Filmwise Condensation Data (Smooth Instrumented Tube, Heatex Insert)	48
Figure 5. Effect of Pressure and Vapor Velocity on the Steam Heat- Transfer Coefficient (Smooth Instrumented Tube, Heatex Insert)	50
Figure 6. Comparison of Experimental Results with Nusselt Theory for Varying Pressure and Vapor Velocities (Smooth Instrumented tube, Heatex Insert)	52
Figure 7. Comparison of Steam Heat-Transfer Coefficients at Atmospheric Conditions for Three Insert Conditions (Smooth Instrumented Tube)	53
Figure 8. Horizontal Tube Wall Temperature Profiles (Smooth Instrumented Tube)	55
Figure 9. Comparison of Experimental Results with the Predictions of Nusselt, Fujii, and Shekrladze-Gomelauri	56
Figure 10. Log-Log Plot of Re versus $\text{Nu}/\text{Pr}^{1/3}(\mu_o/\mu_w)^{0.14}$ for No Insert (Smooth Instrumented Tube)	58

Figure 11. Log-Log Plot of Re versus $\text{Nu}/\text{Pr}^{1/3}(\mu_o/\mu_w)^{0.14}$ for Wire Wrap Insert (Smooth Instrumented Tube)	59
Figure 12. Log-Log Plot of Re versus $\text{Nu}/\text{Pr}^{1/3}(\mu_o/\mu_w)^{0.14}$ for Heatex Insert (Smooth Instrumented Tube)	60
Figure 13. Combined Log-Log Plot of Re versus $\text{Nu}/\text{Pr}^{1/3}(\mu_o/\mu_w)^{0.14}$ for Three Insert Conditions (Smooth Instrumented Tube)	61
Figure 14. Effect of Pressure and Vapor Velocity on the Steam Heat-Transfer Coefficient (Non-instrumented Smooth Tube, Heatex Insert)	67
Figure 15. Comparison of Instrumented Smooth Tube Results with Non-Instrumented Smooth Tube Data After Reprocessing	68
Figure 16. Comparison of the Steam Heat-Transfer Enhancement Data of Van Petten, for the Medium Finned Tube Family	70
Figure 17. Comparison of the Steam Heat-Transfer Enhancement Data of Van Petten and Swensen for the Medium Finned Tube Family	72
Figure 18. Comparison of the Steam Heat Transfer Data of Van Petten and Swensen for the 2.0 mm Fin Spacing Medium Tube.	73
Figure B.1 Horizontal Tube Coolant Flowmeter Calibration Chart	81
Figure B.2 Pressure Transducer Calibration Chart	83
Figure B.3 Friction Temperature Rise Curves for Heatex Insert, Wire Wrap Insert, Twisted Tape Insert, and No Insert	85
Figure C.1 Apparatus Leak Test I	87
Figure C.2 Apparatus Leak Test II	88

NOMENCLATURE

A_i	<i>effective inside surface area (m^2)</i>
A_o	<i>effective outside surface area (m^2)</i>
C_i	<i>Sieder-Tate leading coefficient</i>
C_f	<i>mass flow rate correction factor</i>
c_p	<i>specific heat at constant pressure (J/kg K)</i>
D_i	<i>inside tube diameter (m)</i>
D_o	<i>outside tube diameter (m)</i>
D_r	<i>finned tube outside root diameter (m)</i>
g	<i>gravitational constant (9.81 m/s²)</i>
h_{fg}	<i>specific enthalpy of vaporization (J/kg)</i>
h_i	<i>inside heat transfer coefficient (W/m²K)</i>
h_o	<i>outside heat transfer coefficient (W/m²K)</i>
k_c	<i>thermal conductivity of cooling water (W/mK)</i>
k_f	<i>condensate film thermal conductivity (W/mK)</i>
k_m	<i>thermal conductivity of metal tube (W/mK)</i>
L	<i>length of exposed tube (m)</i>
$LMTD$	<i>log mean temperature difference (K)</i>
L_1	<i>length of inlet portion of tube (m)</i>
L_2	<i>length of outlet portion of tube (m)</i>

m_{act}	<i>Corrected mass flow rate</i>
m_{calc}	<i>Computed mass flow rate</i>
m	<i>mass flow rate (kg/s)</i>
Nu	<i>Nusselt number</i>
P_{sat}	<i>saturation pressure (Pa)</i>
Pr	<i>Prandtl number</i>
Q	<i>heat transfer rate (W)</i>
q	<i>heat flux (W/m²)</i>
Re	<i>Reynolds number</i>
$Re_{2\Phi}$	<i>two phase Reynolds number</i>
R_i	<i>inside resistance (K/W)</i>
R_o	<i>outside resistance (K/W)</i>
R_w	<i>wall resistance (m²K/W)</i>
ΔT_f	<i>temperature across condensate film (K)</i>
T_b	<i>mean bulk fluid temperature (K)</i>
T_m	<i>mean coolant film temperature (K)</i>
T_w	<i>mean inner tube wall temperature (K)</i>
T_{sat}	<i>vapor saturation temperature (K)</i>
T_1	<i>cooling water inlet temperature (K)</i>
T_2	<i>cooling water outlet temperature (K)</i>
U_o	<i>overall heat transfer coefficient (W/m²K)</i>
U_∞	<i>vapor velocity (m/s)</i>

V	<i>cooling water velocity (m/s)</i>
α	<i>dimensionless coefficient</i>
$\epsilon_{\Delta T}$	<i>enhancement ratio based on the constant ΔT</i>
ϵ_q	<i>enhancement ratio based on constant q</i>
μ_c	<i>dynamic viscosity of cooling water at bulk temperature (N·s/m²)</i>
μ_f	<i>dynamic viscosity of condensate film (N·s/m²)</i>
μ_w	<i>dynamic viscosity of cooling water at mean inner tube wall temperature (N·s/m²)</i>
ρ_f	<i>condensate film density (kg/m³)</i>
ρ_v	<i>vapor density (kg/m³)</i>
η	<i>surface efficiency</i>

ACKNOWLEDGEMENTS

The author would like to thank Professor P.J. Marto, for his advice and guidance during this thesis effort. A special thanks is extended to Dr. S.B. Memory for his tireless efforts and guidance throughout each and every phase of this project.

Appreciation is extended to the workers in the Mechanical Engineering Department Machine Shop for their expertise, patience, and support, especially Mr. Charles Crow, Mr. Jim Selby, Mr. Jim Scholfield and Mr. Mardo Blanco.

The author offers a special thank you to his wife and best friend Carol, without her help and support the completion of this work would not have been possible. Her many hours of toil and hard work in typing this thesis are greatly appreciated.

Last of all, the author expresses his appreciation to his children Tyler, Steven, Rachel and Luke for their patience, support, and understanding throughout the duration of this study.

I. INTRODUCTION

A. BACKGROUND

A reduction in size and weight of all types of heat exchangers aboard Naval vessels will allow more efficient use of space. The benefits might include greater equipment accessibility for maintenance or greater heat exchanger capacity (without a corresponding increase in size and weight) with a corresponding increase in fuel efficiency.

For the past ten years, the Naval Postgraduate School in collaboration with the David Taylor Research Center and the National Science Foundation has conducted research that is directed at the development of smaller, more efficient steam condensers. Improved designs can result in significant space savings, always a primary concern on Naval vessels, especially submarines.

Uncertainties in past data using steam were apparently due to the lack of detailed information about the inside heat-transfer correlations used during the data reduction process. Previously, the standard Sieder-Tate correlation was assumed to be valid for the inside heat-transfer coefficient, but it may not be the best correlation to use with the particular test arrangement used in this research program.

A large amount of enhanced condensation data has been collected in previous studies at the Naval Postgraduate School on more than 90 different condenser tubes of varying fin height, fin spacing, and tube material, with a view to finding an

optimum fin geometry for both steam and refrigerant condensation. Satisfactory results have been obtained with refrigerant data using R-113. However, some troublesome questions of possible contamination and instrument inaccuracy still remain with the steam data. It is felt that in order to address these questions, a fundamental evaluation of the heat transfer apparatus on which this data was collected and of the data reduction process was considered appropriate. Current data, taken on a carefully cleaned and calibrated apparatus, could be compared to previously recorded data and a determination as to its validity and reproducibility could be made. In addition, a thorough evaluation of the best inside heat-transfer correlation would lead to more reliable steam condensation results.

B. CONDENSATION

Condensation occurs when a vapor is cooled below its saturation temperature, or when a vapor/gas mixture is cooled below its dew point. Surface condensation occurs in condensers when a cooled surface (kept at a temperature below the saturation temperature of the vapor) contacts the vapor. The vapor molecules that contact such a surface stick to that surface and condense into liquid molecules. Condensation may occur in one of the following modes: filmwise, dropwise, or mixed mode (a combination of filmwise and dropwise) condensation. In the filmwise mode, the liquid wets the cold surface to form a continuous film. If the liquid does not wet the surface but instead forms discrete drops on the cold surface, dropwise or mixed

mode condensation will occur and is often caused by some form of contamination.

[Ref. 1]

The condensate forming on the tube surface offers a resistance to heat transfer between the vapor and the surface, which increases with the thickness of the liquid layer. Even though dropwise condensation results in much larger heat-transfer coefficients than filmwise condensation, it is difficult to maintain a stable dropwise condition over prolonged periods. Therefore, in most cases condenser design calculations are based on the assumption of filmwise condensation, resulting in lower heat-transfer coefficients and more conservative designs. [Ref. 1]

In a condenser, the coolant side, tube wall, and vapor side thermal resistances control the heat transfer rate from vapor to coolant. Also, for experimental work we always use clean tubes, but in real condensers tubeside fouling can play an important role in increasing the coolant side resistance. The magnitudes of these resistances depend on the fluid, tube geometry, and flow conditions on the vapor and coolant side. For steam condensation, it is the coolant side thermal resistance which tends to dominate. Methods to lower this inside resistance include the use of inserts or roped tubing to promote turbulence, thereby raising the convection heat-transfer coefficient. However, such modifications lead to increased pressure drop through the tubes, which must be compensated for by providing extra pumping capacity. Heat transfer through the tube wall is conductive and is fixed once tube thickness and material are selected. The vapor side resistance is due to the condensate film which forms on the outside of the tube. For filmwise condensation, the outside

resistance can be reduced by the addition of low integral fins. These have the effect of not only increasing the outside surface area of the tube, but also of thinning the condensate film around the fins due to surface tension forces. Too small a fin spacing may result in condensate flooding, whereas too large a fin spacing approaches the smooth tube case; there should be an optimum fin spacing somewhere in between these two extremes. Horizontal fin spacing is therefore of prime importance, and finding the optimum spacing is one of the objectives of this long-term research program.

C. CONDENSATION RESEARCH AT NAVAL POSTGRADUATE SCHOOL

The research effort at NPS has included the study of differing fin dimensions (i.e. fin height, fin width, fin spacing) on low-integral finned horizontal tubes. Experimentation has included the use of three different test fluids (steam, R-113, and ethylene glycol) under various operational conditions using a number of different tube diameters.

Van Petten [Ref. 2] provides a summary of research efforts at NPS through the end of 1988. Van Petten and subsequent researchers have analyzed small, medium, and large diameter finned tubes to find the optimum fin spacing for maximum heat-transfer enhancement of the fluids mentioned above. However, discrepancies found by Guttendorf [Ref. 3] in the data processing technique (modified Wilson plot), which resulted in different values of heat-transfer enhancement (for the same tube

under the same operating conditions depending on whether an insert was or was not used), have raised doubts about the accuracy of the inside heat-transfer correlation.

Rouk [Ref. 4] investigated the use of an optimization technique to predict the inside heat-transfer correlation. When the optimization effort proved unsuccessful, he next used the instrumented smooth tube data of Georgiadis [Ref. 5] to develop an inside heat transfer correlation, but could not find a correlation with sufficient accuracy based on previous data. He recommended that once an overhaul on the test apparatus was complete, an increase in data precision would allow the development of an accurate inside heat-transfer correlation. This work is a follow on effort to develop inside heat-transfer correlations which can predict the value of the inside heat-transfer coefficient with good accuracy under a variety of flow conditions. Once an inside correlation can be found, the object of this effort is to reprocess previous data and see if the discrepancies reported by former researchers for finned tubes on this apparatus can be rectified.

D. OBJECTIVES

The main objectives of this thesis were to:

1. Disassemble and meticulously clean the apparatus to eliminate any existing contamination with a view to eliminating dropwise condensation problems experienced in the past.
2. Carefully reassemble the apparatus using new gasket material, and make modifications to improve system performance.
3. Recalibrate all system instrumentation to ensure the greatest achievable accuracy.

4. Investigate the possibility of manufacturing large, medium, and small diameter instrumented smooth tubes.
5. Use the new instrumented tubes and the one existing medium diameter smooth instrumented tube (fabricated by Poole [Ref. 6]) to obtain accurate inside heat-transfer correlations for a number of insert types as well as the no insert condition.
6. Evaluate the accuracy of the currently used data processing technique (modified Wilson plot) using instrumented tube data.
7. Reprocess previous data using the new correlations with a view to comparing current and past smooth tube and finned tube data to provide continuity with previous studies.

II. LITERATURE SURVEY

A. INTRODUCTION

When a vapor condenses in the filmwise mode on a smooth horizontal tube it forms a thin continuous film of condensate on the surface of the tube. The condensate film thickens around the tube due to gravity. This condensate film provides a resistance to heat transfer which may be lowered through the use of fins. For quite some time, it was thought to be impractical to use finned tubes with high surface tension fluids such as water, due to condensate retention and flooding between the fins. However, a number of studies conducted on finned tubes using steam have shown that substantial heat-transfer enhancement may be achieved.

A significant amount of research at the Naval Postgraduate School and elsewhere has addressed the issue of optimum fin height, thickness, and spacing required for maximum heat transfer. Yau et al [Ref. 7] reported that "with an increase in fin density, up to a limit (this limit is not yet known in a generalized manner), the heat-transfer coefficient increases at a rate faster than the increase in the outside area due to the presence of fins. This additional enhancement is due to the thinning effect of the surface-tension forces on the condensate film. Unfortunately, surface-tension forces also adversely affect heat transfer by causing condensate to be retained between fins" [Ref. 8]. Katz et al [Ref. 9] also found that

on finned tubes the portion of the surface occupied by condensate is dependent upon the ratio of condensate surface-tension to density and the fin geometry.

Condensate retention and the behavior of the condensate film on the tube surface under various conditions are critical parameters in the heat transfer process on horizontal finned tubes. Several models have been developed to predict this behavior and the reader is referred to an extensive review of horizontal finned tube heat transfer by Marto [Ref. 10] for a more detailed coverage of the topic.

B. VAPOR SIDE CONSIDERATIONS

The filmwise condensation of vapor on a horizontal tube is a complex two-phase heat transfer process, for which a suitably complex model would be required to accurately predict heat transfer performance under all conditions.

In 1916, Nusselt [Ref. 11] set forth his theoretical work on the study of laminar filmwise condensation of a "stationary" vapor on a vertical or inclined plate and a horizontal tube. Nusselt's simplifying assumptions included the following [Ref. 12]:

1. Pure saturated vapor
2. Negligible vapor velocity ($U_{\infty}=0$)
3. Heat transfer across the condensate film by conduction only
4. Laminar condensate flow governed only by gravitational and viscous forces
5. Condensate properties constant
6. Isothermal condensing surface
7. Negligible interface temperature drop

Nusselt's result for the mean heat-transfer coefficient for a horizontal tube was obtained:

$$Nu = 0.728 \left[\frac{k_f^3 \rho_f (\rho_f - \rho_v) g h_{fg}}{\mu_f D_o \Delta T_f} \right]^{1/4} \quad (2.1)$$

or

$$Nu = 0.655 \left[\frac{k_f^3 \rho_f (\rho_f - \rho_v) g h_{fg}}{\mu_f D_o q} \right]^{1/3} \quad (2.2)$$

where:

Nu	= mean Nusselt number
k_f	= thermal conductivity of condensate film (W/m · k)
ρ_f	= condensate film density (kg/m ³)
ρ_v	= vapor density (kg/m ³)
g	= gravitational constant (9.81 m/s ²)
h_{fg}	= specific enthalpy of vaporization (J/kg)
μ_f	= dynamic viscosity of condensate film (N·s/m ²)
D_o	= outside tube diameter (m)
ΔT_f	= average temperature difference across condensate film (K)
q	= heat flux based on outside area (Q/A _o) (W/m ²)

Many workers have improved on Nusselt's theoretical analysis by accounting for some of the terms he neglected through his simplifying assumptions. However, equations (2.1) and (2.2) have been found to be remarkably accurate over a wide range of conditions for a stationary vapor. High vapor velocity can increase film condensation heat transfer substantially. This enhancement, which refers to the amount of heat transfer above or below the value predicted by the Nusselt analysis, is due to the effect of thinning the condensate film. However, vapor shear is the one

assumption which if applied can lead to significant increases in the heat-transfer coefficient.

The theoretical result of Shekriladze and Gomelauri (1966) [Ref. 13], who considered interfacial shear stress due to vapor velocity, is shown in equation (2.3).

$$\frac{Nu}{Re_{2\Phi}^{1/2}} = 0.64(1 + (1 + 1.69F)^{1/2})^{1/2} \quad (2.3)$$

where:

$$\begin{aligned} Nu &= \text{Nusselt number for the vapor side} \\ Re_{2\Phi} &= \text{two phase Reynolds number, } (\rho_f U_\infty D_o / \mu_f) \end{aligned}$$

For steam condensation, the empirically derived correlation of Fujii et al [Ref. 14] is shown in equation (2.4).

$$\frac{Nu}{Re_{2\Phi}^{1/2}} = 0.96F^{1/5} \quad (2.4)$$

The Nusselt expression (equation (2.1)) can be expressed in similar form:

$$\frac{Nu}{Re_{2\Phi}^{1/2}} = 0.728F^{1/4} \quad (2.5)$$

Whereas the vapor velocity, U_∞ , cancels out in the Nusselt expression (stationary vapor assumption), the Fujii correlation includes the vapor velocity effect. Therefore we can expect equation (2.4) to more accurately predict steam-side heat

transfer coefficients for those cases where vapor velocity begins to have a significant impact.

For further review of basic theoretical studies on the subject of laminar film condensation on smooth tubes the reader is referred to Rose [Ref. 15].

C. COOLANT SIDE CONSIDERATIONS

For a turbulent flow regime inside a pipe ($Re > 10,000$), a number of coolant-side correlations have been used; many of these have taken the form:

$$Nu = C_i Re^m Pr^n \quad (2.6)$$

where:

Nu = mean coolant Nusselt number for turbulent flow

C_i = correlating coefficient

Re = coolant Reynolds number

Pr = coolant Prandtl number

The most common correlations with the same form as equation (2.6) are that of Dittus and Boelter (1930) [Ref. 16]:

$$Nu = 0.023 Re^{0.8} Pr^{0.4} \quad (2.7)$$

and Colburn (1933) [Ref. 17]:

$$Nu = 0.023 Re^{0.8} Pr^{1/3} \quad (2.8)$$

Sieder and Tate (1936) [Ref. 18] applied a correction factor to equation (2.8) to account for cases in which the bulk to inner wall temperature difference is large enough to cause substantial variations in coolant viscosity as follows:

$$Nu = 0.027 Re^{0.8} Pr^{1/3} (\mu_c / \mu_w)^{0.14} \quad (2.10)$$

where:

- μ_c = coolant viscosity evaluated at mean bulk temperature ($N\cdot s/m^2$)
- μ_w = coolant viscosity evaluated at mean inner tube wall temperature ($N\cdot s/m^2$)

The fluid properties in equations (2.7), (2.8), and (2.9) are evaluated at mean coolant bulk temperature $T_{m,bulk}$.

$$T_{m,bulk} = (T_1 + T_2)/2 \quad (2.11)$$

where:

- T_1 = tube coolant inlet temperature (K)
- T_2 = tube coolant outlet temperature (K)

Equations (2.7), (2.8) and (2.9) are valid for $Re > 10^4$ and $0.7 < Pr < 100$, and were developed for long smooth pipes with no inserts [Ref. 12].

The use of inserts and the effect of bends close to the tube entrance region can affect the values of both the leading coefficient, C_i , and Reynolds number exponent, m , in equation (2.6). One of the major focuses of this study is to determine the values of C_i and m for the no insert, wire wrap insert, and Heatex insert cases.

Other well-known turbulent pipe flow heat-transfer correlations (i.e. Petukhov-Popov [Ref. 19], Sleicher-Rouse [Ref. 20], etc.) and the results of an ANL (Argonne National Laboratory) [Ref. 21] study which evaluated several such correlations for accuracy are reviewed in section VI C.

III. APPARATUS AND SYSTEM INSTRUMENTATION

A. SYSTEM OVERVIEW

The apparatus used for this research was basically the same as was used by Van Petten [Ref. 2] and Guttendorf [Ref. 3] with certain modifications. A system schematic is provided in Figure 1. Steam generated from distilled water in the .30 m diameter pyrex glass boiler using ten 4 kW, 440 V Watlow immersion heaters was the working medium for this set of experiments. From the boiler section the steam passed up through a reducing section and a 2.13 m straight length of pyrex glass piping, (ID of 0.15 m), it was then turned through 180 degrees using two 90 degree pyrex glass elbows, and then descended down a 1.52 m straight length of pyrex glass piping. The steam then entered the stainless steel test section containing the horizontally mounted condenser tube (see Figures 1 and 2); any steam not condensing there was condensed in the auxiliary condenser located just beneath the test section. The auxiliary condenser was constructed of a single copper coil mounted to a stainless steel baseplate enclosed within a pyrex glass condenser section. Coolant flow through the auxiliary condenser was used to control system pressure, and all condensed liquid was returned via the condenser baseplate drain to the boiler section by gravity.

Coolant for the auxiliary condenser was provided via a throttled water connection with associated flowmeter. Coolant flow through the single horizontal

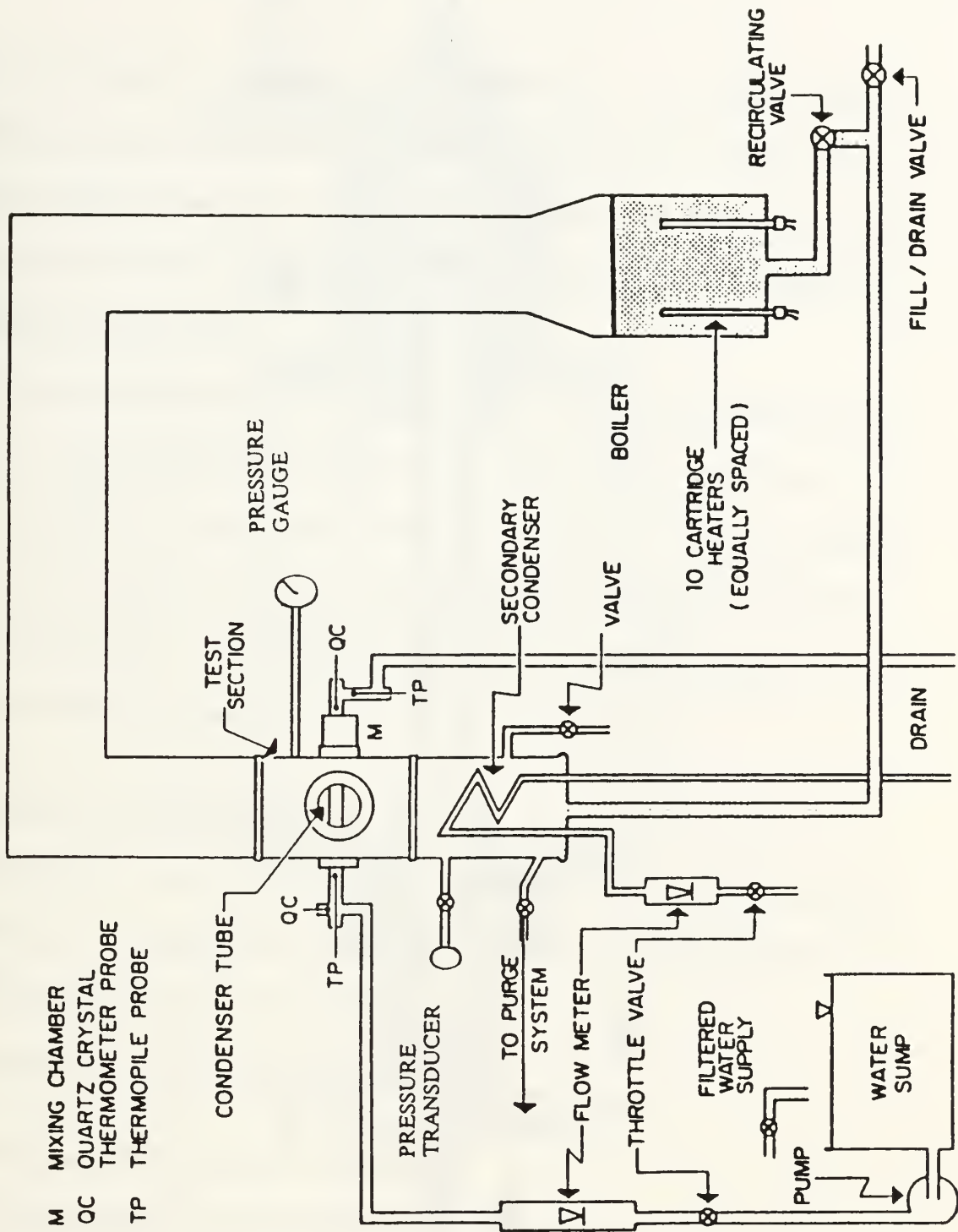


Figure 1. Schematic of Single Tube Test Apparatus

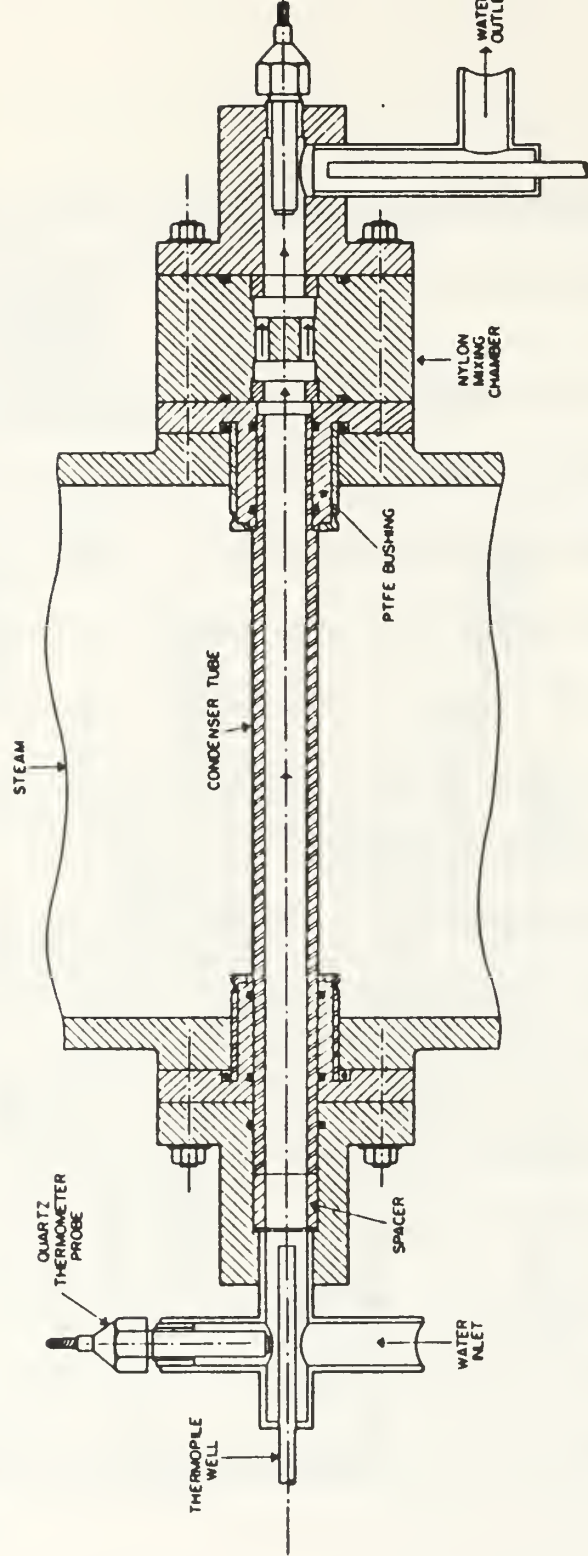


Figure 2. Schematic of Test Section Insert

tube was provided by a separate system consisting of a sump tank with two centrifugal pumps connected in series. Coolant flow rate was measured by a carefully calibrated flowmeter. By varying coolant flow-rate through the single horizontal tube, the rate of steam condensation on the tube (and hence heat-transfer coefficient) could be varied.

Non-condensable gases were removed using the vacuum pump system shown in Figure 3. The condensing coil for this purge system, located in the sump tank, served to condense steam carried through the vacuum line during the purging process. The vacuum line took its suction from the base of the auxiliary condenser, the coolest spot in the apparatus and the place where non-condensable gases (i.e. air) were most likely to accumulate.

B. SYSTEM INSTRUMENTATION

The power to the 440 V heaters was controlled through a panel mounted potentiometer. A description of the power calculation for input into the data acquisition system can be found in Poole [Ref. 6].

System pressure was monitored in three ways:

1. A Setra model 204 pressure transducer
2. A Heise solid front pressure gauge (visual reading only)
3. System saturation pressure from vapor temperature measurement

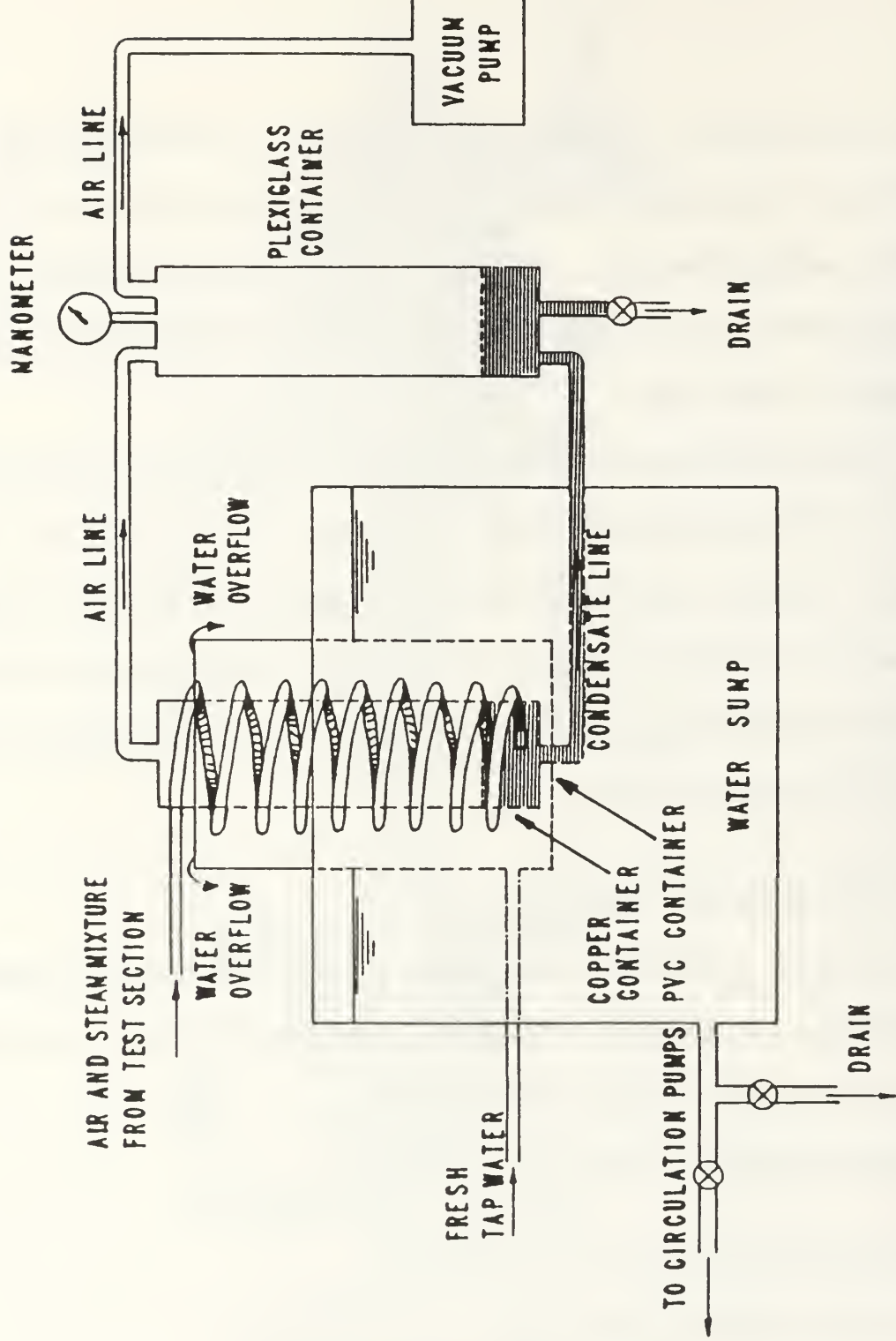


Figure 3. Schematic of Purging System and Cooling Water Sump

System vapor temperature was monitored using both teflon, and metal sheathed type-T copper/constantan thermocouples located juxtaposed in the test section; this position was just upstream of the test condenser tube. Condensate temperature was also monitored using a teflon coated type-T copper/constantan thermocouple located on the condensate return line between the auxiliary condenser and boiler. Coolant temperature rise in the condenser tube was measured using four methods:

1. Two teflon coated type-T copper/constantan thermocouples
2. Two metal sheathed type-T copper/constantan thermocouples
3. Two Hewlett-Packard 2804A quartz crystal thermometers
4. A ten-junction teflon coated type-T copper/constantan thermopile

These were all placed at the inlet to and exit from the condenser tube; at the outlet, all thermocouples were placed just downstream of a coolant mixing chamber.

Two data reduction programs were used to collect and reduce data on this apparatus; "DRPINST", and "DRPKS". The instrumented tube constructed by Poole [Ref. 6] was used to determine an accurate inside heat-transfer correlation for inserts used; this instrumented tube contained six wall thermocouples. For the instrumented tube the appropriate calibration equations were accessed in the data acquisition program "DRPINST". For non-instrumented tubes, the data reduction program "DRPKS" was used. Fluid property equations used in the data reduction programs are given in Appendix A and calibrations were conducted for all system

instrumentation (flowmeter, thermocouples, pressure transducer, etc.) and are included in Appendix B.

The data as monitored by the aforementioned system instrumentation was processed by an HP-3497A data acquisition system controlled by an HP-9826A computer provided with the correct data acquisition program. The raw data was processed and stored on computer disks. Program channel assignments are given in Table 1.

C. SYSTEM MODIFICATIONS

At the beginning of this investigation the apparatus was entirely disassembled to facilitate complete overhaul of the system. Modifications and details of assembly were as follows:

1. The apparatus was taken apart piece by piece, inspected, meticulously cleaned with a warm solution of Sparkleen biodegradable soap and subjected to a complete acetone rinse prior to reassembly.
2. A new pyrex glass riser section above the boiler was 0.31 m shorter than the previous section and allowed the addition of a new aluminum stand on which to place the heater baseplate. This new stand allowed much easier access to the 440 V heater wiring plus the adjustable legs allowed level adjustment of the entire apparatus, to ensure proper alignment of the single horizontal tube.
3. The two pyrex glass elbows were replaced.
4. Every gasket in the system was replaced (using Buna-N rubber) and, using a standard star torque pattern, all flanged joints were tightened to a final torqued of 30 inch-pounds (manufacturer recommended maximum torque

Table 1. DATA ACQUISITION SYSTEM CHANNEL ASSIGNMENT

<u>CHANNEL</u>	<u>QUANTITY MEASURED</u>	<u>APPLICABLE TYPE DESIGNATION</u>
40	Vapor Temperature	T-57 (See Appendix B.1)
41	Vapor Temperature	T-56 (See Appendix B.1)
42	Room Temperature	T-58 (See Appendix B.1)
43	Tube Coolant in 1	T-58
44	Tube Coolant out 1	T-58
45	Tube Coolant in 2	T-55 (See Appendix B.1)
46	Tube Coolant out 2	T-55
47	Condensate Return	T-58
48	Instrumented Tube	T-57 or T-55 as applicable
49	Instrumented Tube	T-57 or T-55 as applicable
50	Instrumented Tube	T-57 or T-55 as applicable
51	Instrumented Tube	T-57 or T-55 as applicable
52	Instrumented Tube	T-57 or T-55 as applicable
53	Instrumented Tube	T-57 or T-55 as applicable
60	10 - Junction Thermopile	T-61 (See Appendix B.1)
61	Voltage	NA
62	Current	NA
64	Pressure Transducer	(See Appendix B.4)

specification was 60 inch-pounds). The bolts holding the flanges together should be checked for tightness on a regular basis, since the thermal cycling of the apparatus has been shown to cause loosening of nut and bolt assemblies.

5. The previous vacuum pump was replaced with a Gast model 2567-V108 vacuum pump which could draw vacuum to 130 mmHg with an installed check valve to prevent pump back spin when the pump was stopped. The new pump could draw vacuum much more rapidly, but could not operate at less than 130 mmHg. Remaining non-condensable gases were removed by flushing the system with steam. The steam flushing procedure for removal of non-condensable gases is given in the operating procedures section. Once the system is completely filled with steam, operating pressures well below 130 mmHg could be achieved utilizing the auxiliary condenser.
6. The double coil auxiliary condenser was replaced with a single coil used originally by Van Petten [Ref. 2]. The single coil was not coated with the special oxide coating used by Guttendorf [Ref. 3]. It was felt to be superior to the double coil in that the baseplate welds were of much higher quality and were preferred on the basis of vacuum tightness.
7. The aluminum side plates attached to the pyrex glass auxiliary condenser housing were replaced with new stainless steel side plates with penetrations for pressure bleed, vacuum line, and a pressure transducer. These three penetrations were fitted with screw threaded stainless steel connectors. The stainless steel connectors were heli-arc welded in place. Prior to this modification (completed 24 January 1992) a leak test conducted from 21 December 1991 to 2 January 1992 revealed a mean vacuum leak rate of \sim 3.4 mmHg per day (see Figure C.1). A subsequent leak test conducted from 6 February 1992 to 19 February 1992 showed an improvement in the mean leak rate to \sim 1.7 mmHg per day (see Figure C.2).
8. System instrument modifications included the addition of the Setra pressure transducer and the Heise pressure gauge, and the removal of the mercury manometer. All system instrumentation was recalibrated and the results incorporated into the data reduction programs.
9. Finally the apparatus was lagged with Halstead insulating foam to reduce heat loss as much as possible. The test section, which was left uncovered previously, was also lagged.

IV EQUIPMENT OPERATION AND EXPERIMENTAL PROCEDURE

A. SYSTEM STARTUP AND SHUTDOWN PROCEDURES

Startup of the system is accomplished in the following manner:

1. Ensure distilled water level in the boiler is 4 to 6 inches above the top of the heating elements. The boiler is filled by gravity drain via a hose connection from the distilled water tank to the boiler fill valve. Ensure the vent valve on the side of the auxiliary condenser is open when filling or draining the boiler. The boiler may be drained by removing the hose connection and opening the fill valve, which allows drainage into the trench directly beneath the boiler.
2. Once the boiler is filled to the appropriate level, shut the boiler fill valve and the distilled water tank valve.
3. Shut the system vent valve.
4. Turn on the data acquisition system, computer and printer. Load the appropriate program (DRPINST or DRPKS) and check for proper operation. Then check all thermocouple outputs, by stepping through the appropriate data acquisition system channels, to verify that all are registering ambient temperature.
5. Open the fill valve to the coolant water sump tank to a level such that the tank overflow drain box does not overflow (the valve is located between the boiler control panel and heat pipe apparatus).
6. Turn on the cooling water supply pumps and adjust the tube flow rate from 20% to 60% of the rotameter setting and check for leaks. Reset flow rate to desired level.
7. Open valves from tap water system to auxiliary condenser and adjust coolant flow rate to at least 30% and check for leaks. Reset flow rate to at least 10%.
8. Energize heaters and adjust voltage to approximately 50 volts (40 volts if the system is already at vacuum below 100 mmHg to limit the vibrational shock to the system from oversized vapor bubble formation). To energize the heaters there are three switches which must be placed in the on position. The first is located in power panel p5 located in the main hallway adjacent to the

lab and is labeled switch 3 / heater controller room 106. The second is the heater load bank circuit breaker located on the side of the boiler control panel. The third is the condensing rig boiler power switch on the front of the boiler control panel. Increase the voltage gradually in 10 volt increments to the desired level.

9. Turn on the vacuum pump and open the vacuum line valve. Allow the vacuum pump to run until system pressure is below 3 psi, then shut the vacuum line valve just prior to turning off the vacuum pump.
10. As system warmup continues and pressure increases to above 4 psi energize the vacuum pump as necessary to flush the non-condensable gases out of the system through the vacuum line by forcing the gases out with steam. To ensure that the non-condensables gather at the base of the auxiliary condenser, where the vacuum line suction is located, ensure that the horizontal tube is not supplied with coolant flow, and adjust coolant flow through the auxiliary condenser as necessary to ensure steam is filling the entire system. The auxiliary condenser may be touched lightly by hand, along its entire length, to ensure the system is completely filled with steam; any cool spots indicate the presence of non-condensable gases which means that the flushing process is not complete. The flushing process takes 15 to 30 minutes to accomplish, and should be repeated periodically for long periods of operation.
11. At the conclusion of the flushing process, shut the vacuum line valve and secure the vacuum pump.
12. In order to ensure that filmwise condensation occurs on the tube, coolant flow through the tube must be initiated as follows:
 - a. Allow the apparatus vapor temperature measurement (channel 40) to reach at least 3800 microvolts.
 - b. Cut in the auxiliary coolant flow (50% or 60% level) to cool the vapor temperature to roughly 3200 microvolts.
 - c. Secure coolant flow through the auxiliary condenser, and allow the vapor temperature level to climb to about 3700-3800 microvolts, which allows a steam blanket to cover the tube.
 - d. Initiate coolant flow through the single horizontal tube at the 80% level.

- e. Cut in coolant flow to the auxiliary condenser to control pressure, and observe the condensation process to ensure that a condensate film has formed on the tube.
13. Run software program DRPINST for an instrumented tube (DRPKS for uninstrumented tubes) by pressing "run" on the keyboard.

To take data for an instrumented tube, the questions for DRPINST can be answered as follows:

- Select fluid ... Enter 0 for steam
- Select option ... Enter 1 to take new data
- Enter month, date and time ... Press enter
- Enter input mode ... Enter 1 for new data
- Give a name for the raw data file ... Enter name
- Enter geometry code ... Enter 1 for finned, 0 for plain
- Select insert type ... Enter 0 for none, 1 for twisted tape, 2 for wire wrap, 3 for Heatex
- No. of thermocouples in wall? ... Enter 4, 5, or 6 depending on the tube
- Select tube diameter type ... Enter 2 for medium
- Enter pressure condition ... Enter 0 for vacuum, 1 for atmospheric
- Give a name for the wall temperature file ... Enter name
- Select input ... Enter 1 for short, 2 for long, or 3 for raw data
- Like to check NG (non-condensable gas) concentration ... Enter 1 for yes, 2 for no; you must answer yes for the first data point
- Enter flowmeter reading (%) ... Enter 2 digit number (i.e. 20 or 58 etc.)
- Connect voltage line ... Flip the voltage line toggle switch, located on the power control panel, to the on position and press enter

- Disconnect voltage line ... Flip the voltage line toggle switch off and press enter
- Enter pressure gauge reading (Pga) ... Enter reading off gauge in psi
- Select measurement ... Enter 0 for teflon, 1 for metal sheath, 2 for quartz, 3 for thermopile
- Change TCOOL rise? ... Enter 1 for yes, 2 for no
- OK to store this data set? ... Enter 1 for yes, 0 for no
- Will there be another run? ... Enter 1 for yes, 0 for no; starts at check NG concentration for following runs.

To take data for an uninstrumented tube the questions for DRPKS can be answered as follows:

- Select fluid ... Enter 0 for steam
- Select option ... Enter 0 to take new data
- Enter month, date and time ... Press enter
- Enter disk number ... Enter number
- Enter input mode ... Enter 0 for new data
- Select Ci ... Enter 0 to find a Ci value, 2 to use a Ci value stored in the program.
- Give a name for the raw data file ... Enter name
- Enter geometry code ... Enter 1 for finned, 0 for plain
- Enter insert type ... Enter 0 for none, 1 for twisted type, 2 for wire wrap, 3 for Heatex
- Select tube type ... Enter 0 for thick wall (only thick wall tubes were tested)
- Select material code ... Enter 0 for copper (only copper tubes were tested)

- Select tube diameter type ... Enter 1 for medium (no small or large diameter tubes were tested)
 - Enter pressure condition ... Enter 0 for vacuum, 1 for atmospheric
 - Want to create a file for NR vs F? ... Enter 1 for yes, 0 for no
 - Give a name for plot data file ... Enter name; easiest to use the raw data file name preceded by a P
 - Select output ... Enter 0 for short, 1 for long, 2 for raw data
 - Like to check NG concentration ... Enter 1 for yes, 2 for no; you must answer yes for the first data point
 - Enter flowmeter reading (%) ... Enter 2 digit number (i.e. 20 or 60 etc.)
 - Connect voltage line ... Flip the voltage line toggle switch on and press enter
 - Disconnect voltage line ... Flip the voltage line toggle switch off and press enter
 - Enter pressure gauge reading (Pga) ... Enter reading off gauge in psi
 - Select measurement ... Enter 0 for teflon, 1 for metal sheath, 2 for quartz, 3 for thermopile
 - Change TCOOL rise ... Enter 1 for yes, 2 for no
 - OK to store this data set ... Enter 1 for yes, 0 for no
 - Will there be another run ... Enter 1 for yes, 0 for no; starts at check NG concentration for following runs.
14. Only answer the program questions up to "Enter flowmeter readings". Monitor system temperature using the vapor thermocouple voltage reading (the program automatically resets to channel 40) closely until system warmup is complete.
15. Monitor system temperature and pressure carefully to prevent a system over pressure during warmup (especially at atmospheric conditions).

16. If conducting a vacuum run, gradually adjust voltage to 90 volts (usually in 10 volt increments). Obtain the desired operating condition by manually controlling coolant flow through the auxiliary condenser until channel 40 reads 1970 ± 20 microvolts ($\sim 48^\circ\text{C}$). Vapor velocity ~ 2 m/s.
17. If conducting an atmospheric run, gradually adjust voltage to 175 volts from the 90 volt level in 10-20 volt increments. Again the desired operating condition is obtained by manually controlling coolant flow through the auxiliary condenser until channel 40 reads 4280 ± 20 microvolts ($\sim 100^\circ\text{C}$). Vapor velocity ~ 1 m/s.
18. Monitor the condensation process using the glass viewing window periodically to ensure that filmwise condensation is maintained. To clear the viewing window of fog and moisture increase coolant flow through the auxiliary condenser briefly to 50% or 60%, then reset to desired flow rate.
19. When taking readings be sure to check the flowmeter setting prior to entering it into the computer (it has a tendency to fluctuate slightly).
20. If conducting vacuum and atmospheric runs on the same day always conduct the vacuum run first. If the atmospheric run is done first it takes too long for the system to cool down to vacuum operating temperatures.

The system is secured in the following manner:

1. Secure power to the heating elements.
2. Secure coolant flow through the tube, through the auxiliary condenser, and to the sump tank.
3. If desired to maintain the system at vacuum conditions until the next run the shutdown is complete. Continued cooling water circulation may be used to assist in cooling down the system.
4. To bring the system back to atmospheric conditions slowly open the vent valve.
5. The data acquisition system may be turned off whenever it is not necessary to monitor system parameters.
6. Periodically change distilled water in the boiler.

7. If an emergency should arise such as abrupt overpressurization or breakage, immediately secure power to the heaters and open the vent valve, then let the system cool down before checking the apparatus for damage.

B. EXPERIMENTAL PROCEDURES AND OBSERVATIONS

Water is a poor wetting medium and therefore great care was taken to ensure that uniform filmwise condensation was the only condensation mode occurring during a data run. Even though the apparatus was meticulously cleaned (as mentioned previously), a continuing problem with dropwise condensation manifested itself. Subsequent to steam cleaning the system with a Sparkleen soap solution, by operating the system with a soapy solution in the boiler (the solution bubbled through the entire apparatus), dropwise condensation was observed on the installed instrumented tube. After taking some data when in the dropwise condition, the tube was removed and rigorously cleaned using a warm Alconox soap solution with a scrub brush. However, after observing the filmwise mode initially, the condensation mechanism soon transitioned to mixed mode and then back to the dropwise mode.

Since only a filmwise condition over several hours would suffice, the tube chemical treatment procedure used by Guttendorf [Ref. 3] and several other researchers was used to produce filmwise condensation. The tube was chemically treated prior to installation as follows:

1. Clean the internal and especially the external surfaces of the tube using a soft brush and mild soap (using the Alconox detergent in warm water), rinse with acetone then rinse thoroughly with distilled water. Repeat the cleaning

procedure until the distilled water rinse perfectly wets the tube surface; any breaks in the wetting film at this point are likely to result in dropwise condensation spots once the tube is installed in the apparatus.

2. Place the tube in a steam bath.
3. Mix equal amounts of ethyl alcohol and a 50% by weight solution of sodium hydroxide. Keep the solution warm so that a watery consistency is maintained.
4. Apply the solution to the tube with a small paint brush, retaining the tube in the steam bath. If the tube has not been treated previously, apply a coating of the solution every 10 minutes for an hour. If the tube has been previously treated, apply a coating every 5 minutes for a period of 20 minutes.
5. Remove the tube from the steam bath and thoroughly rinse the tube with distilled water to remove any excess solution. Install the tube in the test section immediately, being careful not to touch the tube surface. Oil or dirt from any source may contaminate the tube surface and result in mixed mode or dropwise condensation.

The oxide layer which forms on the tube is very thin, and has negligible thermal resistance and high wetting characteristics.

Once the tube was installed in the apparatus (with the desired insert in place), the system startup procedure outlined in section IV A was followed to take data at desired conditions.

At vacuum conditions, when single tube coolant flow was initiated with vapor velocity at ~ 2 m/s, the condensation on the tube did not develop as a perfect film but instead left patches where the film was broken. These patches, or streaks seemed to occur at regular intervals, and it was postulated that they were due to vortex shedding of vapor around the tube. Therefore, the procedure in the startup section IV A, step 12, was used to promote the development of uniform filmwise

condensation by inducing a stationary vapor condition around the tube. This allowed a steam blanket to form around the tube prior to coolant flow initiation. After flow initiation the appearance of the condensate film on the tube surface was continuous with no breaks. Momentary film instabilities were observed at vacuum conditions at pressures below ~ 20 kPa after a continuous film was established at higher pressures. These instabilities seemed to interrupt the film sheet only for an instant and then disappear, and may have been caused by vortex shedding of the vapor around the tube as already mentioned. A possible mechanism to explain these instabilities is that the higher vapor velocity at vacuum conditions momentarily thins the condensate film via vortex shedding, yet this thinning effect is overcome by surface tension forces in the film sheet which tend to restore the continuous film. These instabilities could only be seen for an instant and then would vanish, being very transitory in nature. There also did not appear to be any pattern whatsoever to the instability formation. The instabilities were not observed at pressures above ~ 20 kPa.

The data taking regimen for each data set involved starting, then verifying the existence of a filmwise condensation condition, then taking data at flow rates (in %) of 80, 70, 60, 50, 40, 30, and 20 then back to 80 and 50 to check for repeatability within the data set. Two data points were taken at each of the first seven data points and one each for the last two, which gave a total of 16 data points. It was usually quite clear from the two comparison points, and from data taken previously under similar conditions, whether the data set should be rejected or accepted. After tube installation, the appearance of one or more small patches (breaks in the film) after

~ 7-10 hours of operation signaled the beginning of tube contamination which got worse with time. The tube would then be removed and cleaned.

C. TUBES TESTED

The data taken during this study involved extensive use of the instrumented smooth tube (S01) fabricated by Poole [Ref. 6], (six wall thermocouples spaced 60 degrees apart placed at midwall and midlength). Due to excessive thermocouple wear, only 5 thermocouples in this instrumented tube functioned properly. The tube was positioned in the apparatus to make optimum use of functioning thermocouples. The preferred arrangement placed 4 thermocouples at 10°, 190°, 250°, and 310° from the top dead center position of the tube. This arrangement provided readings from the top and bottom of the tube and two intermediate points, giving the most accurate mean tube wall temperature and best temperature profile readings. At the conclusion of this study, the manufacture of the new instrumented tubes was not yet complete; progress to date (March 1992) is recorded in Appendix F.

Data was also taken on a uninstrumented smooth tube (S02) and four finned tubes (S03, S04, S05, S06) with fin spacings of 0.5 mm, 1.0 mm, and 1.5 mm, and 2.0 mm. All tubes tested were classified as medium tubes, with an outside diameter of 19.05 mm, and an inside diameter of 12.70 mm. The four finned tubes all had the same fin height of 1.0 mm, and fin width of 1.0 mm. Data runs were taken either with no insert, with the wire wrap or the Heatex insert installed. By more efficiently mixing the coolant an insert significantly increases the inside heat-transfer coefficient.

The Heatex insert consists of a central wire core onto which are wound a series of wire loops, each inclined at a common angle to the core. The loops come into direct contact with the tube wall, and each loop provides a significant amount of coolant mixing as the coolant flows through the loop mesh. [Ref. 12].

The wire wrap insert was a copper wire spirally wrapped around a central stainless steel rod with a uniform pitch. This insert induced a swirling coolant motion, which enhanced turbulent mixing within the tube. This particular wire wrap insert was the same insert used by Guttendorf [Ref. 3], Coumbes [Ref. 22], and Van Petten [Ref. 2] to collect data on the medium family of tubes.

A summary of data runs is given in Table 2.

Table 2. DATA RUN SUMMARY

Tube	Filename	Pressure (kPa)	Vapor Velocity (m/s)	Insert
S01	DSOIMVSH2	11	2.17	Heatex
	DSOIMASH4	101	1.06	Heatex
	DSOIMASH5	101	1.06	Heatex
	FSOIMASH3	11	2.11	Heatex
	FIMAVSH1	28	3.53	Heatex
	FIMAVSH2	41	2.45	Heatex
	FIMAVSH3	69	1.53	Heatex
	FIMAVSH4	101	1.08	Heatex
	FIMAVSH5	28	1.01	Heatex
	FIMAVSH6	41	1.04	Heatex
	FIMAVSH7	69	1.02	Heatex
	FIMASW3	101	1.07	wire wrap
	FIMASW4	101	1.07	wire wrap

Tube	Filename	Pressure (kPa)	Vapor Velocity (m/s)	Insert
S01	FIMASW5	101	1.06	wire wrap
	COMPAlW1	101	1.07	wire wrap
	COMPAlW2	101	1.07	wire wrap
	FIMASN4	101	1.08	none
	FIMASN5	101	1.07	none
	FIMASN6	101	1.08	none
	COMPAlN1	101	1.08	none
	COMPAlN2	101	1.08	none
S02	FNMAVSH1	15	6.24	Heatex
	FNMAVSH2	41	2.42	Heatex
	FNMAVSH3	69	1.51	Heatex
	FNMAVSH4	102	1.03	Heatex
	FNMAVSH5	28	1.02	Heatex
	FNMAVSH6	41	1.03	Heatex
	FNMAVSH7	69	1.02	Heatex
	FNMAVSH8	101	1.07	Heatex
S03	FIMAF051	101	1.06	Heatex
	FIMAF052	101	1.06	Heatex
S04	FIMAF101	101	1.07	Heatex
	FIMAF102	101	1.06	Heatex
S05	FIMAF151	101	1.07	Heatex
	FIMAF152	101	1.07	Heatex
S06	FIMAF201	101	1.07	Heatex
	FIMAF202	101	1.07	Heatex

Tube descriptions:

- S01 instrumented smooth tube fabricated by Poole
- S02 uninstrumented smooth tube
- S03 0.5 mm finned tube
- S04 1.0 mm finned tube
- S05 1.5 mm finned tube (this tube designated as F096 by Guttendorf; also a similar 1.5 mm finned tube designated as F006 by Guttendorf and Van Petten was not tested); the 1.5 mm finned tube results were not included in subsequent finned tube analysis since the reason for differences in experimental results for these two tubes has not yet been resolved.
- S06 2.0 mm finned tube

V. THEORETICAL BACKGROUND AND DATA REDUCTION PROCEDURES

A. THEORETICAL BACKGROUND

The overall or total resistance to heat transfer from vapor to coolant consists of the sum of the vapor side resistance (R_o), the tube wall resistance (R_w), and the coolant side resistance (R_i); this neglects any fouling resistance since clean tubes are always used.

$$R_{total} = R_o + R_w + R_i \quad (5.1)$$

The vapor and coolant side resistances are convective in nature and may be expressed by the reciprocal of their respective heat-transfer coefficient and surface area product.

$$R_o = \frac{1}{h_o A_o} \quad (5.2)$$

$$R_i = \frac{1}{h_i A_i} \quad (5.3)$$

where:

- | | |
|-------|---|
| R_o | = outside vapor side resistance to heat transfer (K/W) |
| h_o | = outside heat-transfer coefficient (W/m ² ·K) |
| A_o | = effective outside surface area (m ²) |
| R_i | = inside coolant side resistance to heat transfer (K/W) |
| h_i | = inside heat-transfer coefficient (W/m ² ·K) |
| A_i | = effective inside surface area (m ²) |

The tube wall resistance is conductive in nature and is represented by the radial conduction equation.

$$R_w = \frac{\ln \frac{D_r}{D_i}}{2\pi L k_m} \quad (5.4)$$

where:

- R_w = tube wall resistance (K/W)
- D_r = outside or root (if finned) diameter (m)
- D_i = inside tube diameter (m)
- L = active condensing length (133 mm)
- k_m = thermal conductivity of tube wall (W/m·K)

The effective outside area of the tube is calculated using the following expression:

$$A_o = \pi D_r L \quad (5.5)$$

where:

- D_r = outside or root (if finned) diameter (m)
- L = active condensing length (133 mm)

The effective inside area includes the inside surface area involving the active condensing length and the inside surface area of the insulated inlet and outlet portions of the tube. These portions of the tube act as fins and remove heat via axial conduction. The extended fin assumption with associated fin efficiencies was used to account for these end losses.

$$A_i = \pi D_i (L + \eta_1 L_1 + \eta_2 L_2) \quad (5.6)$$

where:

- D_i = inside diameter of tube (m)
- L = active tube condensing length (m)
- η_1 = fin efficiency of inlet portion of tube
- L_1 = length of inlet portion of tube (m)
- η_2 = fin efficiency of outlet portion of tube
- L_2 = length of outlet portion of tube (m)

The overall thermal resistance to heat transfer may be expressed by:

$$\frac{1}{U_o A_o} = R_o + R_w + R_i \quad (5.7)$$

Substituting equations (5.2) and (5.3) into equation (5.7) yields:

$$\frac{1}{U_o A_o} = \frac{1}{h_o A_o} + R_w + \frac{1}{h_i A_i} \quad (5.8)$$

where:

- U_o = overall heat-transfer coefficient ($\text{W}/\text{m}^2 \cdot \text{K}$)
- A_o = effective outside surface area (m^2)
- h_o = outside heat-transfer coefficient ($\text{W}/\text{m}^2 \cdot \text{K}$)
- R_w = Tube wall resistance (K/W)
- h_i = inside heat-transfer coefficient ($\text{W}/\text{m}^2 \cdot \text{K}$)

The single tube condenser apparatus uses the log mean temperature difference (LMTD) analysis for calculation of the heat transfer between the hot vapor and cold coolant.

$$Q = U_o A_o (LMTD) \quad (5.9)$$

where:

- Q = heat transfer rate to the cooling water (W)
- U_o = overall heat-transfer coefficient ($\text{W}/\text{m}^2 \cdot \text{K}$)
- A_o = effective outside surface area (m^2)
- LMTD = log mean temperature difference between vapor and coolant (K)

The log mean temperature difference (LMTD) is given by:

$$LMTD = \frac{(T_2 - T_1)}{\ln \left[\frac{T_{sat} - T_1}{T_{sat} - T_2} \right]} \quad (5.10)$$

where:

T_1	=	coolant inlet temperature (K)
T_2	=	coolant outlet temperature (K)
T_{sat}	=	vapor saturation temperature (K)

In this and previous studies at NPS, the quartz thermometer output for T_1 and T_2 were used in the calculations for the coolant temperature rise, and the saturation temperature, T_{sat} , was measured using the vapor thermocouple (channel 40).

The total heat transfer across the tube is experimentally determined by measuring the mass flow rate of fluid through the tube and its accompanying temperature rise.

$$Q = mc_p(T_2 - T_1) \quad (5.11)$$

where:

Q	=	heat transfer rate (W)
m	=	mass flow rate of coolant (kg/s)
C_p	=	specific heat of coolant at constant pressure (J/kg·K)
T_1	=	coolant inlet temperature (K)
T_2	=	coolant outlet temperature (K)

Equation (5.11) may be used directly from the experimental data. The resultant heat transfer rate, Q , is then substituted into equation (5.9) to find the overall heat-transfer coefficient, U_o .

$$U_o = \frac{Q}{A_o(LMTD)} \quad (5.12)$$

where:

Q	=	heat transfer rate from eq. (5.11) (W)
A_o	=	effective outside surface area (m^2)
LMTD	=	log mean temperature difference; eq. (5.10) (K)

Since R_w , U_o , A_o , and A_i are known quantities, this leaves only two unknowns in equation (5.8), h_o and h_i , the outside and inside heat transfer coefficients.

Often the coolant side thermal resistance is dominant, and inserts such as those mentioned in section IV C are used to lower the inside resistance. This allows a more accurate computation of the outside heat-transfer coefficient, h_o , when using the modified Wilson plot technique mentioned in section V B. Vapor side heat transfer may also be enhanced through the use of fins, drainage strips, or dropwise condensation promoters.

B. MODIFIED WILSON PLOT TECHNIQUE

The ideal way to solve for h_o and h_i in equation (5.8) is through the use of instrumented, which accurately determine a mean tube wall temperature. The inside and outside mean tube wall temperatures may then be obtained directly by assuming a linear temperature profile across the wall. Since the vapor temperature and mean coolant temperature are known, the inside and outside heat-transfer coefficients may then be calculated directly using equation (5.13).

$$q = h \Delta T \quad (5.13)$$

where:

$$\begin{aligned} q &= \text{heat flux } (\text{W/m}^2) \\ h &= \text{heat-transfer coefficient } (h_i \text{ for inside, } h_o \text{ for outside}) \text{ (W/m}^2\cdot\text{K)} \\ \Delta T &= \text{temperature difference across resistive medium } (\Delta T = T_{\text{sat}} - T_{\text{wall,outside}} \text{ for the vapor side, and } \Delta T = T_{\text{wall,inside}} - T_{\text{coolant}} \text{ for the coolant side}) \end{aligned}$$

For data collection on a large number of tubes, the use of instrumented tubes is impractical due to the high cost and difficulty involved in manufacturing so many tubes. Therefore, the modified Wilson plot technique was developed, which solves for the inside and outside heat-transfer coefficients simultaneously without using wall

thermocouples. To obtain the most accurate results with this method, it is necessary that the inside and outside coefficients be relatively equal in magnitude.

The modified Wilson plot technique requires that the "form" of the equation for both the inside and outside heat-transfer coefficients be known. The Nusselt theory and Sieder-Tate correlation are used to represent the "form" of the outside and inside heat-transfer coefficients respectively. The Nusselt theory when based on q can be represented by:

$$h_o = \alpha \left[\frac{k_f^3 \rho_f^2 g h_{fg}}{\mu_f D_o q} \right]^{1/3} = \alpha Z \quad (5.14)$$

or

where:

h_o	= outside heat-transfer coefficient ($\text{W}/\text{m}^2\cdot\text{K}$); based on q
α	= dimensionless coefficient
k_f	= thermal conductivity of condensate film ($\text{W}/\text{m}\cdot\text{K}$)
ρ_f	= condensate film density (kg/m^3)
g	= gravitational constant ($9.81 \text{ m}/\text{s}^2$)
h_{fg}	= specific enthalpy of vaporization (J/kg)
μ_f	= dynamic viscosity of condensate film ($\text{N}\cdot\text{s}/\text{m}^2$)
D_o	= outside tube diameter (m)
q	= heat flux based on outside area (Q/A_o) (W/m^2)

The Sieder-Tate correlation may be represented by:

$$h_i = C_i \frac{k_c}{D_i} Re^{0.8} Pr^{1/3} \left(\frac{\mu_c}{\mu_w} \right)^{0.14} = C_i \Omega \quad (5.15)$$

where:

h_i	= inside heat transfer coefficient ($\text{W}/\text{m}^2\cdot\text{K}$)
C_i	= Sieder-Tate leading coefficient
k_c	= thermal conductivity of cooling water ($\text{W}/\text{m}\cdot\text{K}$)
D_i	= inside tube diameter (m)
Re	= Reynolds number
Pr	= Prandtl number
μ_c	= dynamic viscosity of cooling water at bulk temperature ($\text{N}\cdot\text{s}/\text{m}^2$)

$$\mu_w = \text{dynamic viscosity of cooling water at mean inner wall temperature (N}\cdot\text{s/m}^2)$$

Substituting equations (5.14) and (5.15) into equation (5.8) gives:

$$\left[\frac{1}{U_o} - R_w A_o \right] Z = \frac{A_o Z}{C_i \Omega A_i} + \frac{1}{\alpha} \quad (5.16)$$

By letting:

$$Y = \left[\frac{1}{U_o} - R_w A_o \right] Z \quad (5.17)$$

$$X = \frac{A_o Z}{A_i \Omega} \quad (5.18)$$

$$m = \frac{1}{C_i} \quad (5.19)$$

$$b = \frac{1}{\alpha} \quad (5.20)$$

then equation (5.16) reduces to:

$$Y = mX + b \quad (5.21)$$

The parameters Ω and Z are both temperature dependent, and must be determined iteratively. A least-squares fit of equation (5.21) is used to determine C_i and α . Once C_i is known, h_i can be calculated using equation (5.15). With h_i and

U_o known, the value of h_o can then be easily determined by rearranging equation (5.7) as in equation (5.22), or by using equation (5.14) with the value of α known.

$$\frac{1}{h_o} = \frac{1}{U_o} - \left[\frac{A_o}{h_i A_i} + R_w A_o \right] \quad (5.22)$$

C. INSTRUMENTED TUBE IMPROVEMENTS FOR DATA REDUCTION

In previous work at NPS, the standard form of the Sieder-Tate equation was used with a Reynolds number exponent of 0.8, as in equation (2.10). One of the aims of this thesis was to use an instrumented tube to directly determine the inside and outside coefficients, h_i and h_o , and then use the data to determine a more "exact" form of the Sieder-Tate-type equation to be used for each insert. The coolant side correlations mentioned in section II C were based on a long, straight entrance length. The sharp 90° bend just prior to the test section tube entrance undoubtedly creates entrance effects which lead to discrepancies between our experimental data and heat transfer behavior predicted by the Sieder-Tate correlation.

Assuming the final form of the inside heat-transfer correlation to be that of equation (2.10) gives the following:

$$Nu = C_i Re^m Pr^{1/3} \left(\frac{\mu_c}{\mu_w} \right)^{0.14} \quad (5.23)$$

where:

m = Reynolds number exponent to be determined

Rearranging equation (5.23) gives:

$$\frac{Nu}{Pr^{1/3} \left(\frac{\mu_c}{\mu_w} \right)^{0.14}} = C_i Re^m \quad (5.24)$$

Taking the natural log of equation (5.24) yields:

$$\ln \left(\frac{Nu}{Pr^{1/3} \left(\frac{\mu_c}{\mu_w} \right)^{0.14}} \right) = \ln C_i + m \ln Re \quad (5.25)$$

Equation (5.25) is in the form of a linear equation, and by plotting $\ln(Nu/(Pr^{1/3}(\mu_c/\mu_w)^{0.14}))$ versus $\ln Re$, the slope and intercept, namely the Reynolds number exponent and Sieder-Tate coefficient may be determined from the instrumented data.

With the unknown parameters of equation (5.23) determined, the new inside heat-transfer correlations (one for each insert) could be used in the data reduction program to give the value of the inside heat-transfer coefficient, h_i , directly and to provide a more accurate calculation of the outside heat-transfer coefficient h_o .

D. ENHANCEMENT RATIO

Following the development of Van Petten [Ref.2], and Nusselt theory, experimental data can be curve fitted, using a least-squares analysis, to an equation of the following form:

$$q = a \Delta T^n \quad (5.26)$$

where:

$$\begin{aligned} q &= \text{heat flux based on outside area } (Q/A_o) \text{ (W/m}^2\text{)} \\ \Delta T &= \text{temperature drop across the condensate film (K)} \end{aligned}$$

Substituting equation (5.12) into his expression yields:

$$h_o = a \Delta T^{n-1} \quad (5.27)$$

From Nusselt theory $n = 0.75$, therefore the enhancement ratio, based on constant temperature drop across the condensate film, can be expressed as:

$$\epsilon_{\Delta T} = \frac{h_{of}}{h_{os}} = \frac{a_f}{a_s} \quad (5.28)$$

where:

$$\begin{aligned} \epsilon_{\Delta T} &= \text{enhancement ratio based on constant temperature drop across the condensate film} \\ f &= \text{subscript denoting finned tube} \\ s &= \text{subscript denoting smooth tube} \\ h_o &= \text{outside heat-transfer coefficient (W/m}^2\text{.K)} \\ a &= \text{constant of proportionality introduced in equation (5.26)} \end{aligned}$$

Also for constant ΔT ; using equation (5.14):

$$\epsilon_{\Delta T} = \frac{a_f}{a_s} = \frac{\alpha_f}{\alpha_s} \left[\frac{q_s}{q_f} \right]^{1/3} = \frac{\alpha_f}{\alpha_s} \left[\frac{a_s \Delta T}{a_f \Delta T} \right]^{1/3} = \frac{\alpha_f}{\alpha_s} \left[\frac{a_s}{a_f} \right]^{1/3} \quad (5.29)$$

If the heat flux is kept constant the values of Z_f and Z_s remain equal, which results in equation (5.30).

$$\epsilon_q = \frac{h_{of}}{h_{os}}|_q = \frac{\alpha_f Z_f}{\alpha_s Z_s} = \frac{\alpha_f}{\alpha_s} \quad (5.30)$$

Combining equations (5.29 and (5.30) gives the relationship between $\epsilon_{\Delta T}$ and ϵ_q in equation (5.33).

$$\epsilon_{\Delta T} = \frac{\alpha_f}{\alpha_s} \left[\frac{a_s}{a_f} \right]^{1/3} = \frac{a_f}{a_s} \quad (5.31)$$

$$\epsilon_q = \frac{\alpha_f}{\alpha_s} = \left[\frac{a_f}{a_s} \right]^{4/3} \quad (5.32)$$

$$\epsilon_q = (\epsilon_{\Delta T})^{4/3} \quad (5.33)$$

Note that $\epsilon_{\Delta T}$ and ϵ_q are independent of q and ΔT .

VI. RESULTS AND DISCUSSION

A. DROPWISE CONDENSATION

As mentioned in section IV B, a dropwise condensation condition was obtained initially. Data were taken during dropwise conditions at vacuum and atmospheric pressure with the instrumented tube, and this data is compared to filmwise data in Figure 4. The figure shows a marked contrast between filmwise and dropwise condensation data. The dropwise heat-transfer enhancement, compared to the filmwise data, varied from ~ 2 to 7 for vacuum conditions and ~ 9 to 10 for atmospheric conditions. Marto et al [Ref. 23] studied the use of organic coatings for the promotion of dropwise condensation of steam, and obtained an outside heat-transfer coefficient of $\sim 55 \text{ kW/m}^2\cdot\text{K}$ for a Fluoroacrylic coating compared to ~ 30 to $85 \text{ kW/m}^2\cdot\text{K}$ found under vacuum conditions in this study (both taken at $P \sim 11 \text{ kPa}$ and vapor velocity $\sim 2 \text{ m/s}$). The difficulty in accurately measuring the temperature drop across the condensate film for the dropwise condition is illustrated by the large amount of scatter in the dropwise data; this problem is caused by the lack of a stable film and the intermittent presence of drops near the instrumented tube wall thermocouples. The exact cause of the dropwise conditions was never determined. Clearly, some organic contamination either from the boiler feed water or from the gasket material was depositing on the test tube. Since this thesis was devoted to filmwise condensation, great efforts were made to clean the test tube and prepare it chemically so that the condensate would wet the surface.

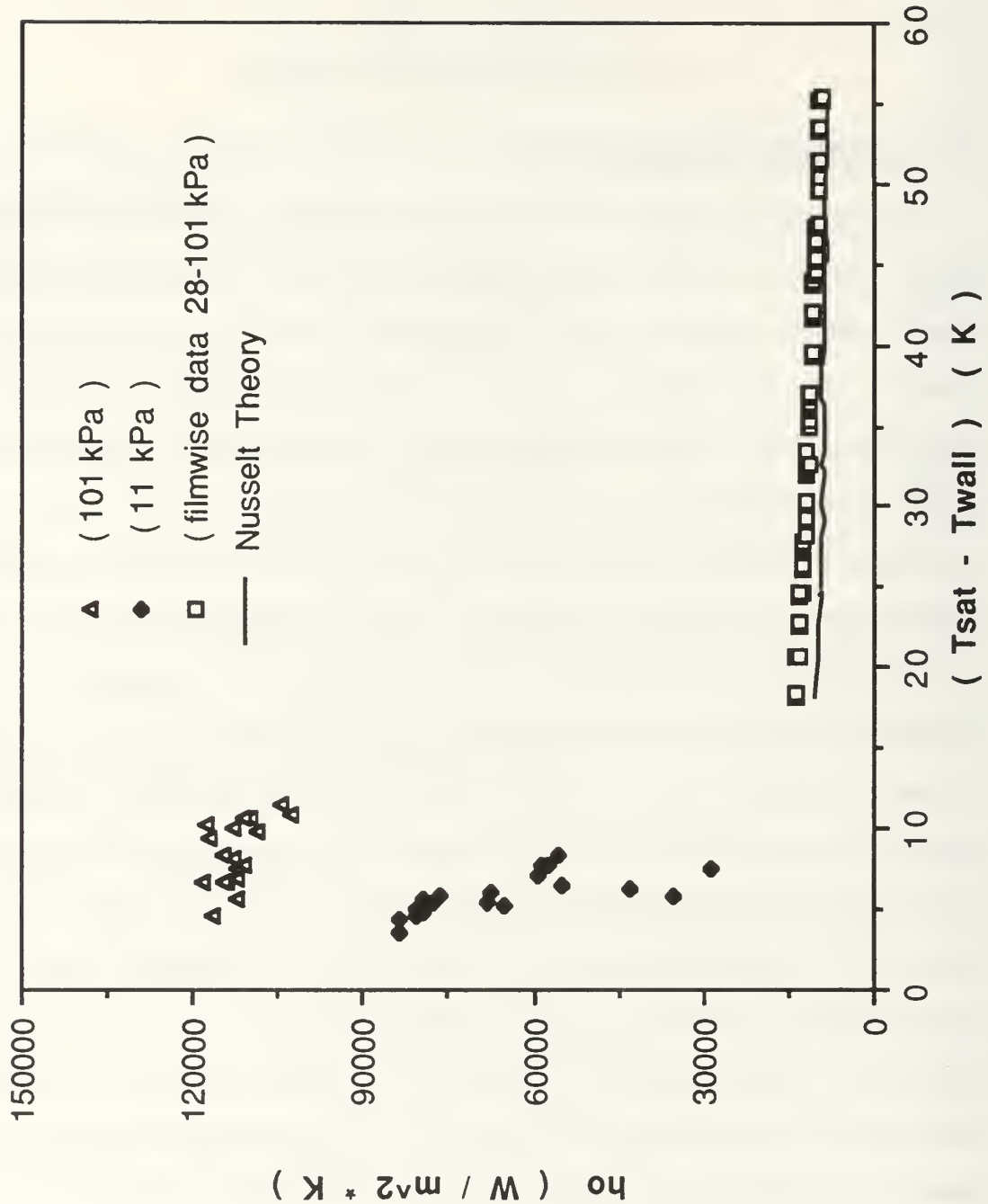


Figure 4. Comparison of Dropwise and Filmwise Condensation Data (Smooth Instrumented Tube, Heatex Insert)

B. INSTRUMENTED TUBE RESULTS

After resorting to the oxide coating procedure mentioned previously to mitigate the dropwise contamination problem, a series of runs were made with the instrumented tube fabricated by Poole [Ref. 6] with the Heatex insert installed. Using a mean wall temperature, the inside and outside heat-transfer coefficients could be evaluated directly.

Figure 5 shows filmwise condensation data taken at various pressures and vapor velocities. The four data sets for increasing vapor velocity (from 1 to 3.5 m/s) and decreasing vapor pressure (from 101 to 28 kPa) show the effect of vapor shear thinning the condensate film, giving an increase in the outside heat-transfer coefficient. This series of data runs was taken by maintaining the heater voltage at 175 volts and adjusting coolant flow through the auxiliary condenser to control pressure.

The four data sets in Figure 5 with constant vapor velocity (~ 1 m/s) and decreasing vapor pressure (from 101 to 28 kPa) show reduction of the outside heat-transfer coefficient with decreasing saturation temperature (due to decreasing saturation pressure). This effect is thought to be due to an increase in condensate viscosity at lower temperatures which tends to prevent the condensate from flowing around and draining from the tube as easily as at higher temperatures. The resulting condensate film thickening provides an additional resistance to heat transfer thereby lowering the outside heat-transfer coefficient. This series of data runs was taken by both adjusting heater power and auxiliary condenser coolant flow to obtain the same pressure conditions as above with a constant vapor velocity of ~ 1 m/s.

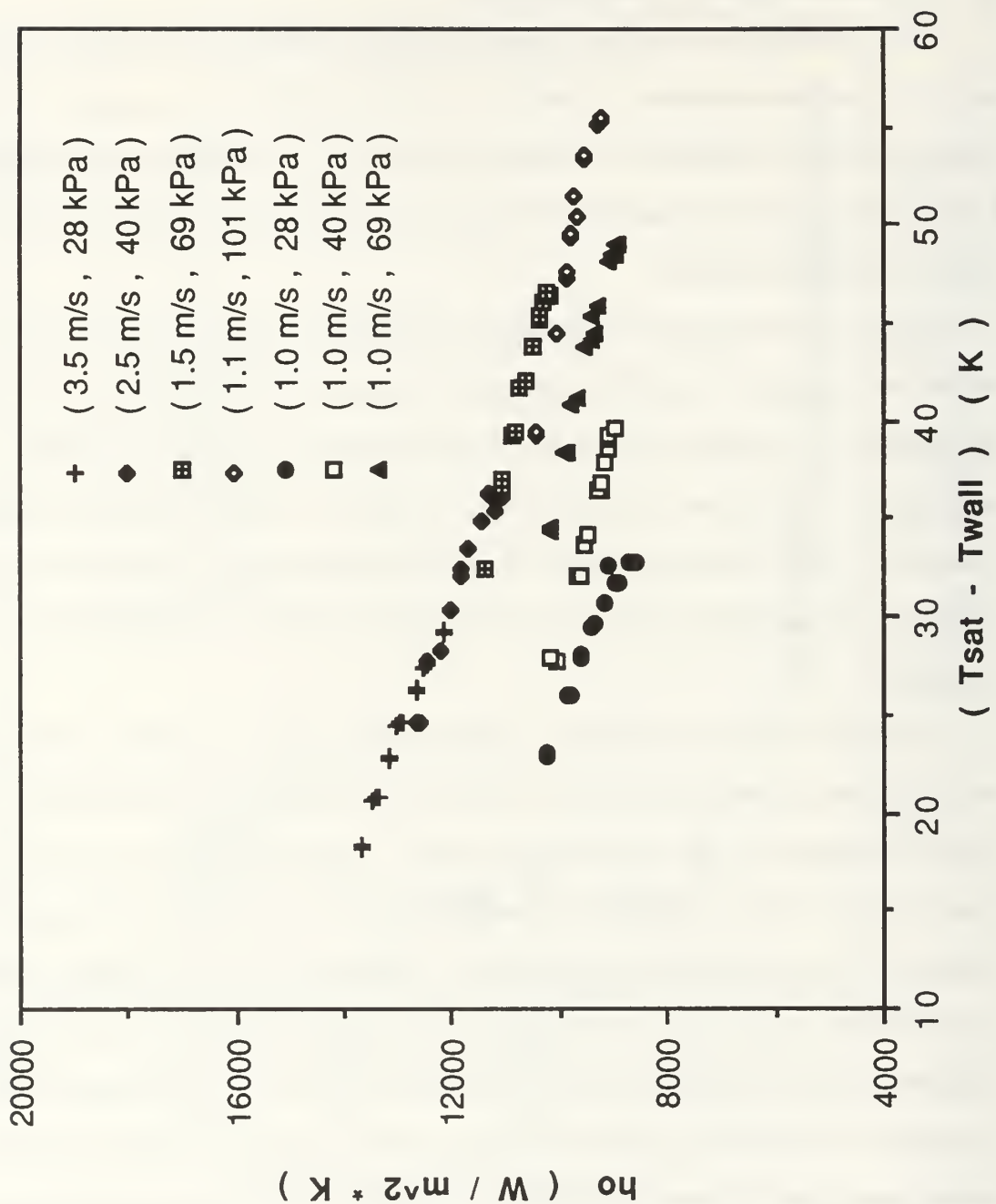


Figure 5. Effect of Pressure and Vapor Velocity on the Steam Heat-Transfer Coefficient (Smooth Instrumented Tube, Heatex Insert)

Figure 6 shows how increased pressure, with vapor velocity held constant, gives a larger increase in the outside heat-transfer coefficient over the predicted Nusselt value. This discrepancy is also thought to be caused by the viscosity effect since the Nusselt treatment seemingly takes into account the other possible causes. Also depicted more clearly is the dramatic enhancement due to vapor shear effects for increased vapor velocity at constant pressure.

As mentioned previously, the use of inserts allows more effective mixing of coolant and facilitates greater accuracy in the calculation of the outside heat-transfer coefficient. Figure 7 shows the outside heat-transfer coefficient determined from the use of the two inserts together with no insert. The results for the wire wrap and Heatex inserts are closely grouped, whereas the no insert data shows much greater scatter. This seems to indicate that the use of an effective insert does indeed enhance accuracy for the instrumented tube data.

The mean temperature difference across the condensate film for the no insert case has a significantly lower value than either of the insert cases; with the outside and tube wall conditions unchanged, this indicates a higher inside resistance for the no insert case. To illustrate this point a mid-range instrumented tube data point at the same conditions for each insert case is shown in Table 3 ($P_{\text{sat}} \sim 101$ kPa, $V_{\text{vapor}} \sim 1.1$ m/s, $V_{\text{coolant}} \sim 2.75$ m/s). It shows that both inserts have a comparable effect (slightly better with Heatex) and roughly provide a factor of two enhancement over the no insert case in the inside heat transfer coefficient. Due to the increased inside resistance for the no insert case, the heat flux shows a decrease of about 15%.

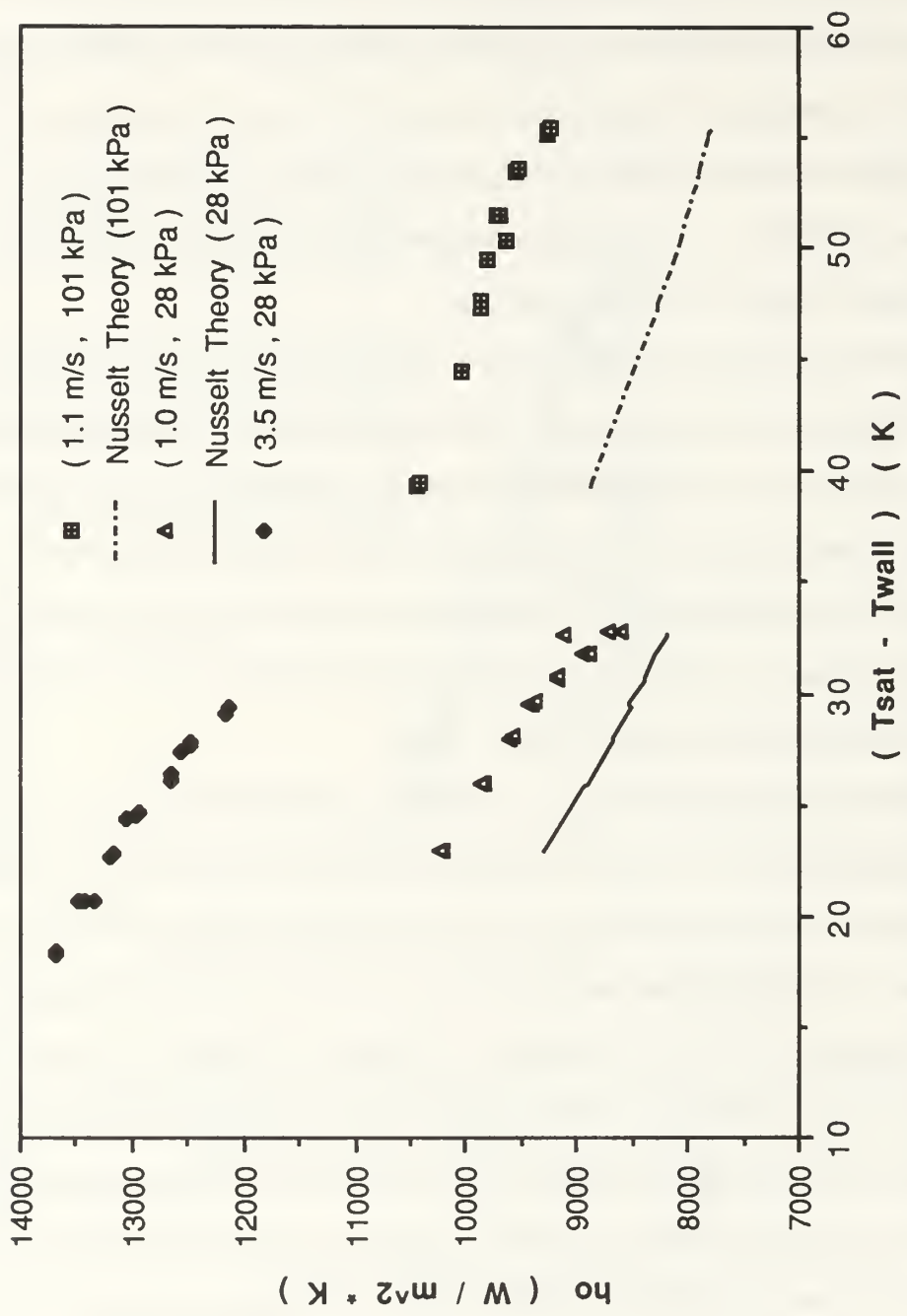


Figure 6. Comparison of Experimental Results with Nusselt Theory for Varying Pressures and Vapor Velocities (Smooth Instrumented tube, Heatex Insert)

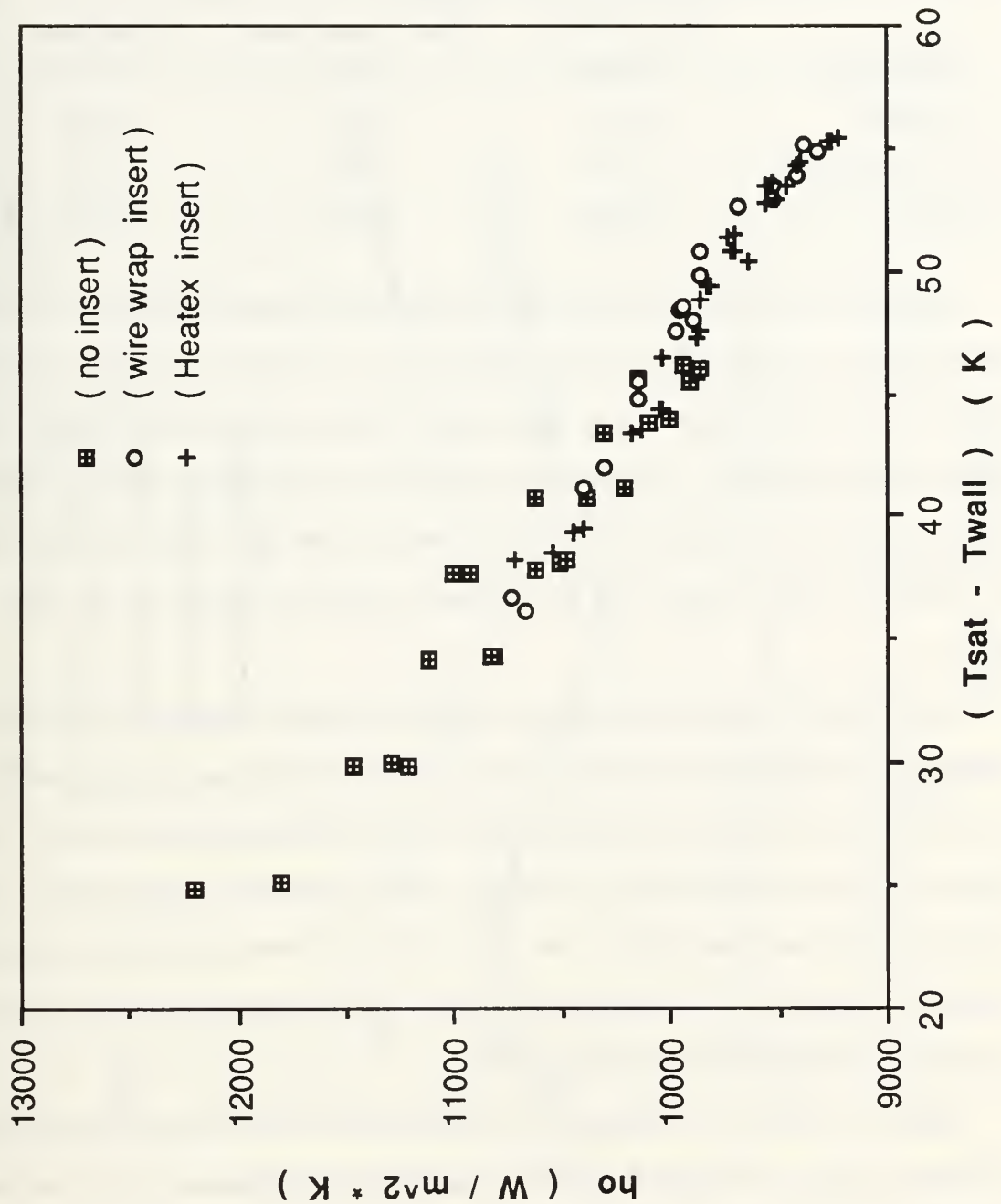


Figure 7. Comparison of Steam Heat-Transfer Coefficients at Atmospheric Conditions ($P_{sat} \sim 101$ kPa, $V_{vapor} \sim 1.1$ m/s) for Three Insert Conditions (Smooth Instrumented Tube)

**Table 3. PERFORMANCE COMPARISON OF TUBE INSERTS
AT ATMOSPHERIC CONDITIONS**

	Heatex Insert	Wire Wrap Insert	No Insert
h_i (kW/m ² ·K)	30.85	27.63	15.31
q (kW/m ²)	481.4	477.7	409.6
h_o (kW/m ² ·K)	9.86	9.82	10.75
ΔT (K)	48.82	48.65	38.10

Figure 8 shows the wall temperature profiles for the data points listed in Table 3 along with a vacuum data set ($P_{sat} \sim 28$ kPa, $V_{vapor} \sim 1$ m/s, $V_{coolant} \sim 2.75$ m/s) for comparison, where 0 degrees is at the top dead center position of the tube. The shape of the temperature profiles shows the effect of condensate film thickening toward the bottom of the tube. The higher resistance through a thicker condensate film results in a lower tube wall temperature toward the bottom of the tube as shown.

As expected, the wire wrap insert and Heatex insert temperature profiles at atmospheric pressure are very similar. The no insert profile has a shape similar to the wire wrap and Heatex profiles, but the mean wall temperature is about 11 K higher and shows the effect of the increased inside resistance to heat transfer. The vacuum run temperature profile shows the effect of a lower temperature gradient between the steam and coolant; the lower heat-transfer potential results in lower heat fluxes and a flatter temperature profile.

Figure 9 shows the comparison of the instrumented data with the predictions of Nusselt, Fujii, and Shekriladze and Gomelauri covered in section II B. The data depicted ranges from $P_{sat} = 28$ kPa and $V_{vapor} = 3.5$ m/s to $P_{sat} = 101$ kPa and $V_{vapor} = 1.1$ m/s. The data seems to follow the Shekriladze and Gomelauri prediction the closest, but is also very near the Fujii prediction.

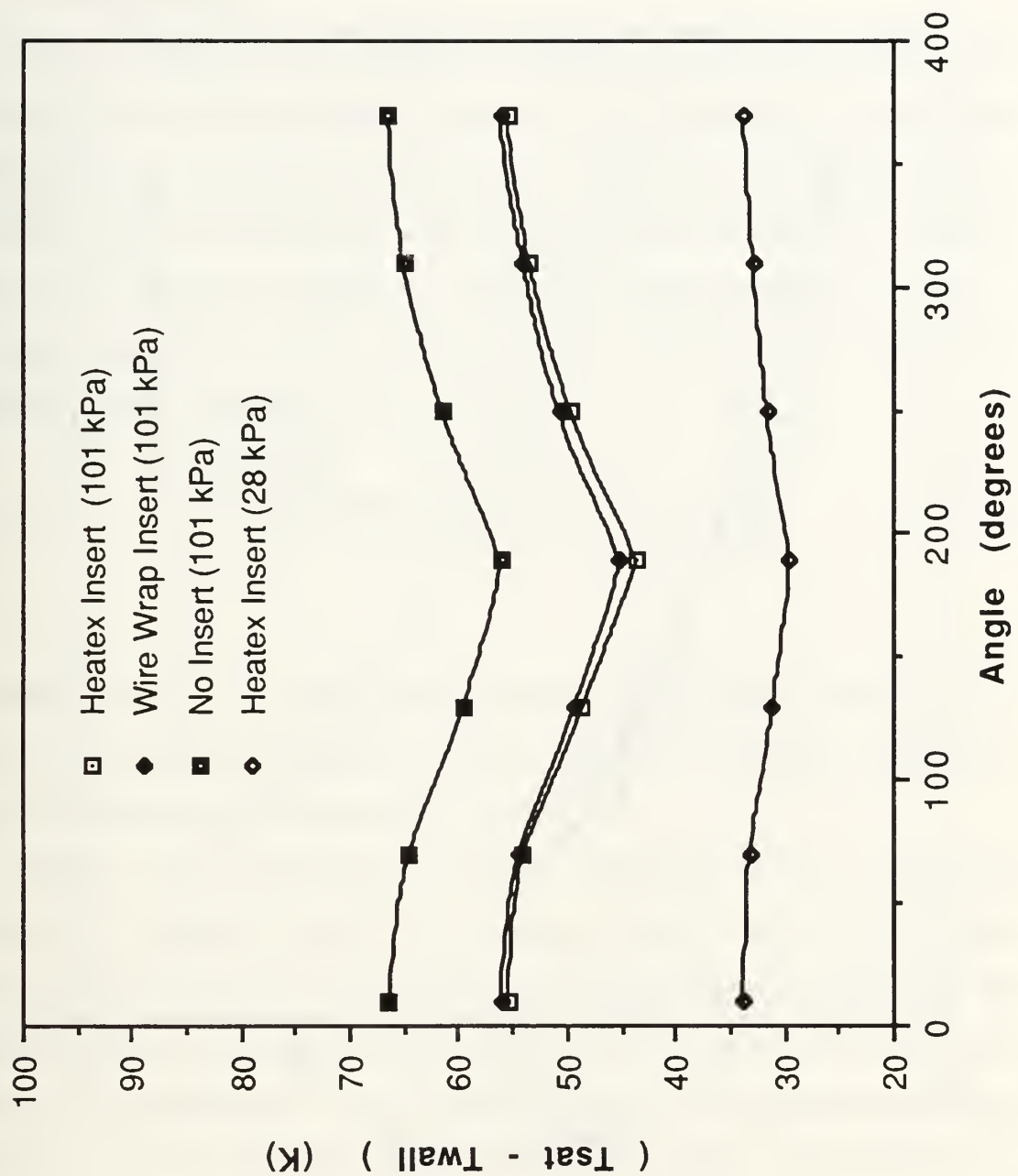


Figure 8. Horizontal Tube Wall Temperature Profiles (Smooth Instrumented Tube, $V_{vapor} \sim 1$ m/s)

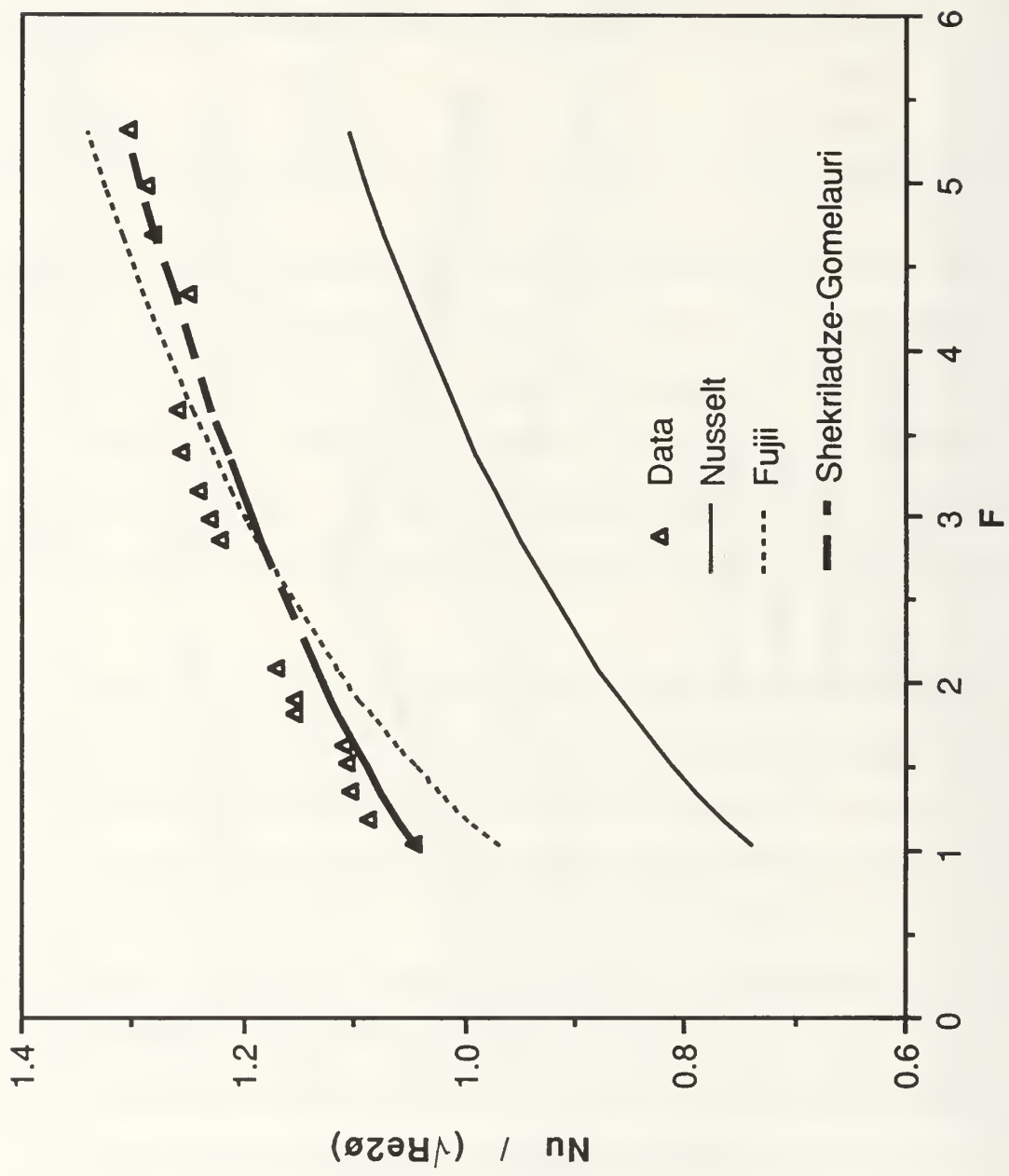


Figure 9. Comparison of Experimental Results with the Predictions of Nusselt, Fujii, and Shekrladze-Gomelauri.

C. INSIDE HEAT-TRANSFER CORRELATIONS FROM INSTRUMENTED TUBE RESULTS

The instrumented tube provides a method of determining an inside heat-transfer coefficient for each insert from direct wall temperature measurements. Wanniarachchi et al [Ref. 8], in a similar effort to resolve the differences between the Sieder-Tate correlation and his experimental results, developed a correlation based on the Sieder-Tate expression. Using an intercept form, with data taken on the same apparatus as used in this study, and a least-squares fitted leading coefficient, the correlation took the following form:

$$Nu = 0.064 Re^{0.8} Pr^{1/3} \left(\frac{\mu_c}{\mu_w} \right)^{0.14} + 26.4 \quad (6.1)$$

However, Rouk [Ref. 4], using an optimization technique, showed that the value of the intercept had little effect on the results, and it was the accurate determination of the Reynolds exponent that was more critical.

With a view to finding the appropriate Reynolds exponent and leading coefficient for equation (5.23), the data for no insert, wire wrap, and Heatex insert were plotted as $\ln Re$ versus $\ln (Nu/Pr^{1/3}(\mu_c/\mu_w)^{0.14})$ as explained in section V C. The plotted data are shown in Figures 10, 11 and 12 for no insert, wire wrap insert, and Heatex insert respectively. A line of best fit (typically with a regression coefficient of 0.99) was used to obtain the value of the intercept. Figure 13 shows the plot of all three cases on the same graph for comparison. Note that the insert data is closely grouped on the upper regions of the graph when compared to the no insert data. The increase in the Nusselt number again indicates more efficient inside heat transfer for the insert vice the no insert case. The Reynolds exponent, or slope,

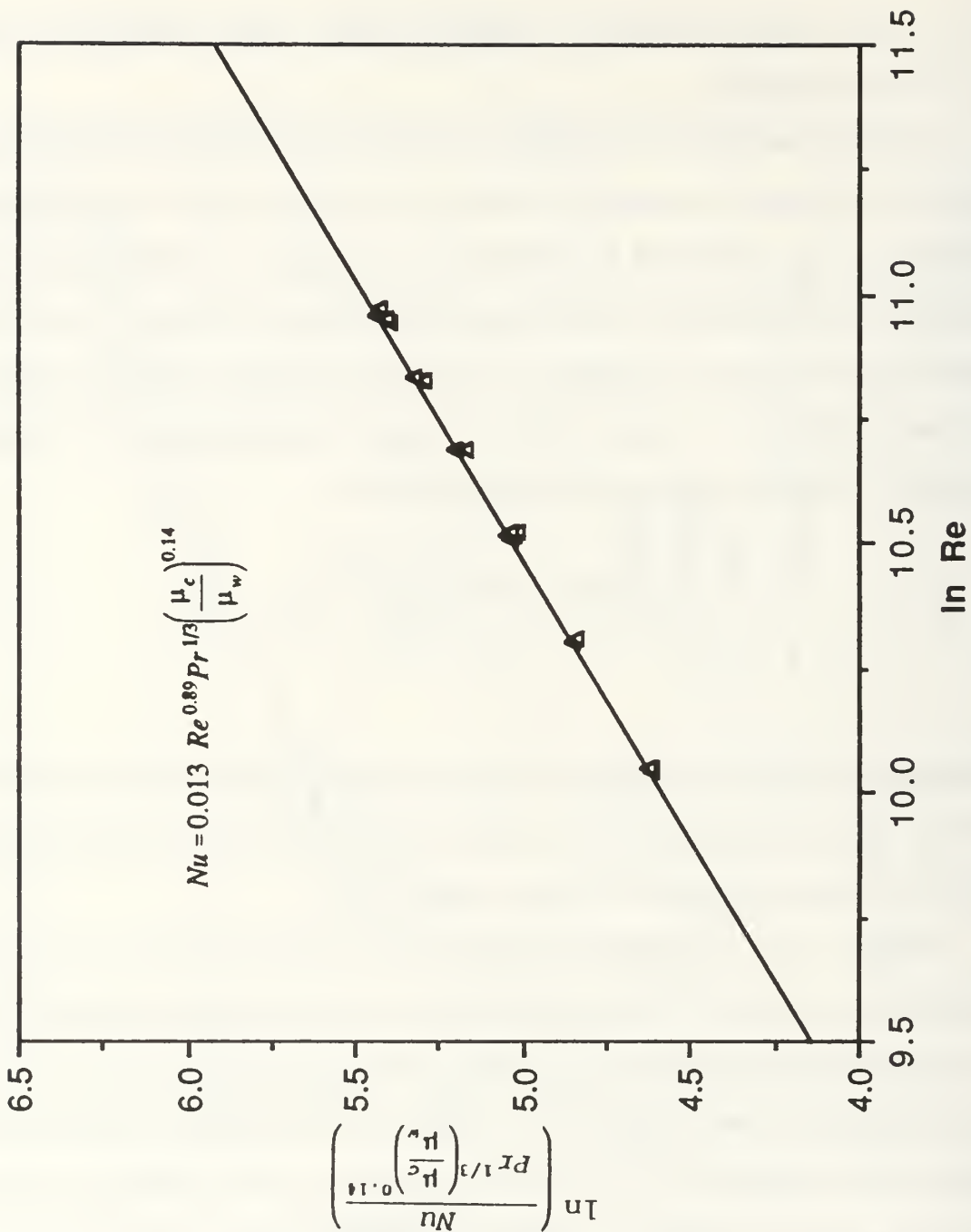


Figure 10. Log-Log Plot of Re versus $Nu/Pr^{1/3}(\mu_c/\mu_w)^{0.14}$ for No Insert (Smooth Instrumented Tube)

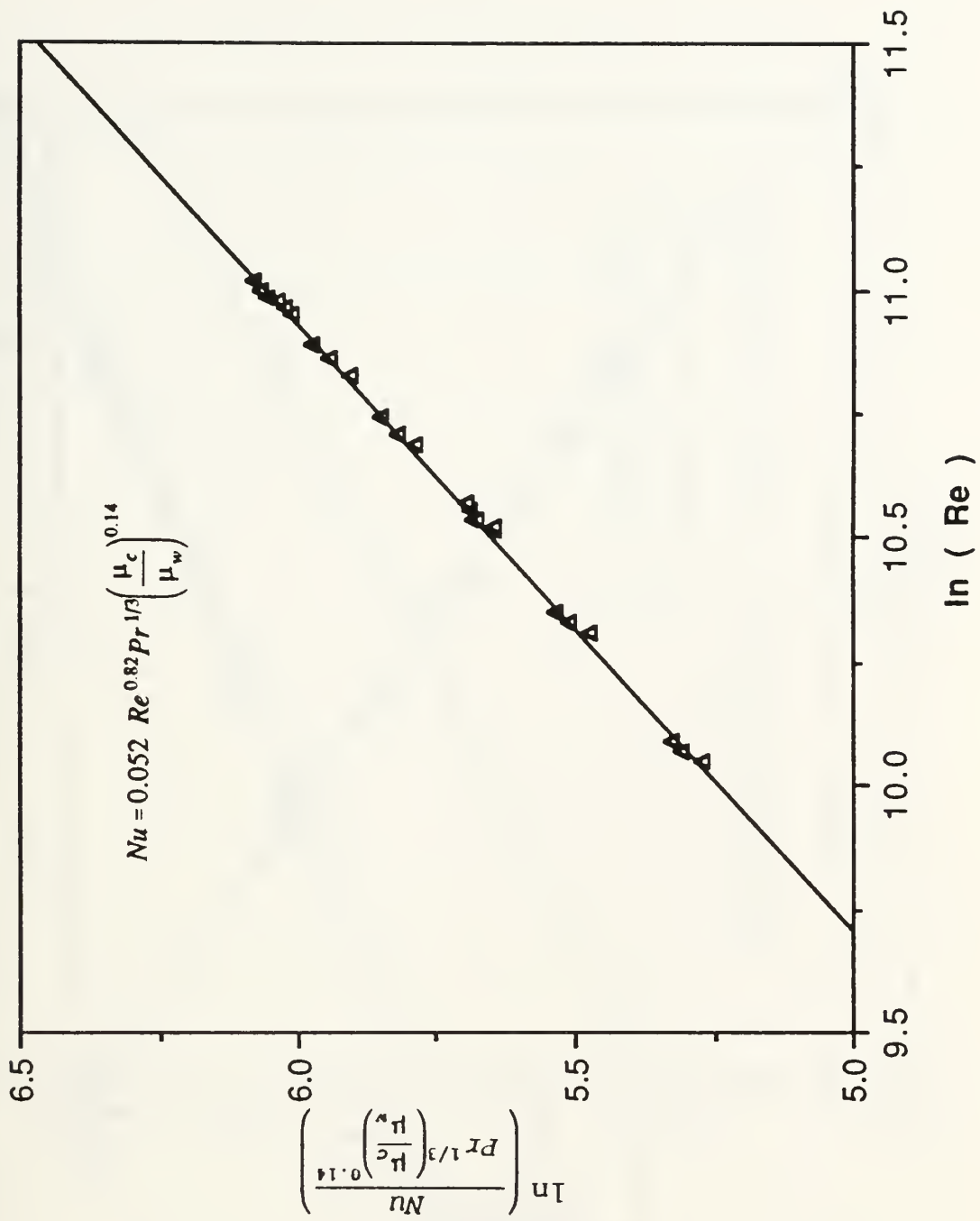


Figure 11. Log-Log Plot of Re versus $Nu/Pr^{1/3}(\mu_c/\mu_w)^{0.14}$ for Wire Wrap Insert (Smooth Instrumented Tube)

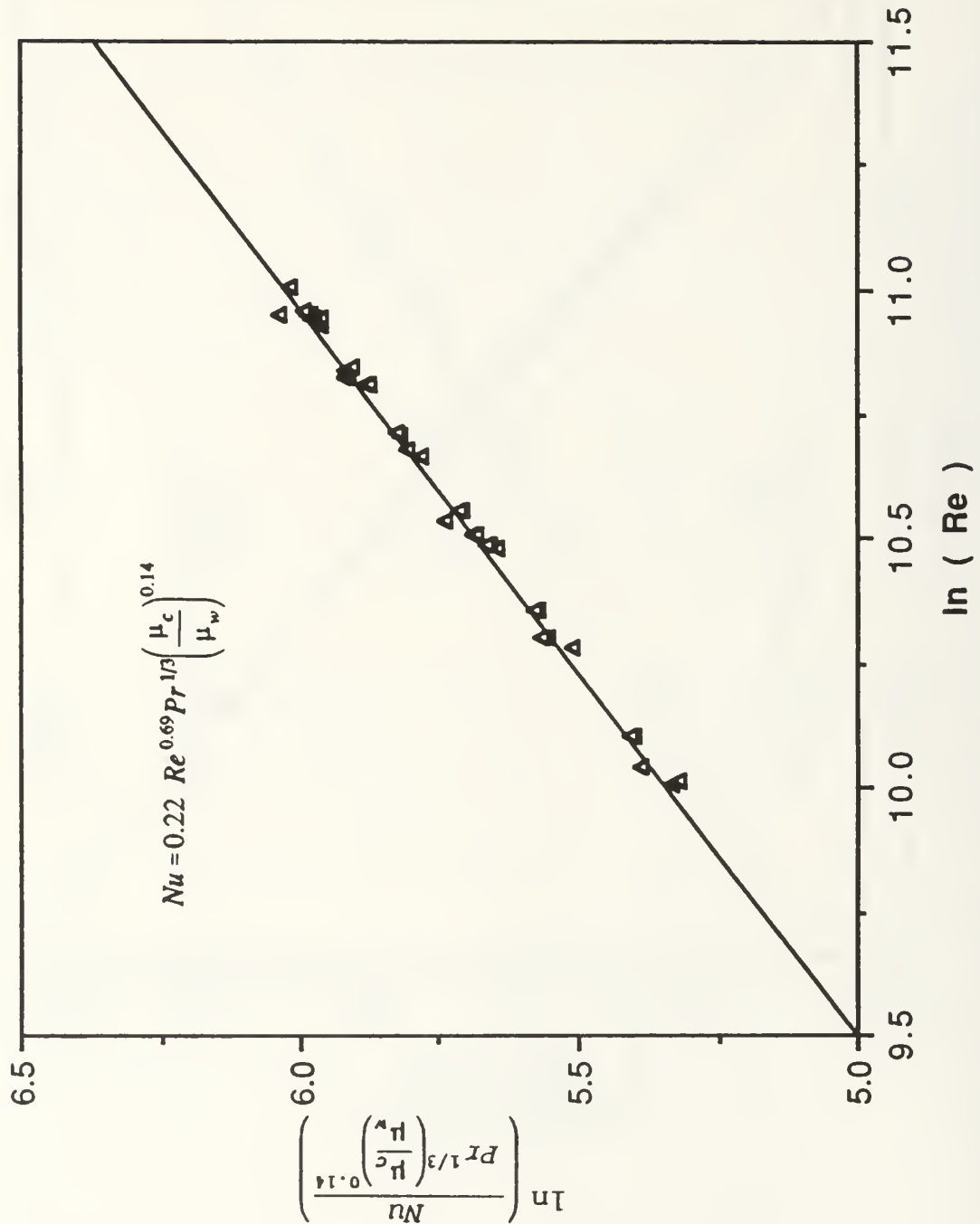


Figure 12. Log-Log Plot of Re versus $\text{Nu}/\text{Pr}^{1/3}(\mu_c/\mu_w)^{0.14}$ for Heatex Insert (Smooth Instrumented Tube)

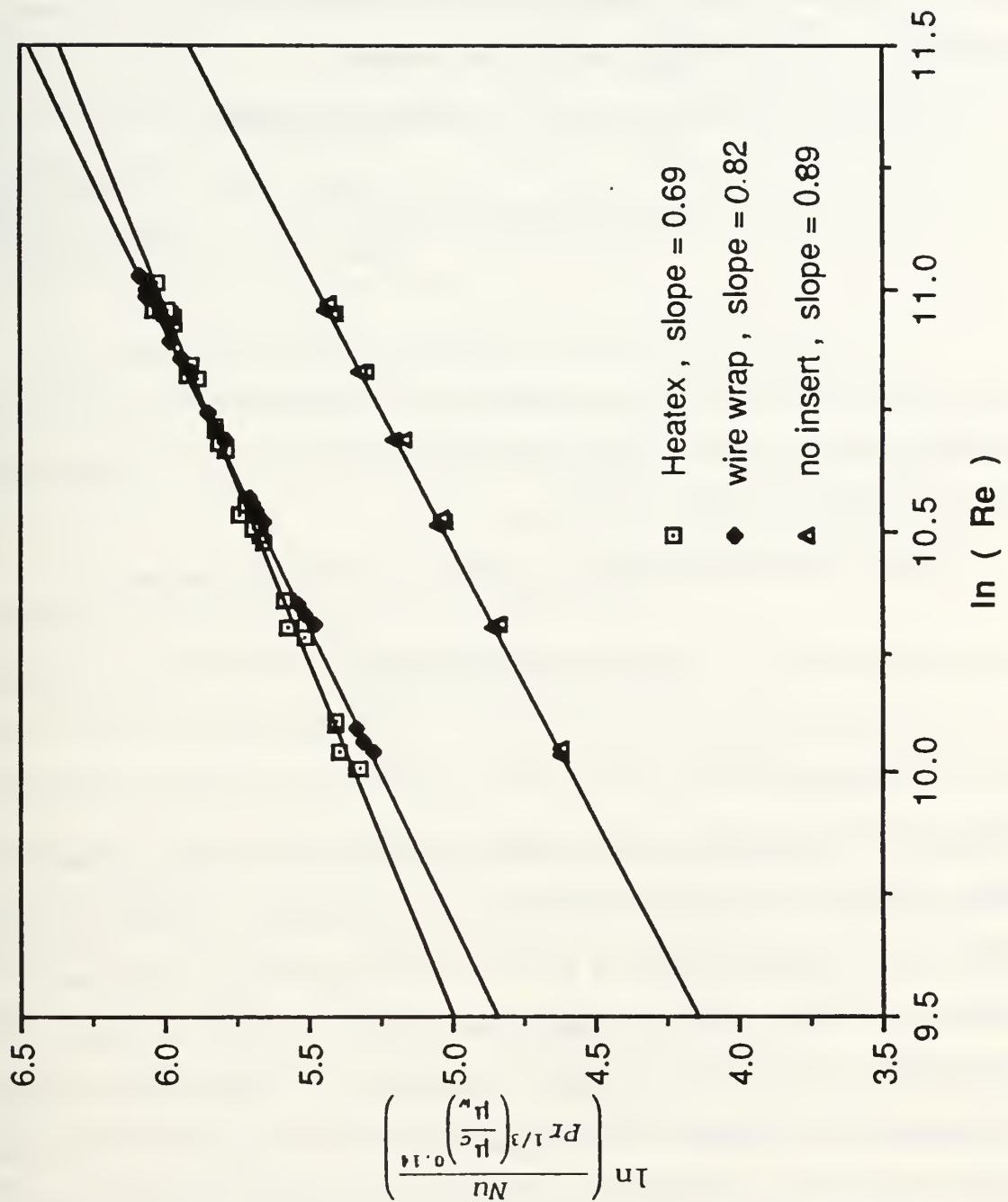


Figure 13. Combined Log-Log Plot of Re versus $Nu/Pr^{1/3}(\mu_c/\mu_w)^{0.14}$ for Three Insert Conditions (Smooth Instrumented Tube)

differs from the Sieder-Tate-type equation of 0.8 in all three cases. The following derived correlations apply specifically only to the medium tube, but should be applicable to any tube with the same inside diameter.

The no insert inside heat-transfer correlation had the form:

$$Nu = 0.013 \ Re^{0.89} Pr^{1/3} \left(\frac{\mu_c}{\mu_w} \right)^{0.14} \quad (6.2)$$

Equation (6.2) was used to reprocess some current smooth tube runs, with no insert, as well as those of Guttendorf [Ref. 3] and Van Petten [Ref. 2] to check their values for the smooth tube Nusselt coefficient α .

The wire wrap insert inside heat-transfer correlation had the form:

$$Nu = 0.052 \ Re^{0.82} Pr^{1/3} \left(\frac{\mu_c}{\mu_w} \right)^{0.14} \quad (6.3)$$

Equation (6.3) was used to reprocess previous data taken on the same apparatus by Guttendorf and Van Petten, who used the wire wrap insert for their finned and smooth tube experiments, with a view to checking their results with this new correlation. Table 4 shows a comparison between the new wire wrap insert correlation (eq. 6.3), and Wanniarachchi's correlation (eq. 6.1) both with and without the intercept value included. This comparison shows that equation 6.1 is actually more accurate without the intercept value included when compared to the results of the new wire wrap insert correlation.

Table 4. COMPARISON OF EQUATIONS (6.1) AND (6.3)
FOR $\text{Pr}^{1/3}(\mu_c/\mu_w)^{0.14} = 1.4$ (held constant for comparison)

Reynolds Number	20,000	30,000	40,000	50,000
Nusselt Number $\text{Nu} = 0.064 \text{ Re}^{0.8} \text{Pr}^{1/3}(\mu_c/\mu_w)^{0.14} + 26.4$	273.7	368.4	456.9	541.0
Nusselt Number $\text{Nu} = 0.064 \text{ Re}^{0.8} \text{Pr}^{1/3}(\mu_c/\mu_w)^{0.14}$	247.3	342.0	430.5	514.6
Nusselt Number $\text{Nu} = 0.052 \text{ Re}^{0.82} \text{Pr}^{1/3}(\mu_c/\mu_w)^{0.14}$	244.9	341.5	432.3	519.1

The Heatex insert inside heat-transfer correlation had the form:

$$\text{Nu} = 0.22 \text{ Re}^{0.69} \text{Pr}^{1/3} \left(\frac{\mu_c}{\mu_w} \right)^{0.14} \quad (6.4)$$

Equation (6.4) was used to reprocess all Heatex data.

Memory [Ref. 12] conducted condensation experiments on a different apparatus with a smooth instrumented tube. He also determined the Reynolds number exponent for no insert, wire wrap insert (made locally and somewhat different from the one used in this study), and Heatex insert. The exponents he obtained are reported in Table 5. The Heatex insert exponent of 0.68 compares very favorably with the value of 0.69 found in this study. The wire wrap exponent of 0.73 was well below the value of 0.82, most likely due to differences in the insert. The no insert case gave a value of 0.85 and compared well to the value of 0.89 found in this study. The difference in the no insert exponent is most likely due to the difference in the tube entrance region; Memory used a long run of straight pipe for the tube entrance, whereas the present work had a sharp bend just prior to the condenser tube.

Rouk [Ref. 4] used the instrumented smooth tube data of Georgiadis [Ref. 5] to find the appropriate value of the Reynolds number exponent for the no insert

and wire wrap cases. His results compare quite well with this study and are also given in Table 5.

ANL (Argonne National Laboratory) [Ref. 21] conducted an assessment of heat-transfer correlations for turbulent pipe flow with water to determine the best correlation(s) on which to base their design of Ocean Thermal Energy Conversion (OTEC) heat exchangers. ANL used two shell-and-tube heat exchangers, with no inserts, for analysis and reported the following:

1. The Dittus-Boelter (eq 2.7) and Sieder-Tate (eq 2.9) correlations underpredicted the data by 5% to 15% and were considered too conservative for design.
2. Overall, the "best" correlations were found to be Petukhov-Popov (eq 6.5) and Sleicher-Rouse (eq 6.6), both of which showed excellent agreement ($\pm 5\%$) with the experimental data (at $Pr=6.0$ and $Pr=11.6$).

$$Nu = \frac{(\epsilon/8)Re Pr}{K_1 + K_2(\epsilon/8)^{1/2}(Pr^{2/3}-1)} \quad (6.5)$$

(valid for $0.5 < Pr < 2000$ and $10^4 < Re < 5 \times 10^6$)

where:

$$\begin{aligned} \epsilon &= (1.82 \log_{10} Re - 1.64)^{-2} \\ K_1 &= 1 + 3.4\epsilon \\ K_2 &= 11.7 + 1.8 Pr^{-1/3} \end{aligned}$$

$$Nu = 5 + 0.015 Re_f^a Pr_w^b \quad (6.6)$$

(valid for $0.1 < Pr < 10^5$ and $10^4 < Re < 10^6$)

where:

$$\begin{aligned} a &= 0.88 - 0.24/(4+Pr_w) \\ b &= 1/3 + 0.5e^{-0.6Pr_w} \end{aligned}$$

3. The most accurate correlations (i.e. Petukhov-Popov and Sleicher-Rouse) seem to yield effective Reynolds exponents in the neighborhood of 0.85 (uncertainty range: $m = 0.82$ to 0.88).
4. The potential sources of uncertainty in the Wilson procedure included waterside flow maldistribution, entrance effects, experimental error in U_o , and the uncertainty in the Reynolds number exponent. Of these, they concluded that the uncertainty in the Reynolds number exponent was, by far, the most significant. In fact, the results of the Wilson procedure were found to be highly sensitive to the value of the Reynolds number exponent.

Table 5. COMPARISON OF REYNOLDS NUMBER EXPONENTS FOR SIEDER-TATE-TYPE CORRELATIONS

	Experimental Data	Rouk	Memory	ANL
No Insert	0.89	0.90	0.85	0.85
Wire Wrap	0.82	0.78	0.73	---
Heatex	0.69	---	0.68	---

D. ANALYSIS OF SMOOTH TUBE RESULTS

When using the modified Wilson plot technique to reprocess data files, the solution option can be specified to use either the stored value of the Sieder-Tate coefficient (for direct computation of h_o) or let the coefficient value "float", which allows the program to calculate its own value of the coefficient. In order to determine which method was most accurate, the instrumented data files were reprocessed using each method and then compared with the values of the heat-transfer coefficient which were obtained by direct measurement of the tube wall temperature. A high, medium, and low coolant flow rate was chosen from each run to facilitate the comparison. The results were tabulated and are shown in Appendix D; it can be seen that the fixed coefficient method yielded the more accurate results at least 75% of the time. The mean error of the fixed method was $\pm 2.0\%$, and that of the floating method was $\pm 5.4\%$. The error for the lowest coolant flow rate (Re

<20,000) was noticeably higher than for higher coolant flow rates for both methods. The choice of using the fixed coefficient method represents a departure from the practice of previous researchers on this apparatus who exclusively used the floating coefficient method.

Prior to the instrumented tube runs reported in Figure 5 (from which the new correlations were empirically derived) a series of data runs were made using a plain smooth uninstrumented tube (S02) of the same dimensions using the Heatex insert. The plain smooth tube data was then reprocessed using the new correlation for the Heatex insert and the results are plotted in Figure 14. These data sets were taken at the same conditions as the instrumented data of Figure 5 except for the set at the highest vapor velocity of 6.2 m/s vice 3.5 m/s for the instrumented tube. Similar effects of vapor shear and vapor pressure, as mentioned previously for Figure 5, are clearly seen, and again illustrate the vapor shear effect on the outside heat-transfer coefficient.

With the exception of the two data runs at high vapor velocity, the data from Figures 5 and 14 are shown together in Figure 15. The close agreement of the reprocessed plain smooth tube data with the instrumented smooth tube data allows a high degree of confidence in the accuracy of the new correlations and the choice of the fixed coefficient method.

To provide a baseline from which to evaluate finned tube performance it was necessary to obtain the smooth tube Nusselt coefficient, α , for the specific conditions under which the comparison was to be made. The condition chosen was atmospheric pressure (101 kPa) and a vapor velocity of ~1 m/s.

For 8 complete sets of data the average value of α , using the fixed method, was found to be 0.876. The average value for each data set was found by taking the

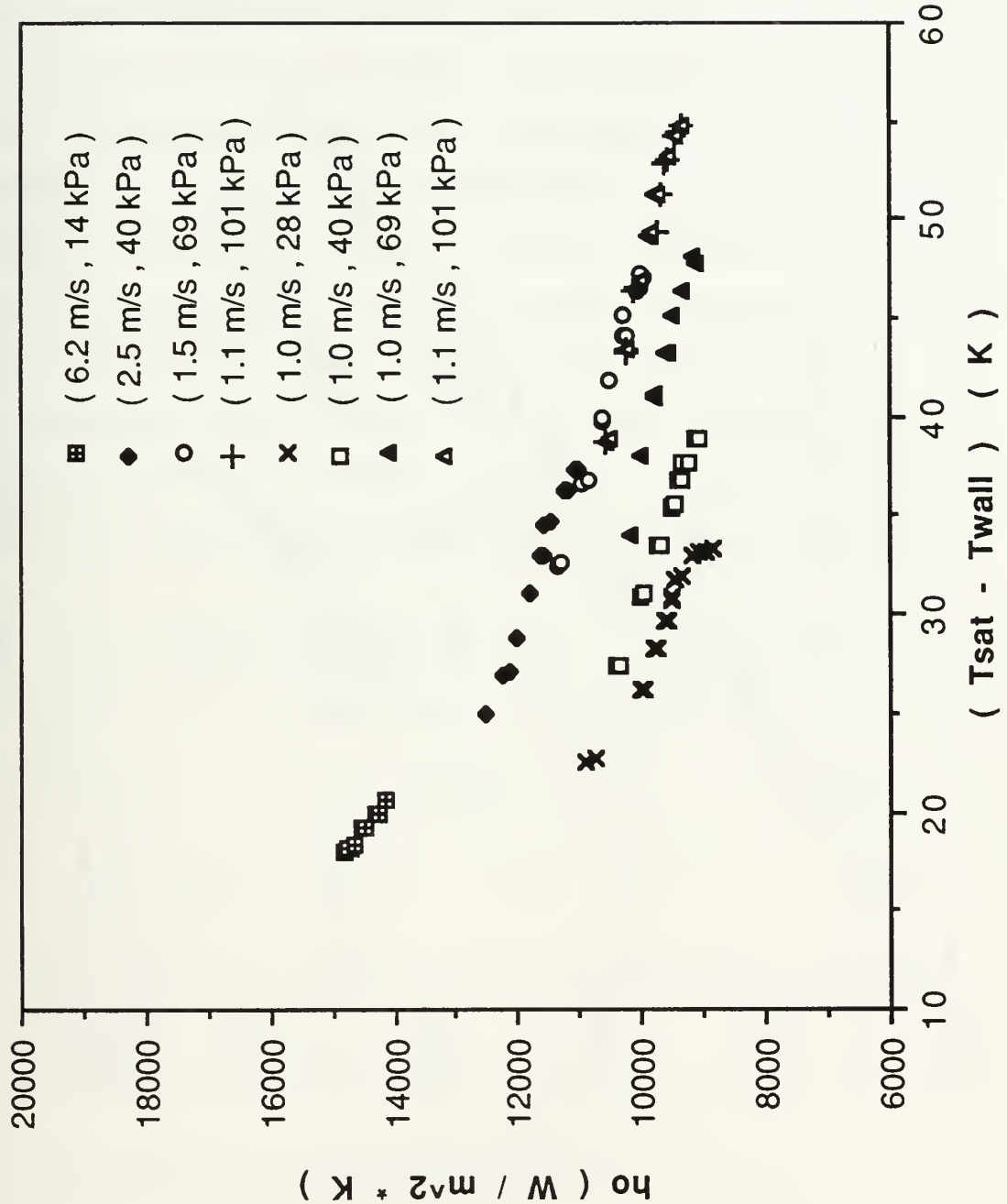


Figure 14. Effect of Pressure and Vapor Velocity on the Steam Heat-Transfer Coefficient (Non-instrumented Smooth Tube, Heatex Insert)

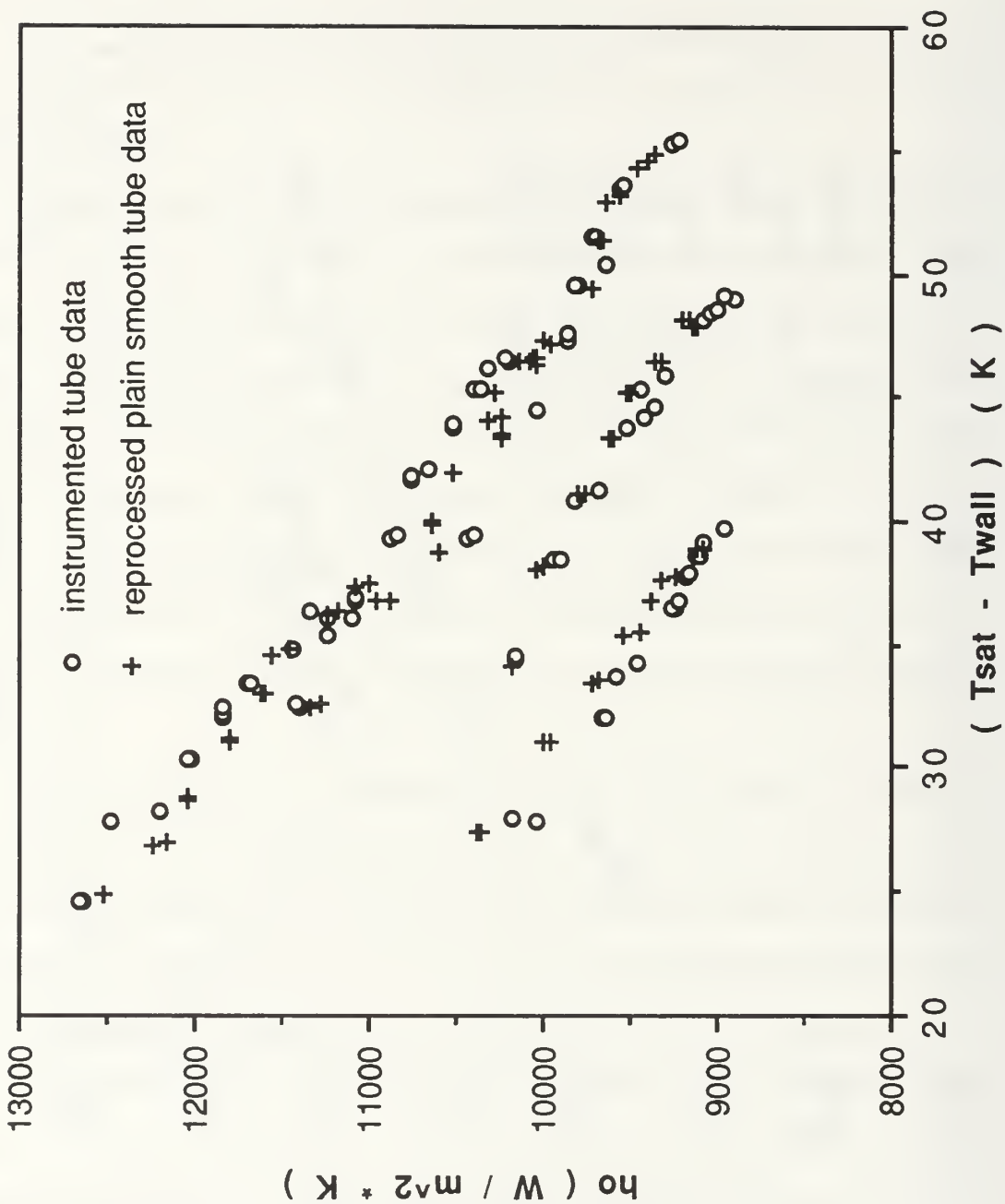


Figure 15. Comparison of Instrumented Smooth Tube Results with Non-Instrumented Smooth Tube Data After Reprocessing with the New Heatex Insert Inside Heat-Transfer Correlation.

measured value of h_o for each data point, dividing it by the Nusselt theory prediction of h_o , and then multiplying by 0.728 (the Nusselt coefficient); the average of all the data points in the set was then taken. Interestingly the Wilson plot floating coefficient method gave a value of 0.835, somewhat lower than the average value. Originally it was thought that this discrepancy might be due to "outlier" data points (high or low coolant velocity) in each set. However, removing the highest or lowest coolant flow rates within a set had little or no effect on the Wilson plot result. The reason for the discrepancy is still not known and merits future study.

The value of α was calculated for several other flow conditions; these are shown in Table 6. The trend of the readings, like that of Figure 6, shows that vapor velocity has a much greater effect than pressure on the value of α , as expected.

Table 6. SMOOTH TUBE α SUMMARY; EFFECT OF PRESSURE AND VAPOR VELOCITY

File Name	P(kPa)	Vapor Velocity (m/s)	α
FIMAVSH1	28	3.5	1.015
FIMAVSH2	41	2.5	.985
FIMAVSH3	68	1.5	.930
FIMAVSH4	101	1.1	.866
FIMAVSH7	69	1.0	.836
FIMAVSH6	41	1.0	.818
FIMAVSH5	28	1.0	.786

E. ANALYSIS OF FINNED TUBE RESULTS

With an accurate value of α , and the newly determined inside heat-transfer correlations, the medium family finned tube data of Van Petten [Ref. 2] was evaluated. Figure 16 shows the data Van Petten reported in his thesis; it also shows his data after being reprocessed using the new wire wrap insert correlation with

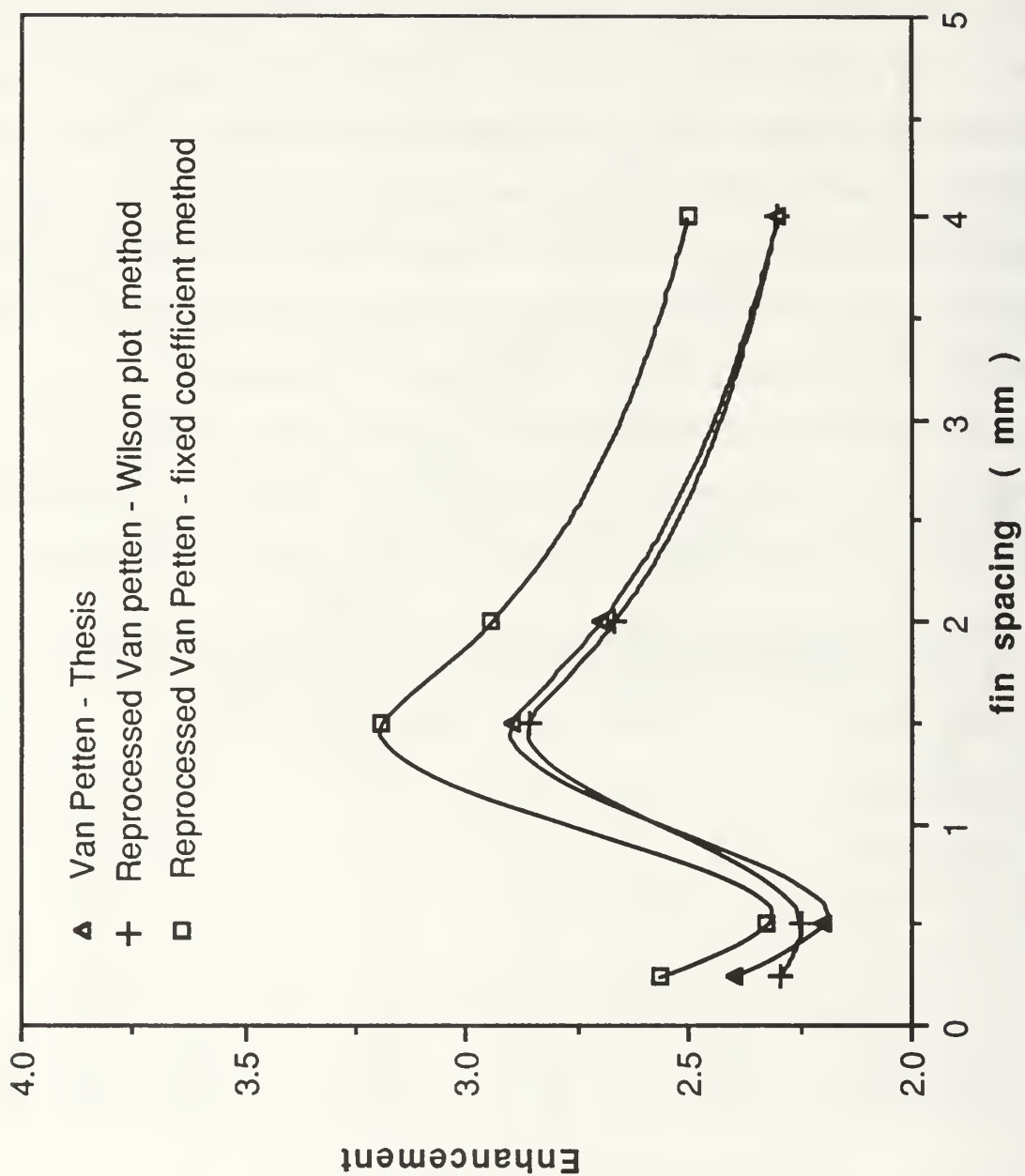


Figure 16. Comparison of the Steam Heat-Transfer Enhancement Data of Van Petten, for the Medium Finned Tube Family, Using the Modified Wilson Plot and New Wire Wrap Insert Inside Correlation.

both the fixed coefficient and Wilson plot floating coefficient methods. Since Van Petten used the Wilson plot method, it is not surprising that the original thesis data and new Wilson plot floating coefficient data are comparable since the Reynolds exponent only varied from 0.8 to 0.82. The fixed coefficient method enhancement is substantially higher than the Wilson plot results.

Since the assertion is that the fixed coefficient method is more accurate than the Wilson plot method, then the conclusion must be that the enhancement for this set of finned tubes is actually higher than previously reported.

During this study, limited medium finned tube experiments were conducted for purposes of comparison. Figure 17 shows the comparison between this data and the newly reprocessed data of Van Petten (using the fixed coefficient method) and shows reasonable agreement. To more clearly illustrate this point, the data taken on the 2.0 mm fin spacing tube has been given in more detail in Figure 18. Excellent agreement is seen between the experimental results of this study and that of Van Petten using the known inside heat-transfer correlation with the fixed coefficient method. Again, as shown in Figure 16, the Wilson plot prediction is significantly below the fixed coefficient results.

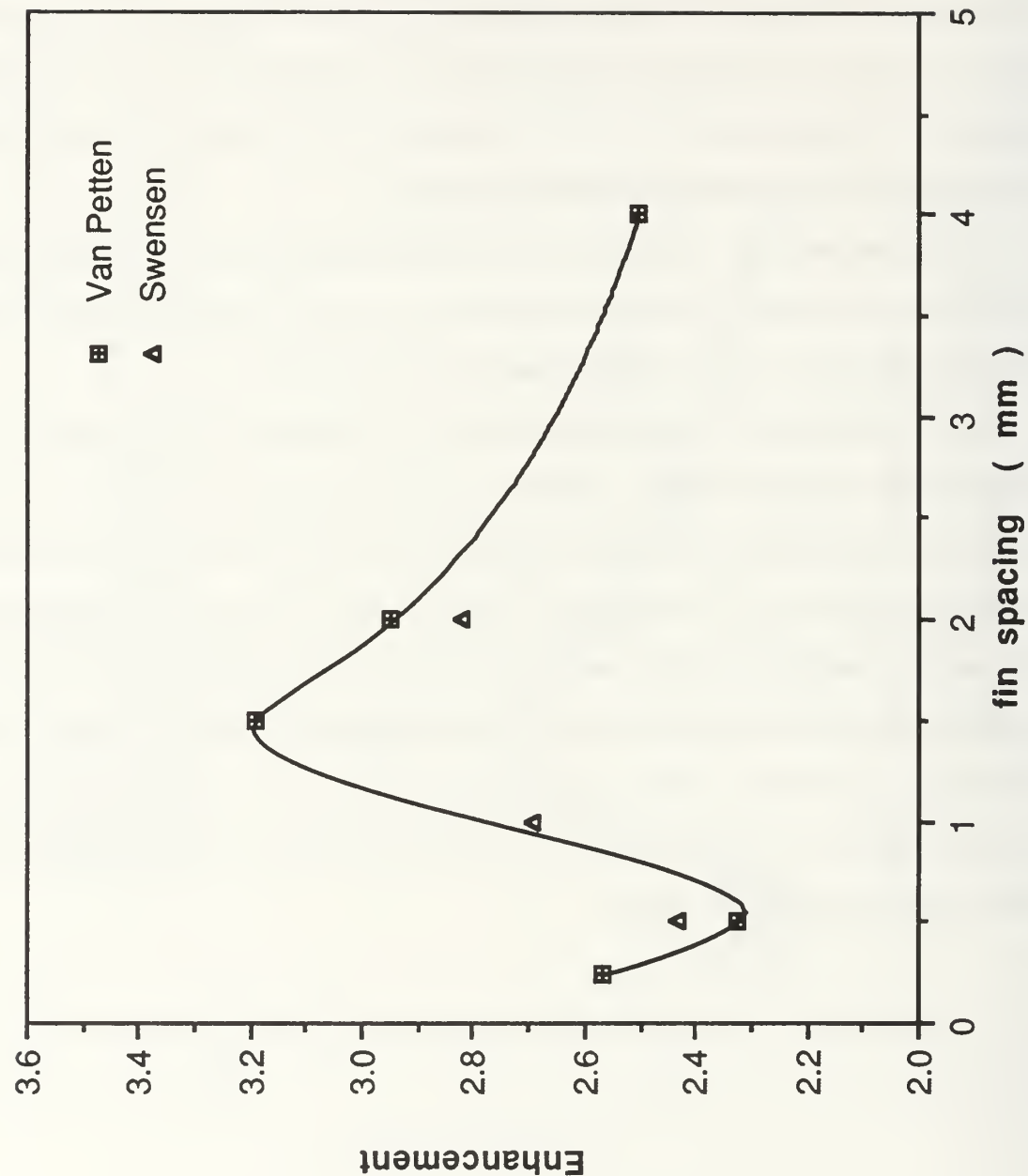


Figure 17. Comparison of the Steam Heat-Transfer Enhancement Data of Van Petten and Swensen for the Medium Finned Tube Family.

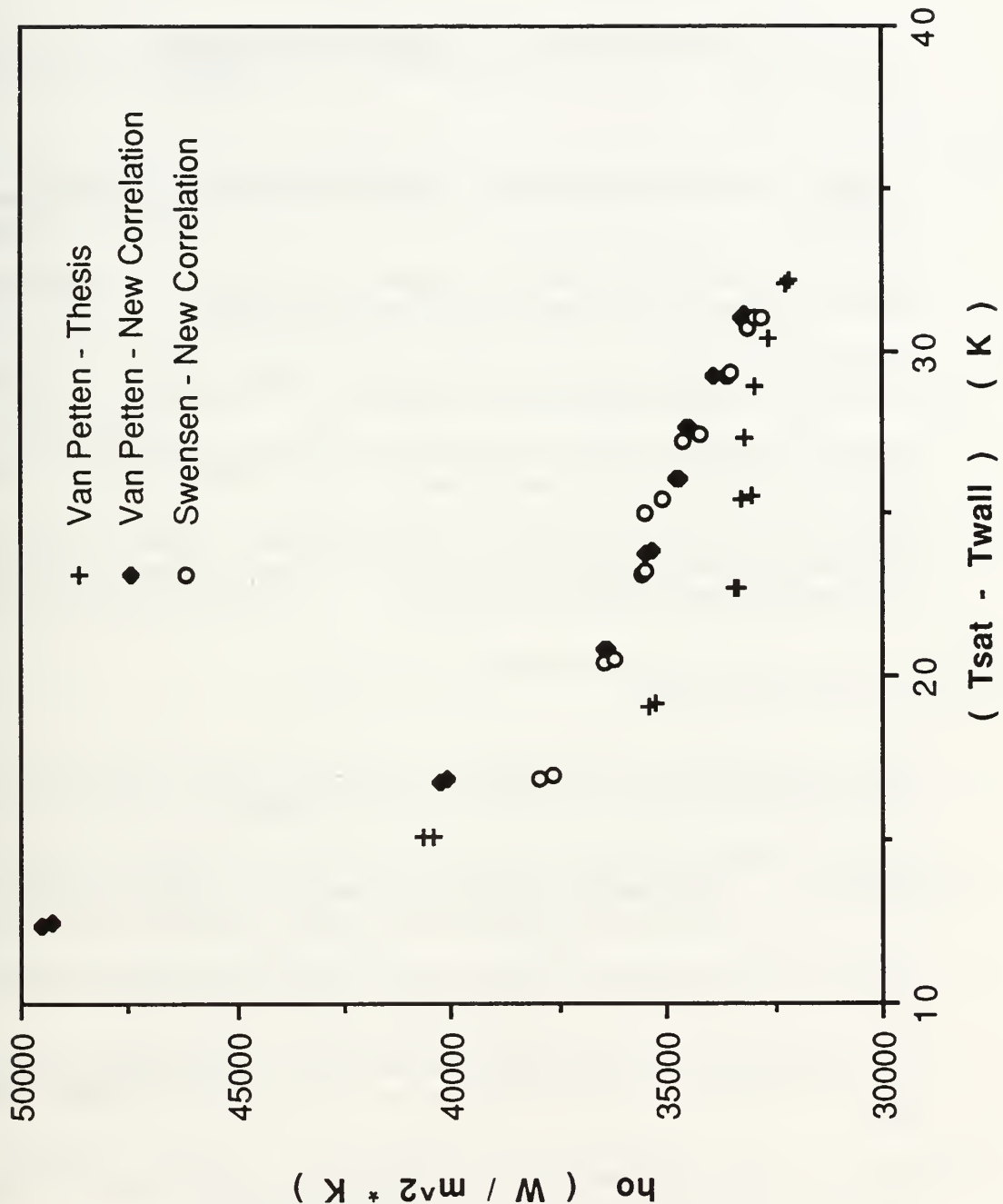


Figure 18. Comparison of the Steam Heat Transfer Data of Van Petten and Swensen for the 2.0 mm Fin Spacing Medium Tube.

VII. CONCLUSIONS AND RECOMMENDATIONS

A. CONCLUSIONS

1. The inside heat-transfer correlation is highly sensitive to the Reynolds number exponent.
2. Each insert condition must be analyzed separately to determine the appropriate "form" of the inside heat-transfer correlation.
3. Calculations based on a known inside heat-transfer correlation are more accurate than modified Wilson plot results.
4. Armed with accurate inside heat-transfer correlations, previous data may be reprocessed to give more accurate results.
5. The source of contamination in the test apparatus, which has caused a dropwise condensation problem for a number of years, is most probably due to a contaminated distilled water source.

B. RECOMMENDATIONS

1. Reprocess all previous medium and large diameter finned tube data using the fixed coefficient method to obtain more accurate results.
2. Continue with construction of smooth instrumented tubes of different diameters (i.e. small, medium, and large) to confirm the medium tube results and develop correlations specifically for the small and large diameter tubes.
3. Construct one representative instrumented finned tube to test the validity of applying instrumented smooth tube results to finned tube data.
4. Test representative water samples that have been collected from both the distiller and boiler to confirm the presence of impurities and validate their origin.
5. Replace current distiller with a deionized pure water source (either commercial purchase of water or new distilling apparatus).

APPENDIX A. PHYSICAL AND THERMODYNAMIC PROPERTIES OF WATER

The physical and thermodynamic properties of water were based on the following equations:

Heat Capacity (J/kg·K):

$$C_p = 4.211 - T * [2.268 \times 10^{-3} - T * (4.424 \times 10^{-5} + 2.714 \times 10^{-7} * T)] \quad (\text{A.1})$$

where: T = temperature (celsius)

Dynamic viscosity, (kg/m·s):

$$\mu = (2.4 \times 10^{-5}) * 10^{[247.8/(T+133.15)]} \quad (\text{A.2})$$

Thermal conductivity (W/m·K):

$$k = -0.9225 + x * (2.8395 - x * (1.8007 - x * (0.5258 - 0.0734 * x))) \quad (\text{A.3})$$

where: x = (T+273.15)/273.15

Density (kg/m³):

$$\rho = 999.5295 + T * (0.0127 - T * (5.4825 \times 10^{-3} - T * 1.2341 \times 10^{-5})) \quad (\text{A.4})$$

Latent heat of vaporization (J/kg):

$$h_{fg} = 2477200 - 2450 * (T - 10) \quad (\text{A.5})$$

Fluid Enthalpy (J/kg):

$$h_f = T * (4.2038 - T * (5.8813 \times 10^{-4} - T * 4.5516 \times 10^{-6})) \quad (\text{A.6})$$

Saturation pressure (Pa):

$$P_{sat} = 22120000 * Pr \quad (\text{A.7})$$

where:

$$Pr = e^{Br}$$

$$Br = \frac{\text{SUM} / [T_r (1 + 4.1671 (1-T_r) + 20.9751 (1-T_r)^2) - (1-T_r)]}{((1.0 \times 10^9)(1-T_r)^2 + 6)}$$

$$\text{SUM} = (-7.6912)(1-T_r) - 26.0802 (1-T_r)^2 - 168.1707 (1-T_r)^3 + 64.2329 (1-T_r)^4 - 118.9646 (1-T_r)^5$$

$$T_r = (T + 273.15) / 647.3$$

APPENDIX B. SYSTEM CALIBRATIONS AND CORRECTIONS

B.1 Thermocouple and Quartz Thermometer Calibration

Several different thermocouples and the quartz crystal thermometer (HP 2804A, Ser. No. 2244AD1192) were calibrated against a platinum resistance probe in a mixed isothermal ethylene glycol bath with a Rosemont Galvanometer model 920A commutating bridge (Ser. no. 013494) from 23 to 26 September, 1991.

NOMENCLATURE

<i>T1</i>	<i>Quartz Thermometer Measuring Probe T1 (Ser. No. 2120A-00707, with dial setting 481)</i>
<i>T2</i>	<i>Quartz Thermometer Measuring Probe T2 (Ser. No. 2120A-60459 with dial setting 510)</i>
<i>T1-T2</i>	<i>The T1-T2 reading on the quartz thermometer</i>
<i>T-55</i>	<i>Large diameter metal sheath thermocouple (diameter = 0.040")</i>
<i>T-56</i>	<i>Small diameter metal sheath thermocouple (diameter = 0.020")</i>
<i>T-57</i>	<i>Old Thermocouple (taken from rig during disassembly set to HP 3497A internal zero); (Type: Omega, TT-T-30, Lot# HCP093HC0306)</i>
<i>T-58</i>	<i>New 1 Thermocouple (set to HP 3497A internal zero); (Type: Omega, TT-T-30 SLE, Lot# OCP1453PTCC01473P)</i>
<i>T-59</i>	<i>New 2 Thermocouple (referenced to ice bath zero)</i>
<i>T-60</i>	<i>10 Junction Thermopile #1 (referenced to ice bath zero)</i>
<i>T-61</i>	<i>10 Junction Thermopile #2 (referenced to ice bath zero)</i>
<i>T-62</i>	<i>10 Junction Thermopile #3 (referenced to ice bath zero)</i>

The calibration was performed by taking the bath temperature up from 290 K to 393 K by 5 K increments then back down to check for hysteresis; no hysteresis was

observed. The data was fitted to a fifth-order polynomial (regression coefficient = 1.000 for each polynomial fit) in each case with the following results:

$$\begin{aligned} T55 &= 273.15 + (2.5943e-2)V - (7.2671e-7)V^2 \\ &\quad + (3.2941e-11)V^3 - (9.7119e-16)V^4 \\ &\quad + (9.7121e-20)V^5 \end{aligned} \quad (\text{B.1})$$

$$\begin{aligned} T56 &= 273.15 + (2.5878e-2)V - (5.9853e-7)V^2 \\ &\quad - (3.1242e-11)V^3 + (1.3275e-14)V^4 \\ &\quad - (1.0188e-18)V^5 \end{aligned} \quad (\text{B.2})$$

$$\begin{aligned} T57 &= 273.15 + (2.5923e-2)V - (7.3933e-7)V^2 \\ &\quad + (2.8625e-11)V^3 + (1.9717e-15)V^4 \\ &\quad - (2.2486e-19)V^5 \end{aligned} \quad (\text{B.3})$$

$$\begin{aligned} T58 &= 273.15 + (2.5931e-2)V - (7.5323e-7)V^2 \\ &\quad + (4.0567e-11)V^3 - (1.2791e-15)V^4 \\ &\quad + (6.4402e-20)V^5 \end{aligned} \quad (\text{B.4})$$

$$\begin{aligned} T59 &= 273.15 + (2.5471e-2)V - (3.7621e-7)V^2 \\ &\quad - (1.0105e-10)V^3 + (2.3928e-14)V^4 \\ &\quad - (1.6440e-10)V^5 \end{aligned} \quad (\text{B.5})$$

$$\begin{aligned} T60 &= 273.17 + (2.5571e-2)V - (1.9980e-7)V^2 \\ &\quad - (1.6385e-10)V^3 + (2.6164e-14)V^4 \\ &\quad - (1.0295e-18)V^5 \end{aligned} \quad (\text{B.6})$$

$$\begin{aligned} T61 &= 273.15 + (2.6119e-2)V - (9.0449e-7)V^2 \\ &\quad + (1.1214e-10)V^3 - (1.5623e-14)V^4 \\ &\quad + (1.0646e-18)V^5 \end{aligned} \quad (\text{B.7})$$

$$T_{62} = 273.15 + (2.5996e-2)V - (7.4405e-7)V^2 \\ + (2.4733e-11)V^3 + (3.3236e-15)V^4 \\ - (3.7460e-19)V^5 \quad (B.8)$$

For T_{55} , T_{56} , T_{57} , T_{59} ; V= Voltage in microvolts (eg. 0.010 volts = 10,000 microvolts).

For T_{60} , T_{61} , T_{62} ; V= Voltage in microvolts/10 (eg. 100,000 microvolts ÷ 10 = 10,000).

The HP 2804A Quartz Crystal Thermometer was also calibrated on 26 September, 1991 with the results summarized in Table B.1.

Table B.1. QUARTZ THERMOMETER CALIBRATION DATA

Reference Temperature (deg C)	T_1 (deg C)	Error (deg C)	T_2 (deg C)	Error (dec C)
17.979	18.003	0.024	18.001	0.022
18.977	18.997	0.020	18.996	0.021
19.984	20.001	0.017	20.002	0.018
20.980	21.007	0.027	21.008	0.028
22.936	22.959	0.023	22.961	0.025
25.014	25.032	0.018	25.037	0.023
30.140	30.153	0.013	30.164	0.024
34.977	34.983	0.006	34.998	0.021

The mean error for the Quartz Thermometer as shown in the Table B.1 is $\sim +0.02$ deg C. However, it is well noted that T_1-T_2 , the critical measurement, indicates an apparent error of less than $+0.005$ deg C when the temperature reading is near or below 25 deg C; T_1 and T_2 tracking well together lowers the error estimate.

B.2 Flow Meter Calibration

The flow meter calibration for coolant flow through the single horizontal tube was completed on Oct 28, 1991 using a stop watch, portable tank, and a Toledo model 31-0851 IV, Se. No. 1326 scale with 1/10 pound graduations. The following relation was obtained via linear regression:

$$m = 6.7409F + 13.027$$

B.9

where:

$$\begin{aligned} m &= \text{mass flow rate (grams per second)} \\ F &= \text{flow meter reading (eg. } 10\% \Rightarrow 10) \end{aligned}$$

The applicable range of the calibration was 10% to 95%. The water temperature on the day of the calibration was 17.5°C (290.6 K) and water density was 998.5 kg/m³. The data is shown in Figure B.1

B.3 Mass Flow Rate Correction

The inlet water temperature from the cooling water sump varies anywhere from 15°C to 25°C depending on environmental conditions. To account for these temperature variations the following function was used to calculate a correction factor for viscosity variation with temperature [Ref. 5].

$$Cf = 1.0365 - (1.9644E - 3) Tin + (5.2500e - 6) Tin^2 \quad (B.10)$$

where:

$$\begin{aligned} Cf &= \text{mass flow rate correction factor} \\ Tin &= \text{inlet temperature (celsius)} \end{aligned}$$

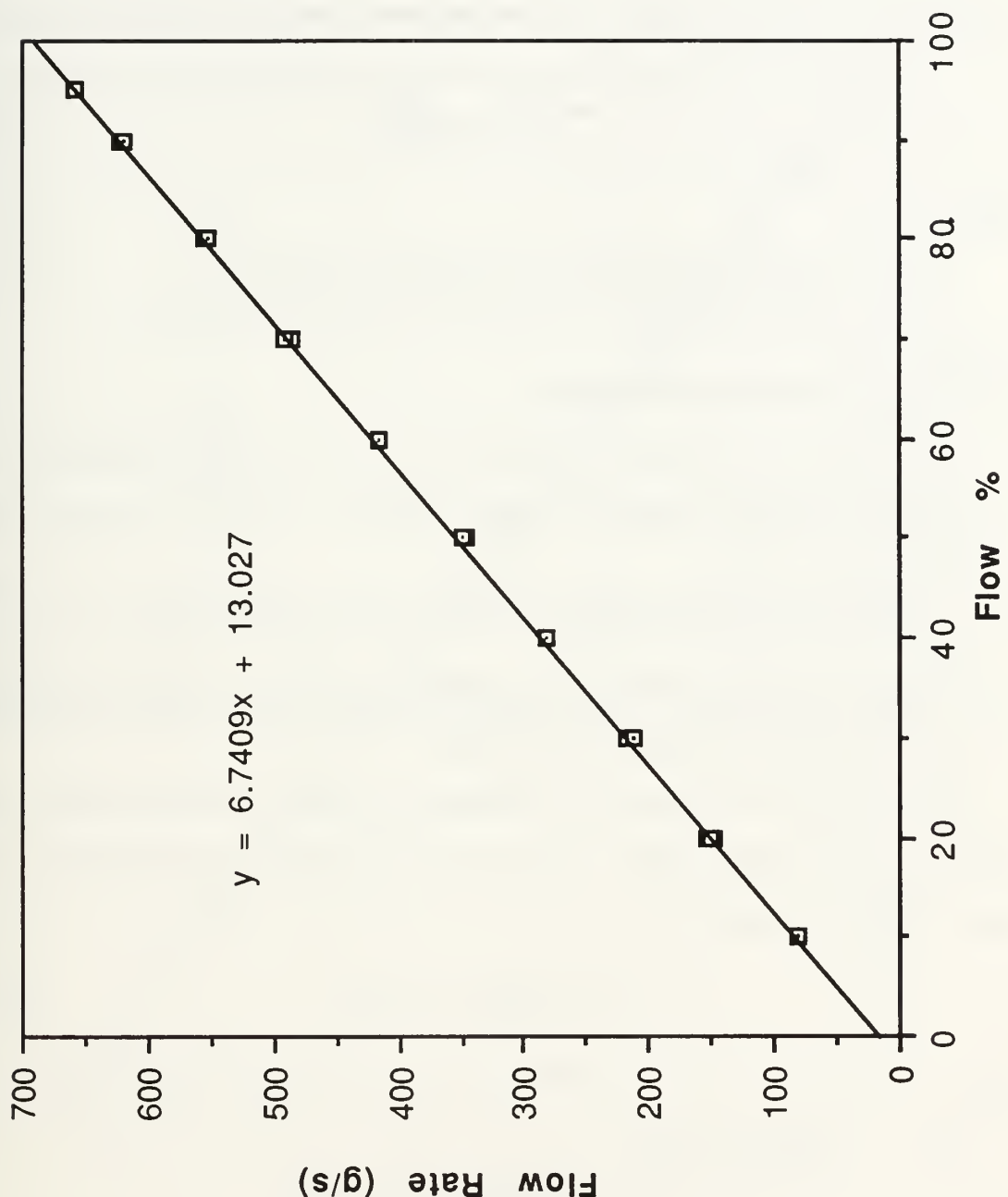


Figure B.1 Horizontal Tube Coolant Flowmeter Calibration Chart

The value of C_f for the flow meter calibration ($T_{in}=17.5^{\circ}\text{C}$) was 1.0037. Therefore, the actual mass flow rate was calculated using the following equation:

$$m_{act} = m_{calc} \frac{C_f}{1.0037} \quad (\text{B.11})$$

where:

m_{act} = corrected mass flow rate (grams per second)
 m_{calc} = computed mass flow rate (eq. B.9) (grams per second)

B.4 Pressure Transducer Calibration

Three methods of pressure measurement were available on the apparatus:

1. Direct pressure reading off the Heise solid front - CM-104119 pressure gauge, (range 0-15 psia).
2. Converted voltage readings from the Setra, model 204, Ser. no. 63982 pressure transducer (range 0-14.7 psia; 0-5 volts; 5V~0 psia).
3. Steam saturation temperature measurement with the apparatus producing steam at steady state. The steam saturation temperature/pressure relation was utilized via standard steam tables.

The pressure transducer was calibrated versus the vapor temperature probe reading on 12 December 1991. Equation B.12 gives the desired relationship. The data is shown in Figure B.2.

$$P = -2.9360V + 14.7827 \quad (\text{B.12})$$

where:

P = pressure (psia)
 V = pressure transducer voltage reading (volts)

B.5 FRICTION TEMPERATURE CORRECTION

As coolant flows through the tube there is a bulk temperature rise due to frictional heating, which is highly dependent on fluid velocity. Although small, this

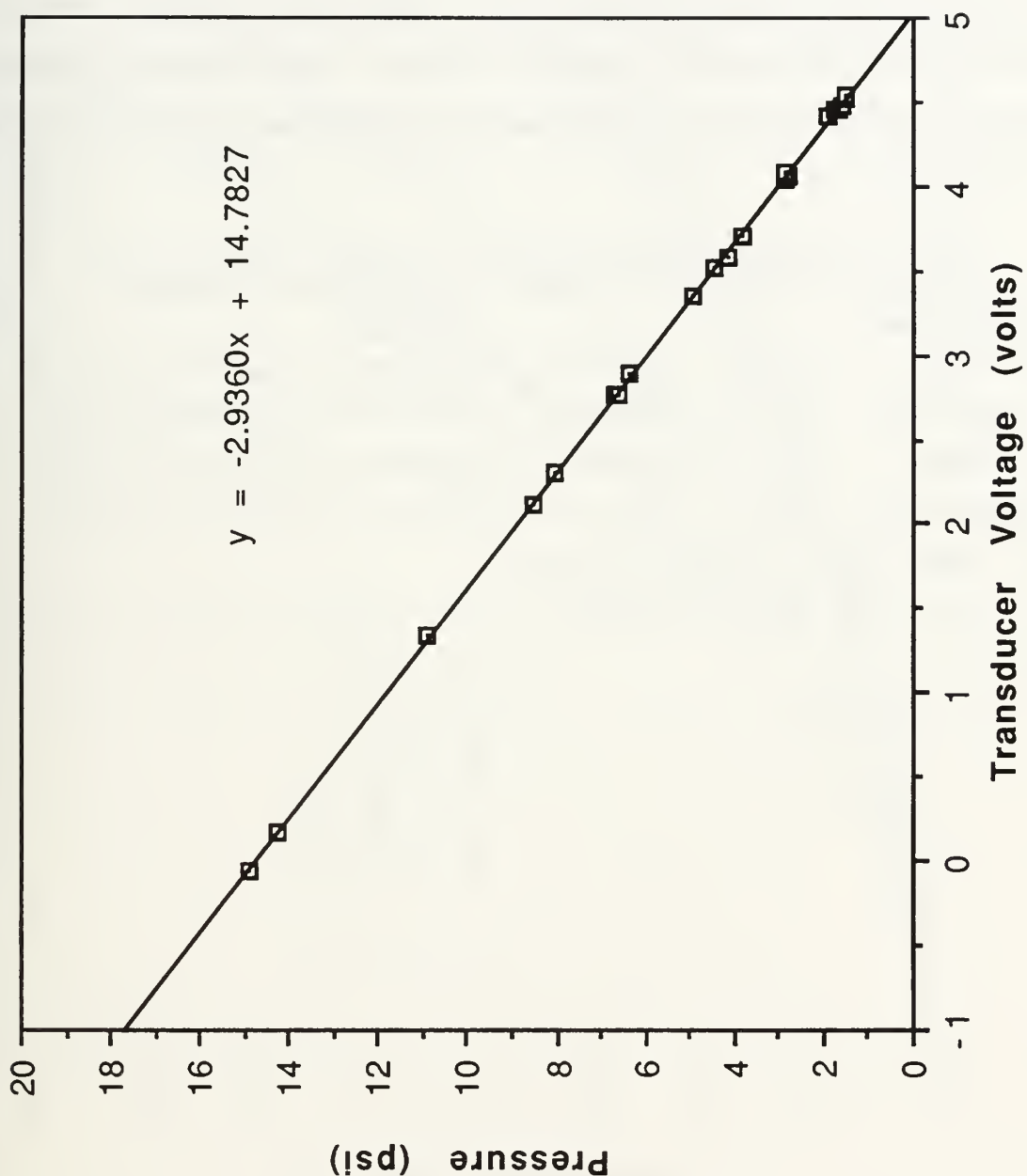


Figure B.2 Pressure Transducer Calibration Chart

can have a significant effect on the calculated overall heat-transfer coefficient. Measurements were made for no insert, Heatex, wire wrap and twisted tape inserts as shown in Figure B.3, on 5 December 1991. Each data set was curve fitted to a third order polynomial which is depicted in Table B.2. Each respective polynomial corrects the temperature rise measurement for the heating due to the particular type of insert used.

Table B.2 FRICTION TEMPERATURE RISE POLYNOMIALS

<u>Insert Type</u>	<u>Polynomial</u>
None	$Trise = -1.960 \times 10^{-5}V^3 + 9.349 \times 10^{-4}V^2 + 1.749 \times 10^{-4}V - 2.728 \times 10^{-4}$
Wire Wrap	$Trise = 8.160 \times 10^{-5}V^3 + 1.4512 \times 10^{-3}V^2 + 2.745 \times 10^{-3}V - 3.991 \times 10^{-4}$
Heatex	$Trise = 8.160 \times 10^{-5}V^3 + 1.080 \times 10^{-3}V^2 + 1.232 \times 10^{-3}V + 8.570 \times 10^{-5}$
Twisted Tape	$Trise = 4.070 \times 10^{-5}V^3 + 4.451 \times 10^{-4}V^2 + 1.711 \times 10^{-3}V - 6.440 \times 10^{-5}$
where: Trise = temperature rise (K) V = fluid velocity (m/s)	

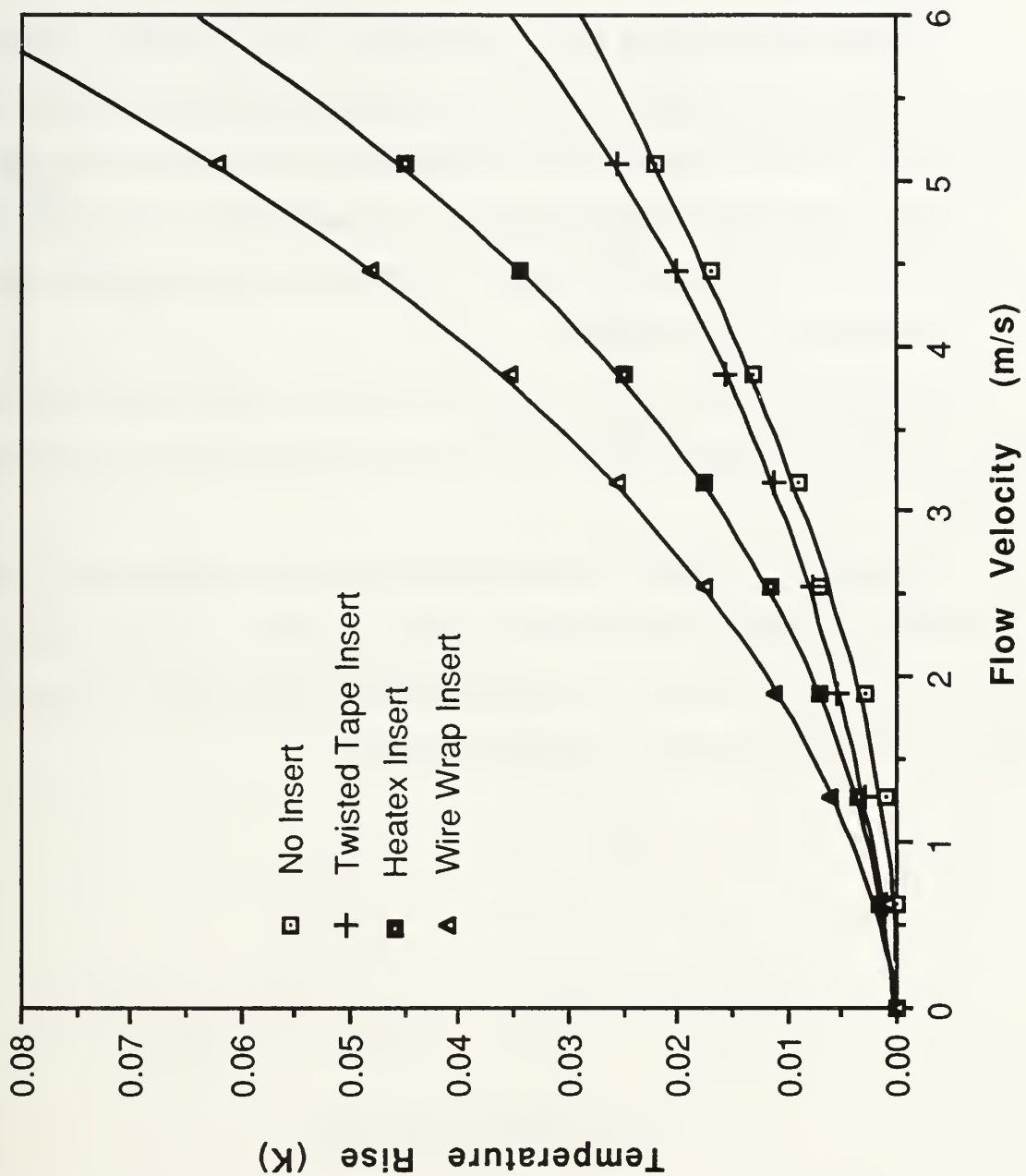


Figure B.3 Friction Temperature Rise Curves for Heatex Insert, Wire Wrap Insert, Twisted Tape Insert, and No Insert.

APPENDIX C. SYSTEM INTEGRITY / LEAK TESTING

As mentioned in section III C, the material for the auxiliary condenser penetration plates was changed from aluminum to stainless steel on 24 January 1992. The stainless steel screw thread connectors in the aluminum side plate had loosened to the extent that leakage could be detected. The cause of this loosening was due to thermal cycling of the apparatus and the differential contraction/expansion of the aluminum/stainless steel combination.

An initial leak test was conducted from 20 December 1991 through 2 January 1992; the results are shown in Figure C.1. The initial mean leak rate was 3.4 mmHg per day.

Subsequent to the structural modification noted above, another leak test was conducted 6-19 February 1992; the results are shown in Figure C.2. The mean leak rate was found to be 1.7 mmHg per day, an noticeable improvement. In general, a leak rate of 2 mmHg per day is considered acceptable.

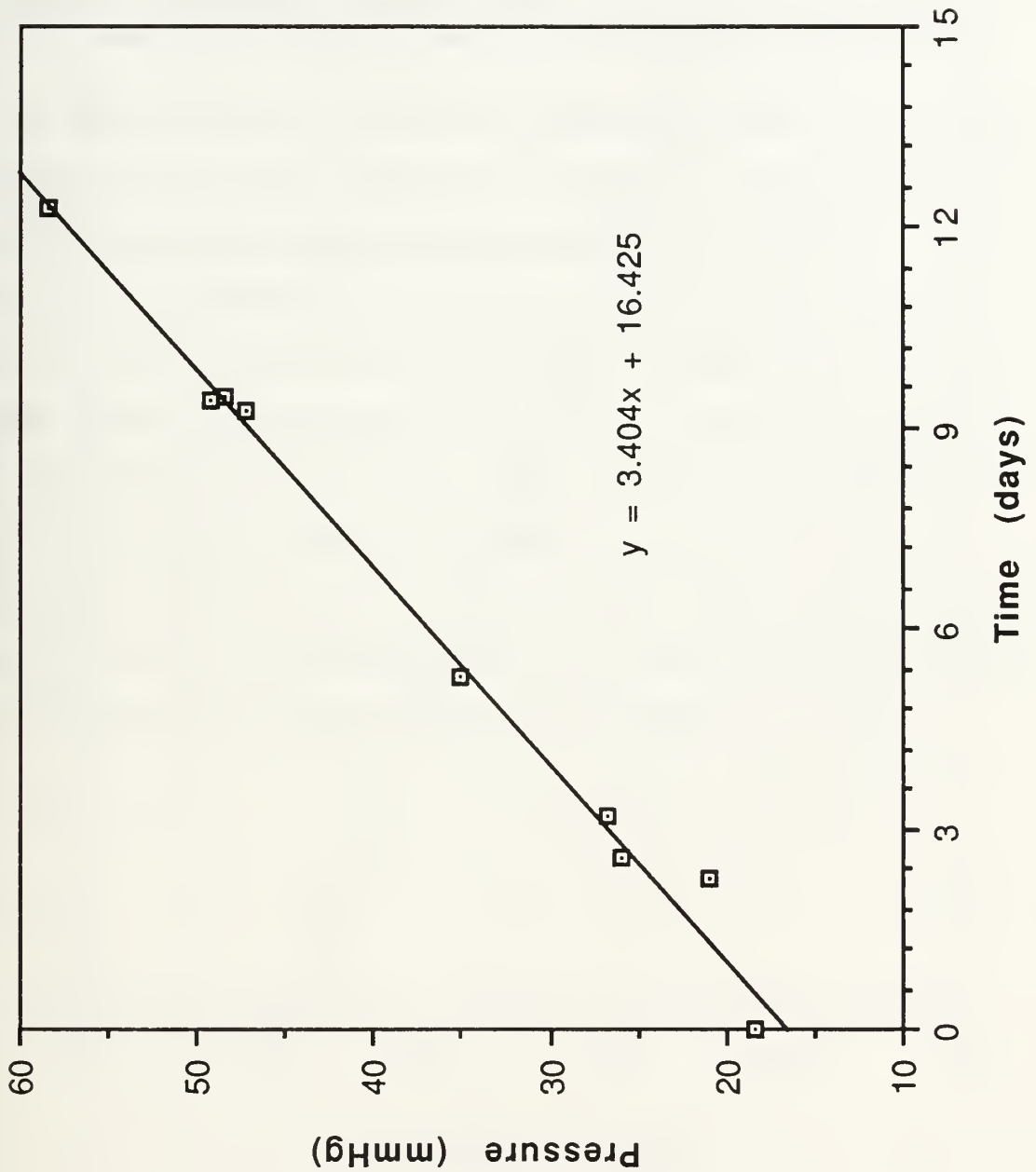


Figure C.1 Apparatus Leak Test I

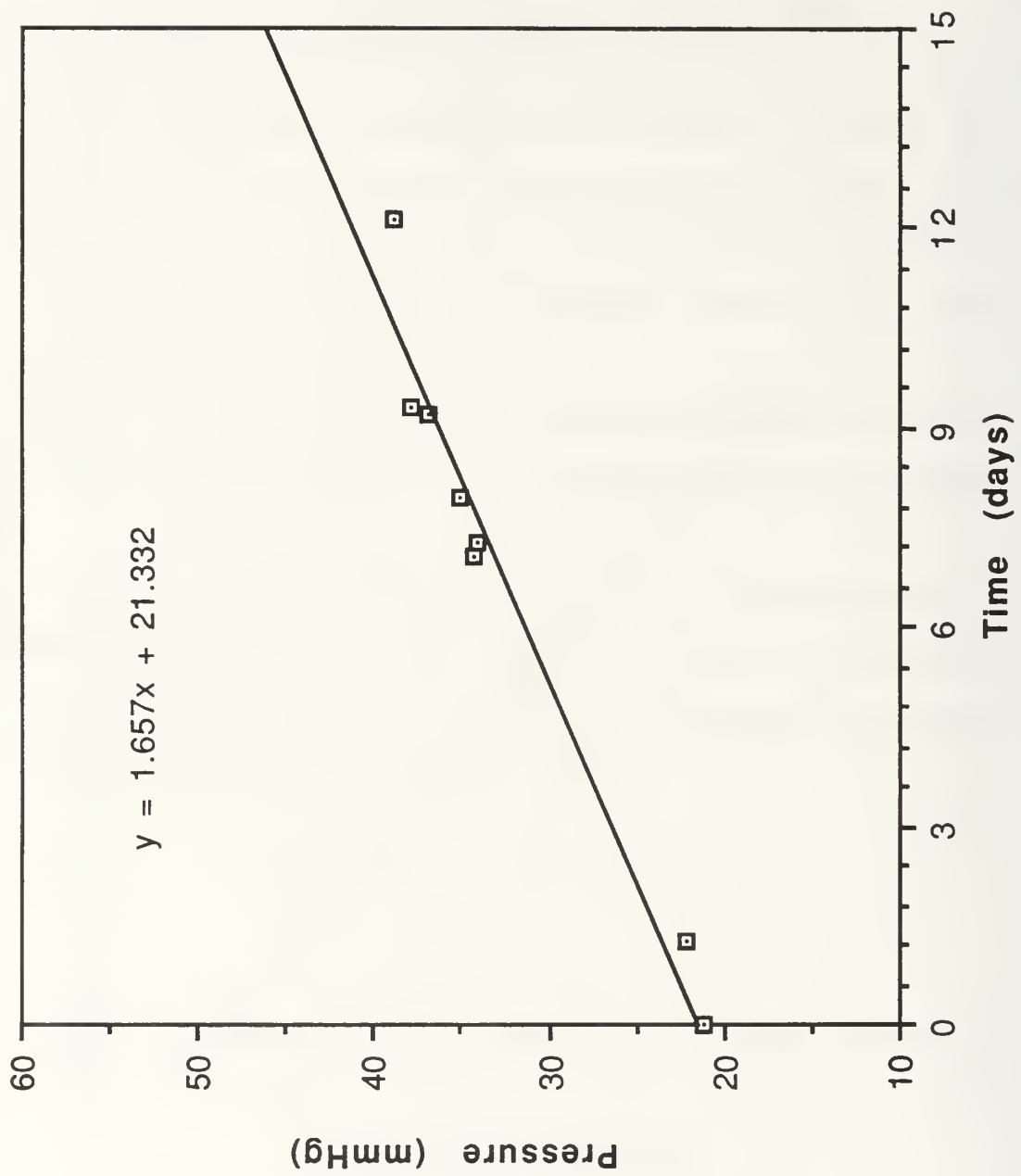


Figure C.2 Apparatus Leak Test II

APPENDIX D. COMPARISON OF FIXED C_i vs FLOATING C_i SOLUTION METHODS FOR MODIFIED WILSON PLOT DATA REPROCESSING.

As related in section VI D the "fixed" C_i method and "floating" C_i method were evaluated against the original instrumented tube results in order to choose the most accurate method of reprocessing non-instrumented data. The results of the fixed coefficient versus modified Wilson plot floating coefficient method comparison are shown in Table D. The fixed coefficient method was determined to be more accurate than the floating coefficient method 75% of the time. For the three coolant flow rates considered for each run, the overall fixed coefficient method mean error was $\pm 2.0\%$, and the floating coefficient method mean error was $\pm 5.4\%$.

For $Re < 20,000$ the error was noticeably higher, which tends to support the assertion of a number of researchers that data with Reynolds numbers below 20,000 should not be used, since the flow may not be fully turbulent.

Table D. COMPARISON OF FIXED C_i vs FLOATING C_i REPROCESSING METHODS

File Name	Flow Vel.	Film ΔT	Inst Tube Data	Fixed Method	% error	Float Method	% error
	V_w (m/s)	T_{cf} (K)	h_o (kW/m ² ·K)	h_o		h_o	
FIMAVSH1	4.35	29.33	12.13	11.93	-1.7	13.19	8.7
	2.21	22.81	13.18	12.82	-2.6	15.17	15.1
	1.16	18.27	13.68	13.16	<u>-3.8</u>	17.20	<u>25.7</u>
					-2.7*		+16.5
FIMAVSH2	4.34	36.09	11.10	11.14	0.4	11.07	0.3
	2.22	30.39	12.03	11.87	-1.3	11.72	-2.6
	1.16	24.62	12.66	12.50	<u>-1.3</u>	12.26	<u>-3.1</u>
					-0.7*		-1.8
FIMAVSH3	4.35	46.10	10.31	10.26	-0.5	10.62	3.0
	2.23	39.35	10.89	10.83	-0.6	11.44	5.1
	1.16	32.56	11.42	11.40	<u>-0.2</u>	12.43	<u>8.8</u>
					-0.4*		+5.6
FIMAVSH4	4.35	55.20	9.263	9.146	-1.3	9.584	3.5
	2.23	47.31	9.869	9.756	-1.1	10.52	6.6
	1.16	39.45	10.41	10.39	<u>-0.2</u>	11.71	<u>12.5</u>
					-0.9*		+7.5
FIMAVSH5	4.35	32.83	8.618	8.478	-1.6	9.018	4.6
	2.23	28.05	9.589	9.341	-2.6	10.36	8.0
	1.16	22.99	10.23	9.865	<u>-3.6</u>	11.66	<u>14.0</u>
					-2.6*		+8.9

File Name	Flow Vel.	Film ΔT	Inst Tube Data	Fixed Method	% error	Float Method	% error
						h_o	
FIMAVSH6	4.35	39.23	9.073	8.953	-1.3	9.084	0.1
	2.23	33.76	9.757	9.447	-1.3	9.667	1.0
	1.16	27.98	10.18	10.25	<u>0.6</u>	10.64	<u>4.5</u>
					-0.7*		+1.9
FIMAVSH7	4.35	49.04	8.960	8.939	-0.2	8.637	-3.6
	2.22	41.25	9.685	9.513	-1.8	9.010	-7.0
	1.16	34.45	10.17	10.01	<u>-1.6</u>	9.209	<u>-9.4</u>
					-1.2*		-6.7
FIMASW3	4.35	55.08	9.379	9.384	0.1	9.223	-1.7
	2.22	45.50	10.15	10.11	-0.4	9.813	-3.3
	1.16	36.67	10.73	11.18	<u>4.2</u>	10.62	<u>-1.0</u>
					+1.3*		-2.0
FIMASW4	4.35	52.83	9.531	9.558	0.3	9.528	0.0
	2.22	44.76	10.15	10.22	0.7	10.17	0.2
	1.16	36.16	10.67	11.18	<u>4.8</u>	11.08	<u>4.2</u>
					+1.9		+1.5*
FIMASW5	4.35	54.28	9.405	9.453	0.5	9.367	0.4
	2.22	45.39	10.08	10.14	0.6	9.985	0.9
	1.16	36.69	10.61	11.20	<u>5.6</u>	10.90	<u>2.7</u>
					+2.2		+1.3*

File Name	Flow Vel.	Film ΔT	Inst Tube Data	Fixed Method	% error	Float Method	% error
	V_w (m/s)	T_{cf} (K)	h_o (kW/m ² ·K)	h_o		h_o	
FIMASN4	4.35	46.24	9.947	10.07	1.2	9.512	-4.4
	2.22	34.27	11.12	11.34	2.0	10.24	-7.9
	1.16	24.82	12.21	--	--	--	--
					+1.6*		-6.2
FIMASN6	4.35	45.93	9.872	9.823	0.5	9.302	5.8
	2.22	34.40	10.84	10.86	0.2	9.898	8.7
	1.16	25.52	11.81	14.35	<u>21.5</u>	11.77	<u>0.3</u>
					+7.4		+4.9*

APPENDIX E. UNCERTAINTY ANALYSIS

In the measurement of a physical quantity, there will always be a difference between the measured value of the quantity and the actual value. The magnitude of this difference depends on the accuracy of the measuring device calibration, operator experience, environmental effects, etc. Eventhough the error associated with a single measurement may be rather small, the error may grow to substantial proportions when combined with other measured quantities in a given calculation scheme. The best estimate of the difference between a calculated or measured quantity and the actual value of the quantity is known as the uncertainty.

The uncertainty may be estimated by the method of Kline and McClintock [Ref. 24]. This states that for a quantity R, which is a function of several measured quantities ($R=R(x_1, x_2, x_3, \dots, x_n)$), the uncertainty in R is given by the following relation:

$$W_R = \left[\left(\frac{\partial R}{\partial x_1} W_1 \right)^2 + \left(\frac{\partial R}{\partial x_2} W_2 \right)^2 + \dots + \left(\frac{\partial R}{\partial x_3} W_3 \right)^2 \right]^{1/2} \quad (\text{E.1})$$

where:

W_R = the uncertainty of the desired dependent variable

$x_1, x_2, x_3, \dots, x_n$ = the measured independent variables

$W_1, W_2, W_3, \dots, W_n$ = the uncertainties in the measured variables.

Georgiadis [Ref. 5] gives a complete description of the uncertainty analysis for this experiment. The uncertainty analysis program written by Mitrou [Ref. 25] was used to calculate uncertainties. The uncertainty for runs using an insert ranged from

$\pm 2.2\%$ to $\pm 4.6\%$. The uncertainty for runs without an insert ranged from $\pm 10.9\%$ to $\pm 17.1\%$. Sample outputs of the uncertainty evaluations are included in this appendix.

DATA FOR THE UNCERTAINTY ANALYSIS:

File Name:	FNMAVSH1	
Pressure Condition:	Vacuum	
Vapor Temperature	=	53.764 (Deg C)
Water Flow Rate (%)	=	50.00
Water Velocity	=	2.76 (m/s)
Heat Flux	=	3.765E+05 (W/m^2)
Tube-metal thermal conduc.	=	385.0 (W/m.K)
Sieder-Tate constant	=	0.2200

UNCERTAINTY ANALYSIS:

VARIABLE	PERCENT UNCERTAINTY
Mass Flow Rate, Md	1.26
Reynolds Number, Re	1.48
Heat Flux, q	1.42
Log-Mean-Tem Diff, LMTD	.48
Wall Resistance, R _w	4.40
Overall H.T.C., U _o	1.50
Water-Side H.T.C., H _i	1.53
Vapor-Side H.T.C., H _o	2.60

DATA FOR THE UNCERTAINTY ANALYSIS:

File Name:	FNMAVSH1	
Pressure Condition:	Vacuum	
Vapor Temperature	=	53.587 (Deg C)
Water Flow Rate (%)	=	80.00
Water Velocity	=	4.38 (m/s)
Heat Flux	=	4.188E+05 (W/m^2)
Tube-metal thermal conduc.	=	385.0 (W/m.K)
Sieder-Tate constant	=	0.2200

UNCERTAINTY ANALYSIS:

VARIABLE	PERCENT UNCERTAINTY
Mass Flow Rate, Md	0.80
Reynolds Number, Re	1.09
Heat Flux, q	1.14
Log-Mean-Tem Diff, LMTD	.68
Wall Resistance, R _w	4.40
Overall H.T.C., U _o	1.33
Water-Side H.T.C., H _i	1.31
Vapor-Side H.T.C., H _o	2.23

DATA FOR THE UNCERTAINTY ANALYSIS:

File Name:	FNMAVSH1	
Pressure Condition:	Vacuum	
Vapor Temperature	=	53.611 (Deg C)
Water Flow Rate (%)	=	30.00
Water Velocity	=	1.70 (m/s)
Heat Flux	=	3.233E+05 (W/m^2)
Tube-metal thermal conduc.	=	385.0 (W/m.K)
Sieder-Tate constant	=	0.2200

UNCERTAINTY ANALYSIS:

VARIABLE	PERCENT UNCERTAINTY
Mass Flow Rate, Md	2.05
Reynolds Number, Re	2.19
Heat Flux, q	2.13
Log-Mean-Tem Diff, LMTO	.34
Wall Resistance, R _w	4.40
Overall H.T.C., U _o	2.16
Water-Side H.T.C., H _i	2.00
Vapor-Side H.T.C., H _o	3.41

DATA FOR THE UNCERTAINTY ANALYSIS:

File Name:	FNMAVSH4	
Pressure Condition:	Atmospheric (101 kPa)	
Vapor Temperature	=	100.086 (Deg C)
Water Flow Rate (%)	=	80.00
Water Velocity	=	4.34 (m/s)
Heat Flux	=	7.258E+05 (W/m^2)
Tube-metal thermal conduc.	=	385.0 (W/m.K)
Sieder-Tate constant	=	0.2200

UNCERTAINTY ANALYSIS:

VARIABLE	PERCENT UNCERTAINTY
Mass Flow Rate, Md	0.80
Reynolds Number, Re	1.12
Heat Flux, q	1.00
Log-Mean-Tem Diff, LMTO	.39
Wall Resistance, R _w	4.40
Overall H.T.C., U _o	1.08
Water-Side H.T.C., H _i	1.33
Vapor-Side H.T.C., H _o	2.26

DATA FOR THE UNCERTAINTY ANALYSIS:

File Name:	FNMAUASH4
Pressure Condition:	Atmospheric (101 kPa)
Vapor Temperature	= 99.778 (Deg C)
Water Flow Rate (%)	= 50.00
Water Velocity	= 2.75 (m/s)
Heat Flux	= 6.713E+05 (W/m^2)
Tube-metal thermal conduc.	= 385.0 (W/m.K)
Sieder-Tate constant	= 0.2200

UNCERTAINTY ANALYSIS:

VARIABLE	PERCENT UNCERTAINTY
Mass Flow Rate, Md	1.27
Reynolds Number, Re	1.49
Heat Flux, q	1.37
Log-Mean-Tem Diff, LMTD	.27
Wall Resistance, R _w	4.40
Overall H.T.C., U _o	1.40
Water-Side H.T.C., H _i	1.55
Vapor-Side H.T.C., H _o	2.54

DATA FOR THE UNCERTAINTY ANALYSIS:

File Name:	FNMAUASH4
Pressure Condition:	Atmospheric (101 kPa)
Vapor Temperature	= 100.429 (Deg C)
Water Flow Rate (%)	= 20.00
Water Velocity	= 1.15 (m/s)
Heat Flux	= 5.70EE+05 (W/m^2)
Tube-metal thermal conduc.	= 385.0 (W/m.K)
Sieder-Tate constant	= 0.2200

UNCERTAINTY ANALYSIS:

VARIABLE	PERCENT UNCERTAINTY
Mass Flow Rate, Md	3.00
Reynolds Number, Re	3.11
Heat Flux, q	3.04
Log-Mean-Tem Diff, LMTD	.13
Wall Resistance, R _w	4.40
Overall H.T.C., U _o	3.04
Water-Side H.T.C., H _i	2.68
Vapor-Side H.T.C., H _o	4.57

DATA FOR THE UNCERTAINTY ANALYSIS:

File Name:	FNMAVSHE
Pressure Condition:	Vacuum
Vapor Temperature	= 76.243 (Deg C)
Water Flow Rate (%)	= 80.00
Water Velocity	= 4.35 (m/s)
Heat Flux	= 5.053E+05 (W/m^2)
Tube-metal thermal conduc.	= 385.0 (W/m.K)
Sieder-Tate constant	= 0.2200

UNCERTAINTY ANALYSIS:

VARIABLE	PERCENT UNCERTAINTY
Mass Flow Rate, Md	0.80
Reynolds Number, Re	1.10
Heat Flux, q	1.08
Log-Mean-Tem Diff, LMTD	.55
Wall Resistance, Rw	4.40
Overall H.T.C., Uo	1.22
Water-Side H.T.C., Hi	1.32
Vapor-Side H.T.C., Ho	2.25

DATA FOR THE UNCEPNTAINTY ANALYSIS:

File Name:	FNMAUSHB
Pressure Condition:	Vacuum
Vapor Temperature	= 76.808 (Deg C)
Water Flow Rate (%)	= 50.00
Water Velocity	= 2.75 (m/s)
Heat Flux	= 4.707E+05 (W/m^2)
Tube-metal thermal conduc.	= 385.0 (W/m.K)
Sieder-Tate constant	= 0.2200

UNCERTAINTY ANALYSIS:

VARIABLE	PERCENT UNCERTAINTY
Mass Flow Rate, Md	1.26
Reynolds Number, Re	1.48
Heat Flux, q	1.40
Log-Mean-Tem Diff, LMTD	.38
Wall Resistance, Rw	4.40
Overall H.T.C., Uo	1.45
Water-Side H.T.C., Hi	1.54
Vapor-Side H.T.C., Ho	2.62

DATA FOR THE UNCERTAINTY ANALYSIS:

File Name:	FNMAUSHE	
Pressure Condition:	Vacuum	
Vapor Temperature	=	76.541 (Deg C)
Water Flow Rate (%)	=	20.00
Water Velocity	=	1.16 (m/s)
Heat Flux	=	3.965E+05 (W/m^2)
Tube-metal thermal conduc.	=	385.0 (W/m.K)
Sieder-Tate constant	=	0.2200

UNCERTAINTY ANALYSIS:

VARIABLE	PERCENT UNCERTAINTY
----------	---------------------

Mass Flow Rate, Md	2.99
Reynolds Number, Re	3.09
Heat Flux, q	3.03
Log-Mean-Tem Diff, LMTD	.19
Wall Resistance, R _w	4.40
Overall H.T.C., U _o	3.04
Water-Side H.T.C., H _i	2.66
Vapor-Side H.T.C., H _o	4.55

DATA FOR THE UNCERTAINTY ANALYSIS:

File Name:	FNMAF051	
Pressure Condition:	Atmospheric (101 kPa)	
Vapor Temperature	=	100.138 (Deg C)
Water Flow Rate (%)	=	80.00
Water Velocity	=	4.32 (m/s)
Heat Flux	=	1.291E+06 (W/m^2)
Tube-metal thermal conduc.	=	385.0 (W/m.K)
Sieder-Tate constant	=	0.2200

UNCERTAINTY ANALYSIS:

VARIABLE	PERCENT UNCERTAINTY
----------	---------------------

Mass Flow Rate, Md	0.81
Reynolds Number, Re	1.16
Heat Flux, q	.95
Log-Mean-Tem Diff, LMTD	.22
Wall Resistance, R _w	4.40
Overall H.T.C., U _o	.99
Water-Side H.T.C., H _i	1.36
Vapor-Side H.T.C., H _o	2.30

DATA FOR THE UNCERTAINTY ANALYSIS:

File Name:	FNMAF051	
Pressure Condition:	Atmospheric (101 kPa)	
Vapor Temperature	=	100.116 (Deg C)
Water Flow Rate (%)	=	50.00
Water Velocity	=	2.73 (m/s)
Heat Flux	=	1.139E+06 (W/m^2)
Tube-metal thermal conduc.	=	385.0 (W/m.K)
Sieder-Tate constant	=	0.2200

UNCERTAINTY ANALYSIS:

VARIABLE	PERCENT UNCERTAINTY
Mass Flow Rate, Md	1.28
Reynolds Number, Re	1.54
Heat Flux, q	1.36
Log-Mean-Tem Diff, LMTD	.16
Wall Resistance, R _w	4.40
Overall H.T.C., U _o	1.37
Water-Side H.T.C., H _i	1.58
Vapor-Side H.T.C., H _o	2.69

DATA FOR THE UNCERTAINTY ANALYSIS:

File Name:	FNMAF051	
Pressure Condition:	Atmospheric (101 kPa)	
Vapor Temperature	=	100.071 (Deg C)
Water Flow Rate (%)	=	20.00
Water Velocity	=	1.16 (m/s)
Heat Flux	=	8.513E+05 (W/m^2)
Tube-metal thermal conduc.	=	385.0 (W/m.K)
Sieder-Tate constant	=	0.2200

UNCERTAINTY ANALYSIS:

VARIABLE	PERCENT UNCERTAINTY
Mass Flow Rate, Md	3.01
Reynolds Number, Re	3.13
Heat Flux, q	3.05
Log-Mean-Tem Diff, LMTD	.09
Wall Resistance, R _w	4.40
Overall H.T.C., U _o	3.05
Water-Side H.T.C., H _i	2.70
Vapor-Side H.T.C., H _o	4.59

DATA FOR THE UNCERTAINTY ANALYSIS:

File Name:	FNMAF201
Pressure Condition:	Atmospheric (101 kPa)
Vapor Temperature	= 99.787 (Deg C)
Water Flow Rate (%)	= 80.00
Water Velocity	= 4.33 (m/s)
Heat Flux	= 1.431E+06 (W/m^2)
Tube-metal thermal conduc.	= 385.0 (W/m.K)
Sieder-Tate constant	= 0.2200

UNCERTAINTY ANALYSIS:

VARIABLE PERCENT UNCERTAINTY

Mass Flow Rate, Md	0.80
Reynolds Number, Re	1.14
Heat Flux, q	.95
Log-Mean-Tem Diff, LMTD	.20
Wall Resistance, R _w	4.40
Overall H.T.C., U _o	.97
Water-Side H.T.C., H _i	1.34
Vapor-Side H.T.C., H _o	2.28

DATA FOR THE UNCERTAINTY ANALYSIS:

File Name:	FNMAF201
Pressure Condition:	Atmospheric (101 kPa)
Vapor Temperature	= 100.076 (Deg C)
Water Flow Rate (%)	= 50.00
Water Velocity	= 2.74 (m/s)
Heat Flux	= 8.941E+05 (W/m^2)
Tube-metal thermal conduc.	= 385.0 (W/m.K)
Sieder-Tate constant	= 0.2200

UNCERTAINTY ANALYSIS:

VARIABLE PERCENT UNCERTAINTY

Mass Flow Rate, Md	1.27
Reynolds Number, Re	1.52
Heat Flux, q	1.35
Log-Mean-Tem Diff, LMTD	.14
Wall Resistance, R _w	2.67
Overall H.T.C., U _o	1.36
Water-Side H.T.C., H _i	1.57
Vapor-Side H.T.C., H _o	2.66

DATA FOR THE UNCERTAINTY ANALYSIS:

File Name:	FNMAF201	
Pressure Condition:	Atmospheric (101 kPa)	
Vapor Temperature	=	100.142 (Deg C)
Water Flow Rate (%)	=	20.00
Water Velocity	=	1.16 (m/s)
Heat Flux	=	6.405E+05 (W/m^2)
Tube-metal thermal conduc.	=	385.0 (W/m.K)
Sieder-Tate constant	=	0.2200

UNCERTAINTY ANALYSIS:

VARIABLE	PERCENT UNCERTAINTY
Mass Flow Rate, Md	3.01
Reynolds Number, Re	3.13
Heat Flux, q	3.05
Log-Mean-Tem Diff, LMTD	.08
Wall Resistance, R _w	2.57
Overall H.T.C., U _o	3.05
Water-Side H.T.C., H _i	2.70
Vapor-Side H.T.C., H _o	4.59

DATA FOR THE UNCERTAINTY ANALYSIS:

File Name:	FSONMASN1	
Pressure Condition:	Atmospheric (101 kPa)	
Vapor Temperature	=	100.155 (Deg C)
Water Flow Rate (%)	=	80.00
Water Velocity	=	4.35 (m/s)
Heat Flux	=	4.548E+05 (W/m^2)
Tube-metal thermal conduc.	=	385.0 (W/m.K)
Sieder-Tate constant	=	0.0130

UNCERTAINTY ANALYSIS:

VARIABLE	PERCENT UNCERTAINTY
Mass Flow Rate, Md	0.80
Reynolds Number, Re	1.11
Heat Flux, q	1.02
Log-Mean-Tem Diff, LMTD	.45
Wall Resistance, R _w	2.57
Overall H.T.C., U _o	1.11
Water-Side H.T.C., H _i	15.41
Vapor-Side H.T.C., H _o	10.91

DATA FOR THE UNCERTAINTY ANALYSIS:

File Name:	FS0NMASN1
Pressure Condition:	Atmospheric (101 kPa)
Vapor Temperature	= 99.842 (Deg C)
Water Flow Rate (%)	= 50.00
Water Velocity	= 2.75 (m/s)
Heat Flux	= 4.012E+05 (W/m^2)
Tube-metal thermal conduc.	= 385.0 (W/m.K)
Sieder-Tate constant	= 0.0130

UNCERTAINTY ANALYSIS:

VARIABLE PERCENT UNCERTAINTY

Mass Flow Rate, Md	1.27
Reynolds Number, Re	1.50
Heat Flux, q	1.38
Log-Mean-Tem Diff, LMTD	.32
Wall Resistance, R _w	2.67
Overall H.T.C., U _o	1.42
Water-Side H.T.C., H _i	15.44
Vapor-Side H.T.C., H _o	17.07

DATA FOR THE UNCERTAINTY ANALYSIS:

File Name:	FS0NMASN1
Pressure Condition:	Atmospheric (101 kPa)
Vapor Temperature	= 100.035 (Deg C)
Water Flow Rate (%)	= 70.00
Water Velocity	= 3.81 (m/s)
Heat Flux	= 4.396E+05 (W/m^2)
Tube-metal thermal conduc.	= 385.0 (W/m.K)
Sieder-Tate constant	= 0.0130

UNCERTAINTY ANALYSIS:

VARIABLE PERCENT UNCERTAINTY

Mass Flow Rate, Md	0.92
Reynolds Number, Re	1.21
Heat Flux, q	1.09
Log-Mean-Tem Diff, LMTD	.41
Wall Resistance, R _w	2.67
Overall H.T.C., U _o	1.17
Water-Side H.T.C., H _i	15.42
Vapor-Side H.T.C., H _o	12.42

APPENDIX F. INSTRUMENTED TUBE CONSTRUCTION

The medium diameter instrumented tube of Poole [Ref. 6], with six wall thermocouples, was fabricated by welding together a copper tube in three pieces after imbedding capillary tubes at mid depth in the tube wall. Teflon thermocouples were inserted into the capillary tubes for tube wall temperature measurement.

An attempt was made during this study to construct instrumented tubes of small, medium, and large diameter in the following steps:

1. Take thick-walled copper tube bar-stock and machine to specified inside diameter, outside diameter, and length.
2. Cut four evenly spaced slots, of given depth and width to accommodate metal sheathed thermocouples, from halfway along the tube to the end.
3. Solder metal sheathed thermocouples into grooves.
4. Cut copper strips from another tube to fit into the top of the slot.
5. Clamp copper strips to the slots (using jubilee clips) and solder in place.
6. Turn off excess copper from strips to original outside diameter.
7. Send tubes to plating shop and plate the whole tube to a given thickness of plate.
8. Return tube to NPS machine shop and machine back down to desired outside diameter.

The process was completed through step 2 of the above procedure and the tubes are ready for step 3. Several of the latter steps were attempted using a practice tube with monel wire placed in the slots on the tube vice thermocouples; this was to ensure the process was safe, and to prevent destruction of assets (small, medium, and large diameter tubes machined to specifications, and the associated

metal sheathed thermocouples). The following summary documents the steps taken and lessons learned.

1. Completed tube fabrication through step 2 of the fabrication procedure (above). A practice tube was used from this point to continue the procedure.
2. Cutting the copper strips proved difficult, so the monel (similar to the stainless steel sheath on the thermocouples) wires were silver soldered after being pinned in place. No lead was permitted in the solder since copper will not plate to lead, but will plate to silver.
3. The practice tube was sent to a local contractor for electroplating. (Bay Custom Chrome, Marina, Ca.)
4. Two different plating procedures were used on the tube:
 - a. First, a cyanide bath treatment was used to electroplate the tube. However, this procedure severely scorched the surface of the tube, resulting in the return of the tube to the NPS machine shop for repair.
 - b. After repair, the tube was again sent off and subsequently treated with an acid bath procedure, which resulted in an acceptable tube surface finish.
5. The original thickness of electroplate was not thick enough for our application, so another acid bath treatment was performed to bring the surface thickness to the desired level.
6. The final product was suitable for our intended application with the exception of the following items which need to be corrected:
 - a. Existing voids (from non-uniform soldering) or flaws in the tube surface would not fill in to give a uniform thickness around the tube.
 - b. The practice wires, tube end pieces, and tube interior were not protected properly during the electroplating process, resulting in unacceptable copper deposition on critical areas.

It is recommended that the instrumented tube efforts be continued with particular attention to the following items:

1. Silver soldering is an acceptable method of fixing the thermocouples in place, since the thermocouple melting temperature is $\sim 1700^{\circ}\text{C}$ (silver solder is applied at $\sim 1100^{\circ}\text{C}$).

2. If the voids left in previous soldering efforts persist, then cut copper strips to place over the thermocouples to hold them in place.
3. Ensure that critical areas on the tube are well protected during the electroplating process.

APPENDIX G. DRPINST PROGRAM LISTING

The program DRPINST, which was used to collect all instrumented data, is listed in this appendix.

1000! DRPINST
1005! WRITTEN FOR INSTRUMENTED TUBES
1009! BY S. MEMORY (10TH DECEMBER 1991)
1009!
1010! USED TO COLLECT DATA ON THE INSTRUMENTED
1011! TUBE FABRICATED BY POOLE (1983) FROM WHICH
1012! NEW INSIDE HEAT-TRANFER CORRELATIONS WERE
1013! EMPIRICALLY DETERMINED FOR NO INSERT, WIRE
1014! WRAP INSERT, AND HEATEX INSERT CASES BY
1015! K. SWENSEN (FEB 1992).
1015!
1017! ALL INSTRUMENT CALIBRATIONS FOR FLOW METER
1018! THERMOCOUPLES, THERMOPILE, PRESSURE TRANSDUCER,
1019! FPICTION TEMP RISE FOR NO INSERT, WIRE WRAP INSERT,
1020! HEATEX INSERT, AND TWISTED TAPE INSERT WERE
1021! PERFORMED BY SWENSEN (SEP-DEC 1991).
1023! VARIOUS PROGRAMS WERE USED TO REPROCESS DATA
1024! COLLECTED; THE APPLICABLE FILES WITH THE APPROPRIATE
1025! REPROCESSING PROGRAMS ARE AS FOLLOWS:
1025!
1027! FILES REPROCESSING PROGRAM
1028! SWENSEN FIMAUSH1-7 DRPINST2
1029! SWENSEN FIMASN4,S DRPINST1
1030! SWENSEN FIMAUSW3-S DRPINST1
1031! SWENSEN NON-INSTRUMENTED DATA DPPHS
1032! (ALL FN.... FILES)
1034! GUTTENDORF DATA DRPKS2
1035! VAN PETTEN DATA DRPKS2
1035!
1037! FILE NAME DEFINITIONS FOR SWENSEN:
1038!
1040! LETTER/NUMBER DEFINITION
1041! POSITION
1044! 1ST CONDENSATION CONDITION
1045! D=DROPWISE, F=FILMWISE
1046! 2ND TUBE TYPE I=INSTRUMENTED
1047! N=NON-INSTRUMENTED
1049! 3RD TUBE TYPE M=MEDIUM
1049! 4TH PRESSURE CONDITION
1050! A=ATMOPHERIC (101 KPA)
1051! U=VACUUM
1052! WHEN A & U APPEAR TOGETHER AS IN
1053! FIMAUSH1 IT REFERS TO A SERIES
1054! OF RUNS AT VARIOUS PRESSURES AND
1055! VAPOR VELOCITIES.
1056! 5TH TUBE TYPE S=SMOOTH

```

1057! F=FINNED
1058!     6TH      TYPE OF INSERT INSTALLED
1059! N=NONE
1060! W=WIRE WRAP
1061! H=HEATEX
1062! THE HEATEX INSERT WAS USED EXCLUSIVELY
1063! FOR FINNED TUBE DATA, SO POSITIONS
1064! 6 & 7 REFER TO THE TUBE FIN SPACING
1065! 05=0.5mm
1066! 10=1.0mm
1067! 15=1.5mm
1068! 20=2.0mm
1069! FINAL POSITION   RUN NUMBER
1070!
1071! MEANING OF ALL FLAGS IN PROGRAM
1072!
1073! IFT:    FLUID TYPE
1074! ISO:    OPTION WITHIN PROGRAM
1075! IM:     INPUT MODE
1076! IFG:    FINNED OR SMOOTH
1077! INN:    INSERT TYPE
1078! IWT:    LOOP NO. WITHIN PROGRAM
1079! ITDS:   TUBE DIAMETER
1080! IPC:    PRESSURE CONDITION
1081! IOU:    OUTPUT REQUIRED
1082 COM /Cc/ C(7)
1083 COM /Cc55/ T55(S)
1084 COM /Cc56/ T56(S)
1085 COM /Cc57/ T57(S)
1086 COM /Cc58/ T58(S)
1087 COM /F1d/ Ift
1088 DIM Emf(13),Tw(5),Tws(6),Tw1(6)
1089 DATA 0.10086091,25727.94368,-767345.8295,78025595.81
1090 DATA -8247486588,6.87688E+11,-2.66192E+13,3.94078E+14
1091 READ C(*)
1092 DATA 273.15,2.5843E-2,-7.2671E-7,3.2841E-11,-8.7719E-16,8.7121E-20
1093 READ T55(*)
1094 DATA 273.15,2.5878E-2,-5.9853E-7,-3.1242E-11,1.3275E-14,-1.0188E-18
1095 READ T56(*)
1096 DATA 273.15,2.5823E-2,-7.3933E-7,2.8625E-11,1.8717E-15,-2.2486E-19
1097 READ T57(*)
1098 DATA 273.15,2.5931E-2,-7.5232E-7,4.0567E-11,-1.2791E-15,6.4402E-20
1099 READ T58(*)
1100 Dssp=.1524 ! Inside diameter of stainless steel test section
1101 Ax=PI*Dssp^2/4
1102 L=.13335 ! Condensing length
1103 L1=.060325 ! Inlet end "fin length"
1104 L2=.034925 ! Outlet end "fin length"
1105 PRINTER IS 1
1106 BEEP

```

```

1107 INPUT "SELECT FLUID (0=STEAM, 1=R-113, 2=EG)",Ift
1108 PRINT USING "4X, ""Select option: """
1109 PRINT USING "5X, "" 1 Take data or re-process previous data"""
1110 PRINT USING "5X, "" 2 Print raw data (NOT COMPLETE)"""
1111 PRINT USING "5X, "" 3 Purge"""
1112 INPUT Iso
1113 IF Iso>1 THEN 3082
1114 PRINTER IS 701
1117 Ijob=0
1120! CLEAR 709
1123 BEEP
1126 INPUT "ENTER MONTH, DATE AND TIME (MM:DD:HH:MM:SS)", Date$
1129 OUTPUT 709;"TD";Date$
1132 OUTPUT 709;"TD"
1135 IF Ijob=1 THEN
1138 BEEP
1141 INPUT "SKIP PAGE AND HIT ENTER",OK
1144 END IF
1147 ENTER 709;Date$
1150 PRINT "           Month, date and time :";Date$
1153 PRINT
1156 PRINT USING "10X, ""NOTE: Program name : DRPINST"""
1171 IF Ijob=1 THEN 1189
1174 BEEP
1177 INPUT "ENTER INPUT MODE (1=NEW DATA 2=EXISTING FILE)",Im
1183 BEEP
1189 IF Im=1 THEN
1192 BEEP
1195 INPUT "GIVE A NAME FOR THE RAW DATA FILE",D_file$
1198 PRINT USING "15Y, ""File name    : "",14A":D_file$
1201 CREATE BOAT D_file$,15
1204 ASSIGN @File TO D_file$
1207 BEEP
1210 INPUT "ENTER GEOMETRY CODE (1=FINNED,0=PLAIN)", Ifg
1211 PRINTER IS 1
1213 Inn=0
1216 BEEP
1219 PRINT "SELECT INSERT TYPE:"
1220 PRINT "  0  NONE (DEFAULT)"
1221 PRINT "  1  TWISTED TAPE"
1222 PRINT "  2  WIRE WRAP"
1223 PRINT "  3  HEATEX"
1225 INPUT Inn
1226 OUTPUT @File;Ifg,Inn
1227 INPUT "NO. OF THERMOCOUPLES IN WALL", Inwt
1228 IF Ifg=1 THEN
1229 INPUT "ENTER FIN HEIGHT, FIN PITCH AND FIN WIDTH (Fh,Fp,Fw) IN MM", Fh,Fp,Fw
1230 ELSE
1231 Fh=0

```

```

1232 Fp=0
1234 Fw=0
1235 END IF
1237 OUTPUT @File;Inwt,Fp,Fw,Fh
1243 ELSE
1246 IF Ijob=1 THEN 1255
1249 BEEP
1252 INPUT "GIVE THE NAME OF THE EXISTING DATA FILE",D_file$
1255 PRINT USING "16X,""This analysis was performed for data in file "",10A";D_
file$*
1258 IF Ijob=1 THEN 1270
1261 Nrun=18
1264 BEEP
1267 INPUT "ENTER NUMBER OF DATA SETS (DEF=18)",Nrun
1270 ASSIGN @File TO D_file$*
1273 ENTER @File;Ifg,Inn
1276 ENTER @File;Inwt,Fp,Fw,Fh
1282 END IF
1295 IF Ijob=1 THEN 1543
1295 PRINTER IS 1
1348 BEEP
1351 PRINT "SELECT TUBE DIA TYPE:"
1354 Itds=2
1357 PRINT "1 SMALL"
1360 PRINT "2 MEDIUM (DEFAULT)"
1363 PRINT "3 LARGE"
1366 INPUT Itds
1369 PRINTER IS 701
1375 Di=.0127      ! ID of medium and large tubes
1378 Do=.01905     ! OD of medium tube
1459 D1=.01905     ! OD of unheated inlet length
1452 D2=.015875    ! OD of unheated outlet length
1453 Dr=.015875    ! Thermocouple burial depth
1465 IF Itds=1 THEN
1466   Di=.009525
1467   Do=.0127
1472   Dr=.01      ! TO BE MODIFIED WHEN KNOWN
1474 END IF
1477 IF Itds=3 THEN
1478   Do=.025
1479   Dr=.02      ! TO BE MODIFIED WHEN KNOWN
1480 END IF
1486 Kcu=385
1498 Rm=Do*LOG(Do/Di)/(2*Kcu) ! Wall resistance based on outside area
1501 BEEP
1504 INPUT "ENTER PRESSURE CONDITION (0=V,1=A)",Ipc
1510 BEEP
1543 PRINT USING "16X,""This analysis includes end-fin effect"""
1546 PRINT USING "16X,""Thermal conductivity      = "",3D.D,"" (W/m.K)""";Kcu
1549 PRINT USING "16X,""Inside diameter, Di      = "",DD.DD,"" (mm)""";Di*1000

```

```

1552 PRINT USING "16X,,"Outside diameter, Do      = "",DD.DD,"" (mm)""";Do*1000
1500 IF Ijob=1 THEN 1648
1509 BEEP
1536 INPUT "GIVE A NAME FOR WALL TEMPERATURE FILE",Wtf$
1539 CREATE BDAT Wtf$,5
1542 ASSIGN @File1 TO Wtf$
1548 IF Ijob=1 THEN
1551 Iov=2
1554 GOTO 1702
1557 END IF
1560 BEEP
1563 INPUT "SELECT OUTPUT (1=SHORT,2=LONG,3=RAW DATA)",Iov
1569 IF Ifg=0 THEN
1572 PRINT USING "16X,,"Tube type : INSTRUMENTED SMOOTH"""
1575 ELSE
1578 PRINT USING "16X,,"Tube type : INSTRUMENTED FINNED"""
1581 PRINT USING "16X,,"Fin pitch, width, and height (mm): "",DD.DD,2X,Z.DD,2X,
Z.DD";Fp,Fw,Fh
1584 END IF
1585 J=0
1586 Go_on=1
1587 Repeat:!
1588 J=J+1
1589 IF Im=1 THEN
1590 BEEP
1594 OUTPUT 709;"AR AF40 AL40 VRS"
1595 OUTPUT 709;"AS SA"
1597 INPUT "LIKE TO CHECK NG CONCENTRATION (1=Y,0=N)?",Ng
1599 IF J=1 THEN
1602 OUTPUT 709;"AR AF40 AL41 VRS"
1605 OUTPUT 709;"AS SA"
1608 END IF
1609 BEEP
1614 INPUT "ENTER FLOWMETER READING",Fm
1617 OUTPUT 709;"AR AF50 AL52 VRS"
1620 OUTPUT 709;"AS SA"
1623 ENTER 709;Etp
1626 OUTPUT 709;"AS SA"
1629 BEEP
1632 INPUT "CONNECT VOLTAGE LINE",Ok
1635 ENTER 709;Bvol
1638 BEEP
1641 INPUT "DISCONNECT VOLTAGE LINE",Ok
1644 IF Bvol<.1 THEN
1645 BEEP
1648 INPUT "INVALID VOLTAGE - TRY AGAIN!",Ok
1651 GOTO 1819
1654 END IF
1657 OUTPUT 709;"AS SA"
1661 ENTER 709;Utran

```

```

1959 OUTPUT 709;"AS SA"
1961 ENTER 709;Bamp
1962 Etp=Etp*1.E+6
1967 OUTPUT 709;"AR AF40 AL53 VRS"
1973 Nn=7+Inwt
1976 FOR I=0 TO Nn
1979 OUTPUT 709;"AS SA"
1982 IF I>7 THEN
1995 Se=0
1998 FOR K=1 TO 20
2001 ENTER 709;E
2004 Se=Se+E
2007 NEXT K
2009 Emf(I)=ABS(Se/20)
2003 ELSE
2006 ENTER 709;E
2012 Emf(I)=ABS(E)
2015 END IF
2016 Emf(I)=Emf(I)*1.E+6
2018 NEXT I
2021 OUTPUT 709;"AS SA"
2024 OUTPUT 713;"T1R2E"
2027 WAIT 2
2030 ENTER 713;T11
2033 OUTPUT 713;"T2R2E"
2036 WAIT 2
2039 ENTER 713;T2
2042 OUTPUT 713;"T1R2E"
2045 WAIT 2
2048 ENTER 713;T12
2051 T1=(T11+T12)*.5
2054 OUTPUT 713;"T3R2E"
2060 BEEP
2061 INPUT "ENTER PRESSURE GAUGE READING (Pga)",Pga
2062 Pvap1=Pga*6894.7 !PSI TO Pa
2072 ELSE
2084 ENTER @File;Bvol,Bamp,Ptran,Etp,Emf(*),Fm,T1,T2,Pvap1
2087 IF J=1 OR J=20 OR J=Nrun THEN
2090 Ng=1
2093 ELSE
2095 Ng=0
2099 END IF
2002 END IF
2008 Tsteam1=FNTvsy57(Emf(0))
2009 Tsteam1=Tsteam1-273.15
2011 Tsteam2=FNTvsy58(Emf(1))
2012 Tsteam2=Tsteam2-273.15
2014! Tsteam=(Tsteam1+Tsteam2)/2.
2015 Tsteam=Tsteam1
2017 Troom=FNTvsy59(Emf(2))

```

```

2018 Tcon=FNTvsv58(Emf(7))
2019 Troom=Troom-273.15
2020 Tcon=Tcon-273.15
2021 Twm=0.
2022 FOR I=0 TO Inwt-1
2023 Tw(I)=FNTvsv57(Emf(I+8))
2024 Tw(I)=Tw(I)-273.15
2025 Twm=Twm+Tw(I)
2026 NEXT I
2032 Twm=Twm/Inwt
2044 Psat=FNPvst(Tsteam)
2057 OUTPUT 709;"AR AF54 AL54 VRS"
2058 OUTPUT 709;"AS SA"    ! PRESSURE TRANSDUCER
2059 Ss=0
2060 FOR K=1 TO 20
2062 ENTER 709;Etran
2065 Ss=Ss+Etran
2066 NEXT K
2067 Ptran=ABS(Ss/20)
2071 BEEP
2072 ! PRESSURE IN Pa FROM TRANSDUCER
2073 Pvap2=(-2.93504*Ptran+14.7827)*5894.7
2075 Ptest1=Pvap1      ! GAUGE
2077 Ptest2=Pvap2      ! TRANSDUCER
2080 ! CORRECTION FOR AIR CONTAMINATION
2081 Pkp=Pvap2*1.E-3   ! TRANSDUCER IN kPa
2083 Pks=Psat*1.E-3    ! SAT. PRESSURE IN kPa
2084 Pg=Psat*1.E-3    ! GAUGE IN kPa
2092 Tsat=FNTvsp(Psat)
2093 Tvap1=FNTvsp(Pvap1)
2094 Tvap2=FNTvsp(Pvap2)
2099 Ust=FNUvst(Tsteam)
2110 Mwv=18.015
2113 IF Ift=1 THEN Mwv=187.39
2116 IF Ift=2 THEN Mwv=62.05
2117 Mfng1=100*(Pvap1-Psat)/(Pvap1-(1.-(Mwv/28.95))*Psat)
2118 Mfng2=100*(Pvap2-Psat)/(Pvap2-(1.-(Mwv/28.95))*Psat)
2134 IF Iov=2 THEN
2135 PRINT
2137 PRINT
2140 PRINT USING "10X,""Date set number           = "",DD";J
2143 OUTPUT 709;"AR AF40 AL40 VRS"
2146 OUTPUT 709;"AS SA"
2149 END IF
2150 PPINT
2152 ! IF Iov=2 AND Ng=1 THEN
2155 PRINT USING "1X,"" Psat      Pga      Ptran      Ttrans      Tsat(P)      NG1%      NG2%"""
2158 PRINT USING "1X,"" (kPa)    (kPa)    (kPa)    (C)        (C)        Molal      Molal"

```

```

2161 PRINT USING "1X,3(3D.00,2X),2(3D.00,2X),2(M3D.0,2X)";Pk$,Pkg,Pkp,Tvac2,Tsa
t,Mfng1,Mfng2
2164 PRINT
2167! END IF
2170 IF Mfng1>.5 THEN
2173 BEEP
2176 IF Im=1 AND Ng=1 THEN
2179 BEEP
2182 PRINT
2185 PRINT USING "10X,,"Energize the vacuum system """
2188 BEEP
2191 INPUT "OK TO ACCEPT THIS RUN (1=Y,0=N)?",Ok
2194 IF Ok=0 THEN
2197 BEEP
2200 DISP "NOTE: THIS DATA SET WILL BE DISCARDED!! "
2203 WAIT 5
2206 GOTO 1780
2209 END IF
2212 END IF
2215 END IF
2218 IF Im=1 THEN
2221 IF Fm<10 OR Fm>100 THEN
2224 Ifm=0
2227 BEEP
2230 INPUT "INCORRECT FM (1=ACCEPT,0=DELETE(DEFAULT))",Ifm
2233 IF Ifm=0 THEN 1804
2236 END IF
2239 END IF
2242! ANALYSIS BEGINS
2245 T11=FNTvsv58(Emf(3))
2246 T12=FNTvsv55(Emf(5))
2247 To1=FNTvsv58(Emf(4))
2248 To2=FNTvsv55(Emf(6))
2249 T11=T11-273.15
2250 T12=T12-273.15
2251 To1=To1-273.15
2252 To2=To2-273.15
2254 Tdel1=To1-T11
2255 Tdel2=To2-T12
2256 Tdel3=T2-T1
2257 Etp1=Emf(3)+Etp/20.
2258 Dtde=2.5931E-2-1.50464E-6*Etp1+1.21701E-10*Etp1^2-5.1154E-15*Etp1^3+3.2201
E-19*Etp1^4
2259 Tris=Dtde*Etp/10.
2262 To3=T11+Tris
2263 PRINT USING "1X,," TIN1 TOUT1 TIN2 TOUT2 TIN3 TOUT3 DELT1 DELT2
DELT3 TPILE """
2264 PRINT USING "1X,," (Teflon) (Metal) (Quartz) """
2265 PRINT USING "2X,10(2D.00,2X)";T11,To1,T12,To2,T1,T2,Tdel1,Tdel2,Tdel3,Tris
2266 Err=ABS(T11-T1)

```

```

2267 Er3=ABS(T12-T1)
2268 PRINTER IS 1
2270 IF Er1>.5 OR Er3>.5 AND Im=1 THEN
2271 BEEP
2272 PRINT "QCT AND TC DIFFER BY MORE THAN 0.5 C"
2275 OK1=1
2278 END IF
2287 IF OK1=0 AND Er1>.5 AND Im=1 THEN 1780
2288 IF OK1=0 AND Er3>.5 AND Im=1 THEN 1780
2290 Er2=ABS((T2-T1)-(Tris))/(T2-T1)
2293 IF Er2>.05 AND Im=1 THEN
2296 BEEP
2299 PRINT "QCT AND T-PILE DIFFER BY MORE THAN 5%"
2302 OK2=1
2305 IF OK2=0 AND Er2>.05 AND Im=1 THEN 1780
2308 END IF
2311 PRINTER IS 701
2312 INPUT "COOLANT TEMP. RISE MEAS. (0=TEFLON, 1=METAL S., 2=QUARTZ, 3=TPILE)" ,
2314 ,Itm
2315 IF Itm=0 THEN
2316 PRINT USING "1X,";"USING SINGLE TEFLON THERMOCOUPLE FOR COOLANT TEMP. RISE"
2317 "
2318 T1i=T1
2319 T2o=Tc1
2323 END IF
2326 IF Itm=1 THEN
2327 PRINT USING "1X,";"USING SINGLE METAL SHEATHED THERMOCOUPLE FOR COOLANT TEM
P. RISE"""
2329 T1i=T12
2332 T2o=Tc2
2335 END IF
2338 IF Itm=2 THEN
2339 PRINT USING "1X,";"USING QUARTZ THERMOMETER FOR COOLANT TEMP. RISE"""
2341 T1i=T1
2344 T2o=T2
2347 END IF
2349 IF Itm=3 THEN
2350 PRINT USING "1X,";"USING THERMOPILE FOR COOLANT TEMP. RISE"""
2351 T1i=T13
2352 T2o=Tc3
2353 END IF
2353 Tavg=(T1i+T2o)+.5
2354 Ift=0
2355 Cpw=FNCpw(Tavg)
2356 Rhow=FNRRhow(Tavg)
2359 Md=(6.7409+Fm+13.027)/1000.
2362 Md=Md*(1.0365-1.95544E-3*T1i+5.252E-6*T1i^2)/1.0037
2368 Mf=Md/Rhow
2371 Uw=Mf/(PI*D1^2/4)
2383 IF Inn=0 AND Uw>.5 THEN T2o=T2o-(-2.73E-4+1.75E-4*Uw+9.35E-4*Uw^2-1.96E-5*

```

```

Vw^3)
2399 IF Inn=1 THEN T2o=T2o-(-6.44E-5+1.71E-3*Vw+4.45E-4*Vw^2+4.07E-5*Vw^3)
2407 IF Inn=2 THEN T2o=T2o-(-3.99E-4+2.75E-3*Vw+1.45E-3*Vw^2+8.16E-5*Vw^3)
2408 IF Inn=3 THEN T2o=T2o-(8.57E-5+1.23E-3*Vw+1.09E-3*Vw^2+8.16E-5*Vw^3)
2413 Q=Md*Cpw*(T2o-T1i)
2416 Qp=Q/(PI*Dc*L)
2417! ITERATE TO FIND OUTER WALL TEMPERATURES
2418 Twm1=Twm
2419 Twm2=Twm
2420 Twm1=(Twm1+Twm2)/2.
2421 Ct=Q*LOG(Do/Dr)/(2.*PI*Kcu*L)
2422 Twm2=Twm+Ct
2423 IF ABS(Twm2-Twm1)>.001 THEN GOTO 2420
2424! ITERATE TO FIND INNER WALL TEMPERATURES
2425 Twm3=Twm
2426 Twm4=Twm
2427 Twm3=(Twm3+Twm4)/2.
2428 Cti=Q*LOG(Dr/Di)/(2.*PI*Kcu*L)
2429 Twm4=Twm-Cti
2430 IF ABS(Twm4-Twm3)>.001 THEN GOTO 2427
2431 Twmo=0.
2432 Twmi=0.
2433 FOR I=0 TO Inwt-1
2434 Two(I)=Tw(I)+Ct
2435 Twi(I)=Tw(I)-Cti
2436 Twmo=Twmo+Two(I)
2437 Twmi=Twmi+Twi(I)
2438 NEXT I
2439 Twmo=Twmo/Inwt
2440 Twmi=Twmi/Inwt
2441 PRINT
2443 PRINT USING "1X,""Position number" : 1 2 3 4
      5   6"""
2444 PRINT USING "1X,""Local outer wall temps. (DEG C) : "",6(00.00,1X)";Two(*)
)
2445 PRINT
2447 PRINT USING "1X,""Average outer and inner wall temps = "",2(00.00,1X)";Twmo,Twmi
2448 PRINT
2450 Ift=0
2451 Kw=FNKw(Tavg)
2452 Muw=FNMuw(Tavg)
2453 Muwi=FNMuw(Twmi)
2454 Rei=Rhow*Vw*Dc/Muw
2457 Prw=FNPrw(Tavg)
2458 Dtw=Q*LOG(Do/Di)/(2*PI*Kcu*L)*.5
2459 Lmtd=(T2o-T1i)/LOG((Twmi-T1i)/(Twmi-T2o))
2460 Perim=PI*Dc
2461 Surfai=PI*Dc*L
2462! PRINT Rei,Prw,Dtw,Lmtd,Perim,Surfai,Q

```

```

2457 Anarea1=PI*(Do^2-Di^2)/4.
2458 Anarea2=PI*(Dr^2-Di^2)/4.
2459 H1=Q/(Surfa1*Lmtd)
2460 Ff1=(Kcu*Perim*Anarea1)^.5
2461 Ff2=(Kcu*Perim*Anarea2)^.5
2472! PRINT Anarea1,Anarea2,H1,Ff1,Ff2
2474 H11=H1
2475 H12=H11
2476 Alam1=((H12*Perim)/(Kcu*Anarea1))^.5
2477 Alam2=((H12*Perim)/(Kcu*Anarea2))^.5
2478 Ff3=Ff1*H12^.5*(Twmi-T1i)
2479 Ff4=Ff2*H12^.5*(Twmi-T2o)
2480 Func6=Ff3*FNTanh(Alam1*L1)
2481 Func7=Ff4*FNTanh(Alam2*L2)
2482 Func8=H12*Surfa1*(Twmi-Tavg)
2483 Funcx=Func6+Func7+Func8-Q
2484 Dfunc6=(.5*Func6/H12)+2.*Ff3*L1/(1.+FNcosh(2.*Alam1*L1))
2485 Dfunc7=(.5*Func7/H12)+2.*Ff4*L2/(1.+FNcosh(2.*Alam2*L2))
2486 Dfunc8=Surfa1*(Twmi-Tavg)
2487 Dfuncx=Dfunc6+Dfunc7+Dfunc8
2488 H11=H12-(Funcx/Dfuncx)
2489 IF ABS(H11-H12)>.05 THEN GOTO 2475
2490 H1=H11
2500! PRINT H1
2521 Hfg=FNHfg(Tsteam)
2527 Tf1lm=Tsteam/3+Twmo*2/3
2530 Kf=FNKw(Tf1lm)
2533 Rhof=FNRhew(Tf1lm)
2534 Cpf=FNCPw(Tf1lm)
2536 Muf=FNMuw(Tf1lm)
2572 Q1=500
2575 Qloss=Q1/(100-25)*(Tsteam-Troom) ! TO BE MODIFIED
2576 Cpsc=FNCPw((Tcon+Tsteam)^.5)
2584 Mdv=0
2587 Bp=(Bvol*100)^2/5.76
2590 Hsc=Cpsc+(Tsteam-Tcon)
2593 Mdvc=(Bp-Qloss)-Mdv+Hsc)/Hfg
2596 IF ABS((Mdv-Mdvc)/Mdvc)>.01 THEN
2599 Mdv=(Mdv+Mdvc)^.5
2602 GOTO 2593
2605 END IF
2608 Mdv=(Mdv+Mdvc)^.5
2611 Vg=FNUVst(Tsteam)
2614 Vv=Mdv*Vg/Ax
2624 Tdcf=Tset-Twmo
2634 Ho=Qp/Tdcf
2635 Pr=Muf*Cpf/Kf
2636 Retp=(Vv*Do*Rhof)/Muf
2637 Nuss=(Ho*Do)/Kf
2638 Nunel=Nuss/Retp^.5

```

```

2639 Ff=9.81*Do*Muf*Hfg/(Vv^2*Kf*Tdef)
2640 Hnuss=.728*(Kf^3*9.81*Hfg*Rhof^2/(Muf*Do*Tdef))^25
2642 PRINT
2643 PRINT USING "1X," Uinf Tdef Qf1 Ho"""
2644 PRINT USING "1X,2(DD.DD,2X),2(MZ.3DE,2X)";Vv,Tdef,Qp,Ho
2645 PRINT
2646 PRINT USING "1X," Nu Retp NuRe Pr F Hnus
s"""
2648 PRINT USING "1X,2(MZ.3DE,2X),2(DD.DD,2X),2(MZ.3DE,2X)";Nuss,Retp,Nurel,Pr,
Ff,Hnuss
2654 Rat=Muw/Muw1
2654 Anus=Hi*D1/Kw
2674 Ares=(Uw*D1+Rhow)/Muw
2675 Aprs=Muw*Cpw/Kw
2676 Stco=Anus/(Ares^.8*Aprs^.3333*Rat^.14)
2677 Nupr=Anus/(Aprs^.3333*Rat^.14)
2679 PRINT
2680 PRINT USING "1X," Ucool Rec Hi Nuc Stcoef
f Nu/Pr"""
2681 PRINT USING "1X,6(MZ.3DE,2X)";Uw,Re1,Hi,Anus,Stco,Nupr
2682 INPUT "CHANGE TOOL RISE? 1=Y 2=N",Itr
2683 IF Itr=1 THEN GOTO 2312
2684 OUTPUT @File1;Two(*)
2704 IF Im=1 THEN
2707 BEEP
2710 INPUT "OK TO STORE THIS DATA SET (1=Y,0=N)?",Ok
2713 IF Ok=1 THEN
2725 OUTPUT @File1;Bvol,Bamp,Ptran,Etp,Emf(*),Fm,T1,T2,Pvap1
2738 END IF
2758 BEEP
2761 INPUT "WILL THERE BE ANOTHER RUN (1=Y,0=N)?",Igo
2764 Nrun=J
2767 IF Igo=1 THEN 1777
2770 ELSE
2773 IF J<Nrun THEN 1777
2783 END IF
2833 BEEP
2836! INPUT "ENTER PLOT FILE NAME",Fplot$
2838! ASSIGN @File4 TO Fplot$
2842! FOR I=1 TO Nrun
2845! ENTER @File4;Qp,Ho
2866! NEXT I
3001 PRINT USING "10X,""NOTE: "",ZZ,"" data runs were stored in file "",10A";J,
O_file$
3007 BEEP
3010! IF Ip=1 THEN
3013 PRINT
3016! PRINT USING "10X,""NOTE: "",ZZ,"" X-Y pairs were stored in plot data file
"",10A";J,P_file$
3019! END IF

```

```

3073 ASSIGN @File TO *
3076 ASSIGN @File1 TO *
3079! ASSIGN @File4 TO *
3082 IF Iso=2 THEN CALL Raw
3092 IF Iso=3 THEN CALL Purg
3115 END
3118 DEF FNPyst(Tc)
3121 COM /F1d/ Ift
3124 DIM K(8)
3127 IF Ift=0 THEN
3130 DATA -7.691234564,-26.08023696,-168.1706546,64.23285504,-118.9646225
3133 DATA 4.16711732,20.9750676,1.E9,6
3136 READ K(*)
3139 T=(Tc+273.15)/547.3
3142 Sum=0
3145 FOR N=0 TO 4
3148 Sum=Sum+K(N)*(1-T)^(N+1)
3151 NEXT N
3154 Br=Sum/(T*(1+K(5)*(1-T)+K(6)*(1-T)^2)-(1-T)/(K(7)*(1-T)^2+K(8)))
3157 Pr=EXP(Br)
3160 P=22120000*Pr
3163 END IF
3166 IF Ift=1 THEN
3169 Tf=Tc+1.8+32+459.6
3172 P=10^(33.0655-4330.98/Tf-9.2635*LGT(Tf)+2.0539E-3*Tf)
3175 P=P*101325/14.696
3179 END IF
3181 IF Ift=2 THEN
3184 A=9.394585-3056.1/(Tc+273.15)
3187 P=133.32*10^A
3190 END IF
3193 RETURN P
3196 FNEND
3199 DEF FNHfg(T)
3202 COM /F1d/ Ift
3205 IF Ift=0 THEN
3208 Hfg=2477200-2450*(T-10)
3211 END IF
3214 IF Ift=1 THEN
3217 Tf=T+1.8+32
3220 Hfg=7.0557957E+1-Tf*(4.838052E-2+1.2619048E-4*Tf)
3223 Hfg=Hfg*2326
3226 END IF
3229 IF Ift=2 THEN
3232 Tk=T+273.15
3235 Hfg=1.35264E+6-Tk*(6.38263E+2+Tk*.747462)
3238 END IF
3241 RETURN Hfg
3244 FNEND
3247 DEF FNMuw(T)

```

```

3250 COM /F1d/ Ift
3253 IF Ift=0 THEN
3256 A=247.8/(T+133.15)
3258 Mu=2.4E-5*10^A
3262 END IF
3265 IF Ift=1 THEN
3268 Mu=9.9629919E-4-T*(1.1084609E-5-T*5.566829E-8)
3271 END IF
3274 IF Ift=2 THEN
3277 Tk=1/(T+273.15)
3280 Mu=EXP(-11.0178+Tk*(1.744E+3-Tk*(2.80335E+5-Tk*1.12661E+8)))
3283 END IF
3286 RETURN Mu
3288 FNEND
3292 DEF FNUvst(Tt)
3295 COM /F1d/ Ift
3298 IF Ift=0 THEN
3301 P=FNPvst(Tt)
3304 T=Tt+273.15
3307 X=1500/T
3310 F1=1/(1+T*1.E-4)
3313 F2=(1-EXP(-X))^2.5*EXP(X)/X^.5
3316 B=.0015*F1-.000842*F2-.0004882*X
3319 K=2*P/(461.52*T)
3322 V=(1+(1+2*B*K)^.5)/K
3325 END IF
3328 IF Ift=1 THEN
3331 Tf=Tt+1.8+32
3334 V=13.955357-Tf*(.16127262-Tf+5.1726190E-4)
3337 V=V/16.018
3340 END IF
3343 IF Ift=2 THEN
3346 Tk=Tt+273.15
3349 P=FNPvst(Tt)
3352 V=133.95+Tk/P
3355 END IF
3358 RETURN V
3361 FNEND
3364 DEF FNCpw(T)
3367 COM /F1d/ Ift
3370 IF Ift=0 THEN
3373 Cpw=4.21120858-T*(2.26826E-3-T*(4.42351E-5+2.71428E-7*T))
3376 END IF
3378 IF Ift=1 THEN
3382 Cpw=9.2507273E-1+T*(8.3400433E-4+1.7207792E-6*T)
3385 END IF
3388 IF Ift=2 THEN
3391 Tk=Tt+273.15
3394 Cpw=4.1868*(1.6894E-2+Tk*(3.35083E-3-Tk*(7.224E-6-Tk*7.61748E-9)))
3397 END IF

```

```

3400 RETURN Cpw*1000
3403 FNEND
3405 DEF FNRhow(T)
3409 COM /F1d/ Ift
3412 IF Ift=0 THEN
3415 Ro=999.5294E+T*(.01269-T*(5.492513E-3-T*1.234147E-5))
3418 END IF
3421 IF Ift=1 THEN
3424 Ro=1.6207479E+3-T*(2.218634E+T*2.3578291E-3)
3427 END IF
3430 IF Ift=2 THEN
3433 Tk=T+273.15-338.15
3436 Uf=9.24849E-4+Tk*(6.2795E-7+Tk*(9.2444E-10+Tk*3.057E-12))
3439 Ro=1/Uf
3442 END IF
3445 RETURN Ro
3448 FNEND
3451 DEF FNPrw(T)
3454 Prw=FNCpw(T)*FNMuw(T)/FNKw(T)
3457 RETURN Prw
3460 FNEND
3463 DEF FNKw(T)
3466 COM /F1d/ Ift
3469 IF Ift=0 THEN
3472 X=(T+273.15)/273.15
3475 Kw=-.92247+X*(2.8395-X*(1.8007-X*(.52577-.07344*X)))
3478 END IF
3481 IF Ift=1 THEN
3484 Kw=8.2095238E-2-T*(2.2214285E-4+T*2.3809524E-8)
3487 END IF
3490 IF Ift=2 THEN
3493 Tk=T+273.15
3496 Kw=4.1868E-4*(519.442+.320920*Tk)
3499 END IF
3502 RETURN Kw
3505 FNEND
3508 DEF FNTanh(X)
3511 P=EXP(X)
3514 Q=EXP(-X)
3517 Tanh=(P-Q)/(P+Q)
3520 RETURN Tanh
3523 FNEND
3526 DEF FNTvsy(U)
3529 COM /Cc/ C(7)
3532 T=C(0)
3535 FOR I=1 TO 7
3538 T=T+C(I)*U^I
3541 NEXT I
3544 T=T+4.73385E-3+T*(7.692934E-3-T*9.077927E-5)
3547 RETURN T

```

```

3550 FNEND
3553 DEF FNHf(T)
3556 COM /F1d/ Ift
3559 IF Ift=0 THEN
3562 Hf=T*(4.203849-T*(5.98132E-4-T*4.55160317E-6))
3565 END IF
3568 IF Ift=1 THEN
3571 Tf=T*1.8+32
3574 Hf=8.2078571+Tf*(.19467957+Tf*1.3214296E-4)
3577 Hf=Hf*2.326
3580 END IF
3583 IF Ift=2 THEN
3586 Hf=250 ! TO BE VERIFIED
3589 END IF
3592 RETURN Hf+1000
3595 FNEND
3610 DEF FNTvsp(P)
3613 Tu=190
3616 T1=10
3619 Ta=(Tu+T1)*.5
3622 Pc=FNPvst(Ta)
3625 IF ABS((P-Pc)/P)>.0001 THEN
3628 IF Pc<P THEN T1=Ta
3631 IF Pc>P THEN Tu=Ta
3634 GOTO 3619
3637 END IF
3640 RETURN Ta
3643 FNEND
3653 DEF FNTvsV55(V)
3656 COM /Cc55/ T55(5)
3673 T=T55(0)
3683 FOR I=1 TO 5
3693 T=T+T55(I)*V^I
3703 NEXT I
3713 RETURN T
3723 FNEND
3733 DEF FNTvsV56(V)
3734 COM /Cc56/ T56(5)
3735 T=T56(0)
3736 FOR I=1 TO 5
3737 T=T+T56(I)*V^I
3747 NEXT I
3748 RETURN T
3749 FNEND
3753 DEF FNTvsV57(V)
3754 COM /Cc57/ T57(5)
3755 T=T57(0)
3756 FOR I=1 TO 5
3757 T=T+T57(I)*V^I
3767 NEXT I

```

```

3768 RETURN T
3769 FNEND
3773 DEF FNTvsy58(V)
3774 COM /C658/ T58(5)
3775 T=T58(0)
3776 FOR I=1 TO 5
3777 T=T+T58(I)*V^I
3778 NEXT I
3797 RETURN T
3807 FNEND
3817 DEF FNCosh(X)
3827 P=EXP(X)
3837 Q=EXP(-X)
3847 Cosh=.5*(P+Q)
3857 RETURN Cosh
3867 FNEND
3877 SUB Raw
3878 COM /F1d/ Ift
3879 DIM Emf(13)
3880 BEEP
3881 INPUT "ENTER FILE NAME",File$
3882 ASSIGN @File TO File$
3883 BEEP
3884 INPUT "ENTER PRESSURE CONDITION (0=V, 1=A)",Ipc
3885 INPUT "ENTER NUMBER OF RUNS",Nrun
3886 PRINTER IS 701
3887 PRINT
3888 PRINT
3889 PRINT USING "10X,","File Name:      ",14A";File$"
3890 IF Ipc=0 THEN
3891 PRINT USING "10X,","Pressure Condition: Vacuum"""
3892 ELSE
3893 PRINT USING "10X,","Pressure Condition: Atmospheric"""
3894 END IF
3895 ENTER @File;Ifg,Ion
3896 ENTER @File;Inwt,Fp,Fw,Fh
3897 PRINT
3898 PRINT USING "10X,","Data    Vw    Tin    Tout    Ts"""
3899 FOR I=1 TO Nrun
3900 ENTER @File;Bvol,Bamp,Ptran,Etp,Emf(+),Fm,T1,T2,Pvap1
3902 PRINT Bvol,Bamp,Ptran,Etp,Emf(+),Fm,T1,T2,Pvap1
3903 NEXT I
3904 ASSIGN @File TO *
3906 SUBEND
3907 SUB Purge
3908 BEEP
3909 INPUT "ENTER FILE NAME TO BE DELETED",File$
3917 PURGE File$
3927 GOTO 3908
3937 SUBEND

```

LIST OF REFERENCES

1. Incropera, F.P. and DeWitt, D.P., *Introduction to Heat Transfer*, John Wiley and Sons, New York. pp 566-67, 1990.
2. Van Petten, T.L., *Filmwise Condensation on Low Integral-Fin Tubes of Different Diameters*, Master's Thesis, Naval Postgraduate School, Monterey, California, December 1988.
3. Guttendorf, M.B., *Further Development of Filmwise Condensation of Steam on Horizontal Integral Finned Tubes*, Master's Thesis, Naval Postgraduate School, Monterey, California, June 1990.
4. Rouk, P., *Some Considerations of Data Reduction Techniques in Film Condensation Heat Transfer Measurements*, Master's Thesis, Naval Postgraduate School, Monterey, California, June 1992.
5. Georgiadis, I.V., *Filmwise Condensation of Steam on Low Integral-Finned Tubes*, Master's Thesis, Naval Postgraduate School, Monterey, California, September 1984.
6. Poole, W.M., *Filmwise Condensation of Steam on Externally-finned Horizontal Tubes*, Master's Thesis, Naval Postgraduate School, Monterey, California, December 1983.
7. Yau, K.K., Cooper, J.R., and Rose, J.W., *Effect of Fin Spacing on the Performance of Horizontal Integral-Fin Condenser Tubes*, ASME Journal of Heat Transfer, vol. 107, pp. 337-383, 1985.
8. Wanniarachchi, A.S., Marto, P.J., and Rose, J.W., *Film Condensation of Steam on Horizontal Finned Tubes: Effect of Fin Spacing*, Journal of Heat Transfer, vol. 108, pp. 960-966, November 1986.
9. Katz, D.L., Hope, R.E., and Datsko, S.C., *Liquid Retention on Finned Tubes*, Department of Engineering Research, University of Michigan, Ann Arbor, Michigan, project M592, 1946
10. Marto, P.J., *An Evaluation of Film Condensation on Horizontal Integral-Fin Tubes*, Journal of Heat Transfer, vol. 110, pp. 1287-1305, November 1988
11. Nusselt, W., "Die Oberflächen-Kondensation des Wasserfampfes," *VDI Zeitung*, vol. 60, pp. 541-546, 569-575, 1916.
12. Memory, S.B. *Forced Convection Film Condensation on a Horizontal Tube at High Vapor Velocity*, PHD Thesis, University of London, London, England, September 1989.

13. Shekrladze, I.G. and Gomelauri, V.I., *Theoretical Study of Laminar Film Condensation of Flowing Vapour*, International Journal of Heat and Mass Transfer, vol. 9, pp. 581-591, 1966.
14. Fujii, T., Honda, H., and Oda, K., *Condensation of Steam on a Horizontal Tube -- the Influences of Oncoming Velocity and Thermal Condition at the Tube Wall*, Condensation Heat Transfer, The 18th National Heat Transfer Conference, San Diego, California, pp. 35-43, August 1979.
15. Rose, J.W., *Fundamental of Condensation Heat Transfer: Laminar Film Condensation*, JSME International Journal, Series II, vol. 31, no. 3, pp. 357-375, 1988.
16. Dittus, F.W. and Boelter, L.M.K., *Heat Transfer in Automobile Radiators of the Tubular Type*, University of California Publications in Engineering, vol. 2, no. 13, pp. 443-461, 1930.
17. Colburn, A.P., *A Method of Correlating Forced Convection Heat Transfer Data and a Comparison with Fluid Friction*, Transactions of AIChE, vol. 29, pp. 174, 1933.
18. Sieder, E.N., and Tate, C.E., *Heat Transfer and Pressure Drop of Liquids in Tubes*, Industrial Engineering Chemistry, vol. 28, pp. 1429, 1936.
19. Petukhov, B.S., *Heat Transfer and Friction in Turbulent Pipe Flow with Variable Physical Properties*, Advances in Heat Transfer, vol. 6, pp. 503, 1970.
20. Sleicher, C.A. and Rouse, M.W., *A Convenient Correlation for Heat Transfer to Constant and Variable Property Fluids in Turbulent Pipe Flow*, International Journal of Heat and Mass Transfer, vol. 18, p. 677, 1975.
21. Lorenz, J.J., Yung, D., Panchal, C., and Layton, G., *An Assessment of Heat Transfer Correlations for Turbulent Pipe Flow of Water at Prandtl Numbers of 6.0 and 11.6*, Argonne National Laboratory, Argonne, Illinois, January, 1981.
22. Coumes, J.M., *Some Aspects of Film Condensation of Steam on Horizontal Finned Tubes*, Master's Thesis, Naval Postgraduate School, Monterey, California, December 1989.
23. Marto, P.J., Looney, D.J., Rose, J.W., and Wanniarachchi, A.S., *Evaluation of Organic Coatings for the Promotion of Dropwise Condensation of Steam*, International Journal of Heat and Mass Transfer, vol. 29, no. 8, pp. 1109-1117, 1986.
24. Kline, S.J., and McClintock, F.A., *Describing Uncertainties in Single-Sample Experiments*, Mechanical Engineering, vol. 74, pp. 3-8, January 1953.
25. Mitrou, E.S., *Film Condensation of Steam on Externally Enhanced Horizontal Tubes*, Master's Thesis, Naval Postgraduate School, Monterey, California, March 1986.

INITIAL DISTRIBUTION LIST

No. Copies

1.	Defense Technical Information Center Cameron Station Alexandria, VA 22304-6145	2
2.	Library, Code 0142 Naval Postgraduate School Monterey, CA 93943-5002	2
3.	Department Chairman, Code ME/He Department of Mechanical Engineering Naval Postgraduate School Monterey, CA 93943-5004	1
4.	Naval Engineering Curricular Officer, Code 34 Department of Mechanical Engineering Naval Postgraduate School Monterey, CA 93943-5004	1
5.	Professor Paul J. Marto, Code ME/Mx Department of Mechanical Engineering Naval Postgraduate School Monterey, CA 93943-5004	3
6.	Professor Stephen B. Memory, Code ME/Me Department of Mechanical Engineering Naval Postgraduate School Monterey, CA 93943-5004	1
7.	Professor John W. Rose Department of Mechanical Engineering Queen Mary College, University of London London E1 4NS, England	1
8.	Mr. David Brown David W. Taylor Naval Ship Research and Development Center Annapolis, MD 21402	1
9.	LT. Keith A. Swensen 1260 Spruance Rd. Monterey, CA 93940	3

~~744-343~~

744-343

DUDLEY KNOX LIBRARY
NAVAL POSTGRADUATE SCHOOL
MONTEREY CA 93943-5101

GAYLORD S



DUDLEY KNOX LIBRARY



3 2768 00018904 7